SIMULATION OF THE HYDROLOGICAL PROCESSES ON RECONSTRUCTED WATERSHEDS USING SYSTEM DYNAMICS

By

Antarpreet Singh Jutla[1]

Amin Elshorbagy[1]

Jim Kells[2]

[1]Centre for Advanced Numerical Simulation (CANSIM), Department of Civil & Geological Engineering, University of Saskatchewan, Saskatoon, SK, Canada

[2] Department of Civil & Geological Engineering, University of Saskatchewan, Saskatoon, SK, Canada

CANSIM SERIES REPORT NO. CAN-06-01

Centre for Advanced Numerical Simulation (CANSIM)

Department of Civil & Geological Engineering,

University of Saskatchewan, Saskatoon, SK, CANADA

January, 2006

ABSTRACT

The mining of oil sands in the sub-humid region of Northern Alberta, Canada causes large-scale landscape disturbance, which subsequently requires extensive reclamation to re-establish the surface and subsurface hydrology. The reconstructed watersheds examined in this study are located at the Syncrude Canada Limited mine site, 40 km North of Fort McMurray, Alberta, Canada. The three experimental reconstructed watersheds, with nominal soil thicknesses of 1.0 m, 0.50 m and 0.35 m accompanied a thin layer of peat (15-20 cm) over varying thicknesses of secondary (till) soil, have been constructed to cover saline sodic overburden and to provide sufficient moisture storage for vegetation while minimizing surface runoff and deep percolation to the underlying shale overburden. In order to replicate the hydrological behavior, assess the sustainability, and trace the evolution over time of the reclaimed watersheds, a suitable modeling tool is needed.

In this research, a model is developed using the system dynamics approach to simulate the hydrological processes in the three experimental reconstructed watersheds and to assess their ability to provide the various watershed functions. The model simulates the vertical and lateral water movement, surface runoff and evapotranspiration within each watershed. Actual evapotranspiration, which plays an important role in the hydrology of the Canadian sub-humid regions, is simulated using an indexed soil moisture method. The movement of water within the various soil layers of the cover is based on parametric relationships in conjunction with conceptual infiltration models. The feedback relationships among the various dynamic hydrologic processes in the watershed are captured in the developed System Dynamic Watershed Model (SDWM).

Most hydrological models are evaluated using runoff as the determining criterion for model calibration and validation, while accounting for the movement of moisture in the soil as a water loss. Since one of the primary objectives of a reconstructed watershed is to maintain the natural flora and fauna, it is important to recognize that soil moisture plays an important role in assessing the performance of the reconstructed watersheds. In turn, soil moisture becomes an influential factor for quantifying the health of the reconstructed watershed. The developed model has been calibrated and validated with data for two years (2001-2002), upholding the sensitive relationship between soil moisture and runoff. Accurate calibration of the model based on simulations of soil moisture in the various soil layers improves its overall performance. The model was subsequently used to simulate the three sub-watersheds for five years, with changing the calibrated model parameters to use them as indicators of watershed evolution. The simulated results were compared with the observed values.

The results of the study illustrate that all three watersheds are still evolving. Failure to identify a unique parameter set for simulating the watershed response supports the hypothesis of watershed evolution. Soil moisture exchange between the till and peat layers changed with time in all of the watersheds. There was also a modest change in the water movement from the till to shale layers in each of the sub-watersheds. Vegetation is increasing in all of watersheds although there is an indication that one of the sub-watersheds may be sustaining deep rooted vegetation. The results demonstrate the successful application of the system dynamics approach and the developed model in simulating the hydrology of reconstructed

watersheds and the potential for using this approach in assessing complex hydrologic systems.

ACKNOWLEDGEMENTS

Financial support provided by the Natural Science and Engineering Research Council (NSERC) of Canada and the in-kind support of Syncrude Canada Ltd. to do the research work is greatly acknowledged. Facilities provided by the Centre For Advanced Numerical Simulation (CANSIM), Department of Civil Engineering, University of Saskatchewan, Canada is also acknowledged.

TABLE OF CONTENTS

LIST OF TABLES

LIST OF FIGURES

Chapter 1

Introduction

1.1 Background

Surface mining results in the large-scale destruction of natural landscapes, which affects the local ecosystems and the hydrology of the region. Canadian mining industry produces more than 500 million tons of solid waste in the form of overburden and tailings sands (O'Kane et al., 1998). Until the late 1960s, the problem posed by these residual wastes on the environment was considered minimal, but global concerns about degradation of the natural environment have since forced many governments to impose stringent laws that require mine operators to adopt reasonable final closure and reclamation strategies for the mine before receiving certification (Haigh, 2000).

Prior to mining, the soil and overburden material are removed so as to provide access to the desired mined product (e.g., coal, oil). The overburden and tailings materials are stockpiled and contoured, and then topsoil is placed over then. The process of reestablishing the disturbed landscape and developing sustainable soil-vegetation-water relationships to achieve land capability corresponding to the undisturbed condition is called land reclamation (Gilley et al., 1977). Reclamation of the landscape following mining is a multifaceted process that involves reconstruction and redesign of a complete landscape profile. The reclamation process is followed by a series of developmental activities, including the growing of vegetation, preparing the land for agriculture, and monitoring the long-term behavior of such lands (Ward et al., 1983). Accordingly, Haigh (2000) divided land reclamation strategies into three sub-categories: (i) cosmetic land reclamation, which involves temporary development of drains, thin soil coverings, and little vegetation (the land reclaimed in this category often erodes away, subsides, and requires re-establishment later on); (ii) sustainable reclamation, which requires higher engineering skills to design appropriate soil covers, drainage, and growth of vegetation (the soil covers in this category require continuous maintenance and management); and (iii) self-sustainable reclamation that aims at using ecological and engineering principles to reclaim land surfaces and to develop interaction between the local flora and fauna. This type of reclamation helps in creating a dynamic, self-evolving and biologically sound hydrologic system that will mimic a natural watershed within few years of the reconstruction (Haigh, 2000). The landforms resulting from this category are often termed reconstructed landscapes and are called 'reconstructed watersheds' throughout this document. The global aim of this type of reclamation is to make the land self-sustainable over time, which altogether negates the use of the first two sub-categories of reclamation strategy.

1.2 Area of Interest: Restoration of Hydrology

A self-sustainable reclamation strategy is the most appropriate technique for the closure of an open pit mine (Sawatsky et al., 2000). Hence, it is proposed that mining industries should

adopt strategies based on sub-category (iii) as a final plan for landscape restoration. Soil covers minimize the influx of water and oxygen into the underlying overburden material, conserve soil moisture in the root zone and promote vegetation growth (Swanson et al., 2003). Thus, the major issue requiring attention with reconstructed watersheds is how to re-establish the natural hydrology in the region. Kilmartin (2000) suggested that research into the hydrology of an open pit mine focuses on surface runoff, infiltration, vegetation, and drainage.

Land reclamation and the design of soil covers are affected by local climate. In regions where potential evapotranspiration is greater than annual rainfall, often called a semi-arid climate, a soil cover should minimize runoff, retain soil moisture for the growing season and prevent deep percolation. In regions where the annual rainfall is greater than the potential evapotranspiration, called a wet climate, a soil cover should allow runoff without much soil erosion and should retain appropriate soil moisture (Swanson et al., 2003).

Runoff response from the reconstructed watersheds has been studied by many researchers (e.g., Cutris, 1974; Lusby and Toy 1976; Gilley et al., 1977; Schroeder, 1987). These studies indicate that soil covers in wet climates produce more runoff than soil covers constructed in dry climates. Infiltration is one of the most important and fundamental variables in a reconstructed watershed, which serves to define the success of any reclamation strategy (Ward et al., 1983). Runoff from reclaimed watersheds can be minimized only through enhanced infiltration and evapotransiration. Kilmartin (2000) reported the major factors controlling infiltration in such watersheds is the structure of the soil matrix in the surface layer. Other researchers (Prunty and Kirkham, 1979; Potter et al., 1988; Rogowski and Weinrich, 1981) studied the effects of infiltration in reconstructed watersheds and concluded that infiltration rates were higher when compared to that of natural watersheds.

Vegetation is a good indicator of the success of a reclamation strategy, but it is highly dependent on the soil moisture conditions and physical properties of the soils. Wright (1978) noticed that the rooting depth of the vegetation has a significant hydrological effect for arid and semi-arid regions; vegetation decreases overland flow and increases evapotranspiration. However, there is limited literature available to support such claims in reconstructed watersheds. In addition to vegetation, groundwater may play a vital role in describing the water balance in the watershed. Surface mining also lowers the groundwater levels (Ngah et al., 1984). In arid and semi-arid regions, under low precipitation, surface recharge plays only a small role in groundwater recharge. High groundwater levels and saturation of the overburden waste material like can lead to lateral drainage of the water along the slope of a reconstructed watershed (Ringler, 1984). The impact of hydrological processes and their interrelationships on the reconstructed watershed can be better understood by simulating the watershed as a whole hydrologic system. Simulating such a system could help in the proper management and possible future design of reclamation strategies. Simulating reconstructed watersheds to model the various hydrologic processes, and to assess the hydrologic performance of such watersheds is the area of interest for this study.

1.3 Problem Definition

The interrelationships among the several variables and hydrological processes in reconstructed watersheds define the watershed response and develop a closed loop network of interactions. During the initial stages of development of the watershed, soil moisture in the upper soil layers plays a significant role in vegetation growth, but as the watershed matures, runoff and lateral flow may increase (Kilmartin, 2000). This process can be further complicated by time and scale factors. Rick (1995) suggests that the monitoring period for reconstructed watersheds should be five years with two additional years of passive management as a factor of safety.

Syncrude Canada Limited initiated an instrumented reconstructed watershed research program at South Bison Hills near Fort McMurray, Alberta, Canada in 1999. Three experimental soil covers, with thicknesses of 1.0 m, 0.50 m and 0.35 m comprising a thin layer of peat mineral (15-20 cm) over varying thicknesses of secondary (glacial/till) soil, have been constructed to cover saline sodic overburden and to provide sufficient moisture storage for vegetation while minimizing runoff and weathering of the underlying overburden shale (Boese, 2003). The data from these three soil covers have been used in this research.

The three experimental soil covers need to be evaluated with regard to their ability to hold sufficient moisture for vegetation and to minimize deep percolation of water into the underlying waste material. The evolution of the soil covers over time is an important factor for the sustainability of the reclamation strategy. A simulation model that captures the short term behavior of the reconstructed watersheds, and which has the potential to predict the long-term hydrologic performance, is essential for the mining industry. The watershed simulation model can maximize the benefits gained from the monitoring program and allow for testing different scenarios that may help direct the design of future reclamation landscapes and direct further monitoring. It may be added here that most work on reclamation sites to date has been limited to a geotechnical focus, with the cumulative effects of hydrological processes either being ignored or with each process being dealt with separately (Woyshner and Yanful, 1995; Swanson at al., 2003). In order to evaluate the various hydrologic functions in the reconstructed watershed, a suitable and flexible modeling structure is required.

1.4 Research Objectives

This report is directed towards the development of a suitable watershed model for reconstructed watersheds. The modeling exercise will enhance the understanding of the interactions among the various hydrological processes within the reconstructed watershed under consideration. The model developed in this research is a lumped parameter model that takes no explicit account of the spatial variability of the processes while calibrating and validating the model to the research site. The broad aim of this study is to understand, evaluate and model the hydrologic processes in a reconstructed watershed. The specific objectives of the research reported in this report are to:

- Develop a hydrologic model for the reconstructed watersheds
- Calibrate and validate the developed model, and
- Run the model for several consecutive years in order to assess evolution of the reconstructed watersheds.

1.5 Scope of the Research Program

Watershed models can be classified on the basis of processes, scale, and the underlying mathematical approach. Details on such classifications can be found in Singh (1995). A watershed model is called a lumped model if it considers ordinary differential equations (based upon simplified hydraulic laws), taking no account of the spatial variability of the processes, inputs, boundary conditions, and system geometric characteristics. Distributed models explicitly take into account the spatially-variable processes, inputs, boundary conditions and/or system geometric characteristics.

The present report is a part of a large research program that aims at developing a framework to help understand the dynamics of the hydrologic processes that are dominant in reconstructed watersheds as a result of different reclamation strategies. The overall goal of the research is to help the oil sands mining industry as well as the industry regulators develop, adopt, and enforce a sustainable reclamation strategy. Such a strategy requires a comprehensive understanding of both short-term and long-term evolution of reclaimed (reconstructed) watersheds. The sizable amount of meteorological, hydrological, hydrogeological, and ecological data collected, although apparently useful and desirable, can lead to paralysis of analysis in the absence of a framework that guides all stakeholders through the decision-making process.

The overall research framework, shown in Figure 1.1, is founded on the ongoing program of extensive monitoring. Initial understanding is used to go through two parallel approaches of mechanistic and inductive (data-driven) modeling of the reconstructed watersheds as partially understood system. The outputs from the two different approaches will be used to encapsulate the initial understanding of the system from the perspective of a decision analysis (DA) approach that entails comprehensive and detailed sensitivity and uncertainty analyses. The DA approach, along with the initial understanding of the system of reconstructed watersheds, which is supplemented with knowledge gained from a comparison with natural systems, will be utilized to provide feedback to the monitoring program and the modeling exercise. Re-directed monitoring and refined modeling will help achieve the desired comprehensive understanding of the system of reconstructed watersheds. Finally, the system understanding can be quantified towards modifying existing regulations and reclamation practices to develop sustainable reclamation strategy (SRS).

The overall framework for general research requires the following specific tasks to be completed:

- Develop a watershed simulation methodology that helps develop an understanding of the dynamics of various watershed (hydrologic) processes associated with reconstructed watersheds. The overriding objective of this task is to develop a simulation-for-understanding tool rather than simulation-for-prediction (this objective of the research program will be covered in the present research work);

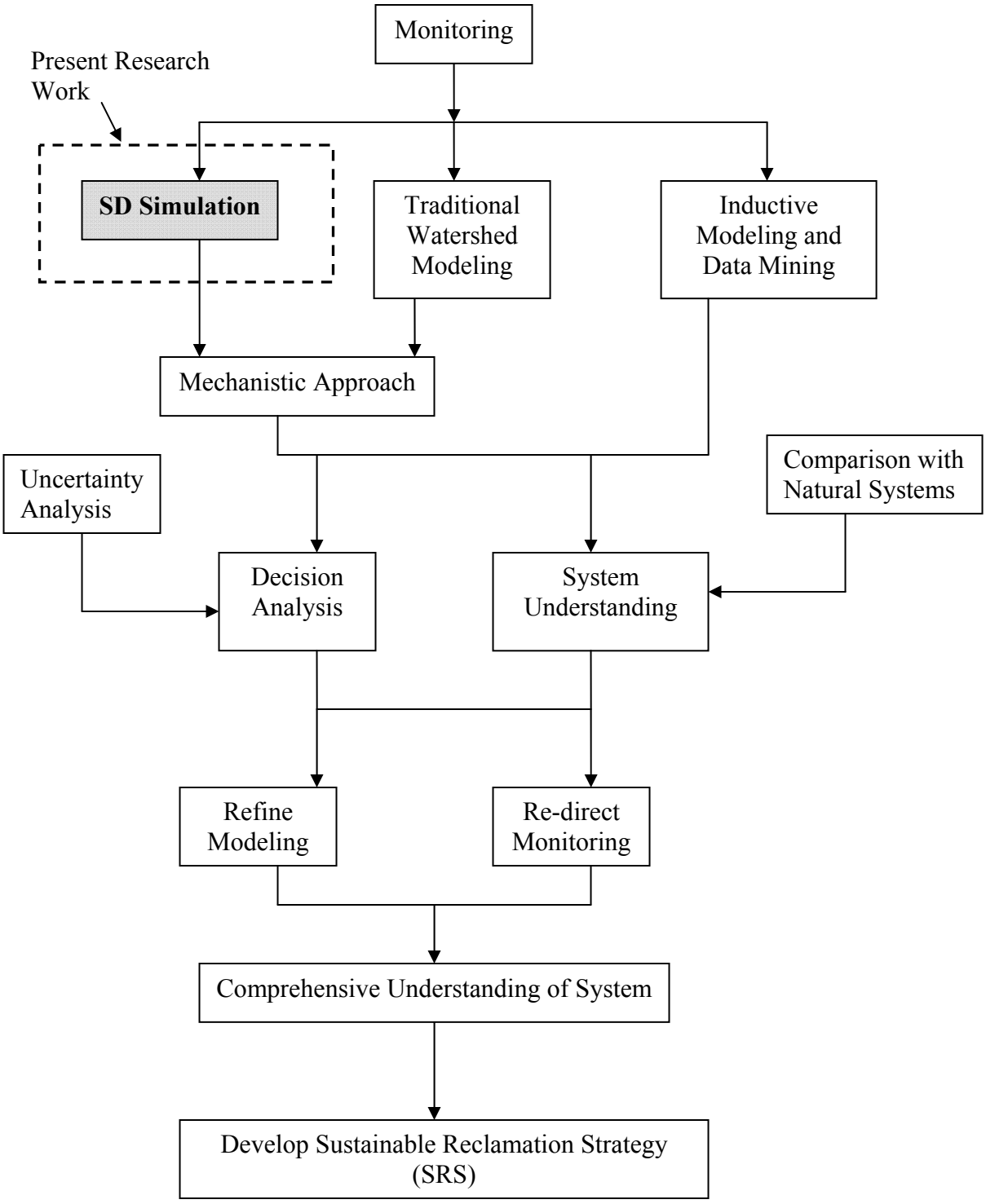

Figure 1.1. Framework of the Research Program for Developing a Sustainable Reclamation Strategy.

- Simulate the reconstructed watersheds using some of the readily available watershed models (e.g., HSPF, SLURP), and conduct a comparison between the available models and the model developed in Task 1. The objective of this task is to identify the type of mechanistic models and modeling approaches that are suitable for modeling reconstructed watersheds in sub-humid regions, and also to identify the levels of detail and data resolution needed for this exercise;
- Develop an inductive modeling approach to model or estimate the various hydrologic processes, individually and as a system, without relying heavily on the underlying physics of the different processes. Hopefully, the inductive approach could count for processes that are difficult to be modeled using a the mechanistic approach;
- Conduct a comparison between reconstructed and natural watershed systems using both mechanistic and inductive modeling approaches. The objective of this task is to identify the possibility of knowledge augmentation to fill in the knowledge gap of reconstructed watersheds with regard to their evolution over time, and also to identify the data requirements for modeling and decision making;
- Develop an integrated or hybrid modeling approach that benefits from the advantages of both mechanistic and inductive modeling approaches. The objective of this task is to develop and propose to both industry and scientists the best possible tool for modeling reconstructed watersheds;
- Develop a multi-criterion decision analysis (MCDA) framework to evaluate different reclamation alternatives. The objective of this task is to encapsulate all of the knowledge gained with regard to different reclamation strategies into a decision analysis context that addresses the important question of `*What is it that really matters?*`. The most important parameters to be measured, the most important processes to be modeled, the most appropriate modeling approach to be adopted, and the most sustainability-oriented reclamation strategy are the key issues to be addressed using the MCDA technique; and
- Conduct a comprehensive uncertainty analysis. The objective of this task is to identify the impacts of uncertainty about the measured parameters, the model structure, the model parameters, and the scale and the representation of various processes on the decision-making process with regard to the reclamation alternatives.
- The scope of this report is limited to develop the model that should meet the objective described in Task 1. Simply it is represented by the shaded rectangle in Figure 1.1.

1.6 Synopsis of the report

The remainder of the report document is organized as follows: Key issues as well as a literature review on watershed modeling are provided in Chapter 2. The modeling approach used to simulate the reconstructed watershed is explained in Chapter 3. Chapter 4 provides a description of the case study where the developed model is applied. Chapter 5 explains the various model formulations and assumptions. Presentation of results, analysis and discussion are presented in Chapter 6 and, finally, Chapter 7 presents a summary of the research, the conclusions reached, and possible areas of future research.

Chapter 2

Watershed Modeling: Literature Review

This chapter gives an overview of the dominant hydrological processes in a watershed and methods for quantifying these processes. The chapter also provides insight into the role of hydrological processes in the calibration and validation of watershed models.

2.1 Overview of Watershed Modeling

Watershed modeling plays an important role in the domain of hydrological sciences. Watershed models are required for: (1) understanding hydrological processes and their impact on each other, (2) quantifying non-measurable hydrological processes, (3) application to ungauged watersheds, and (4) hydrologic forecasting (Beven, 2000). According to Singh (1995), watershed models can be classified on the basis of hydrological processes, scale, or methods of solution. Process-based models can be lumped, distributed, or quasi-distributed. A lumped model is based on ordinary differential equations and takes no account of the spatial variability of the processes and boundary conditions. Examples of a lumped model include HEC-1 (Hydrologic Engineering Centre, 1981), and HYdrologic Model-HYMO (Williams and Hann, 1972). On the other hand, distributed models, such as European hydrological system – Systeme Hydrologique European, SHE (Abbott et al., 1986) and National Weather Service River Forecasting System, NWSRFS (Burnash, 1995), take explicit account of spatially variable processes, input, and boundary conditions. In many cases, models are quasi-distributed, such as Hydrologic Simulation Program-Fortran, HSPF (Donigian et al., 1995) and Simple LUmped Reservoir Parametric, SLURP (Kite, 1995), in which some processes, inputs and boundary conditions are lumped.

On the basis of a description of the process, a model can be deterministic, stochastic or mixed. If the variables in a mathematical model are regarded as random variables having probability distributions, the model is called a stochastic model. If all of the variables are considered free from random variation, then the model is deterministic. A mixture of deterministic and stochastic variables makes the model mixed or hybrid.

According to Diskin and Simon (1979), watershed models can be classified based upon time intervals as: (1) continuous-time or event-based, (2) daily, (3) monthly, or (4) yearly models. The models can also be classified by spatial scale as small scale models (area $\leq$ 100 km^2), medium scale models (area between 100 and 1000 km^2), and large scale models (area >1000 km^2) (Singh, 1995). This classification is arbitrary, although it is related to the concept of homogeneity and the validity of averaging of hydrological processes over a particular area. According to the method of solution of the governing equations, a model can be a numerical model, an analog model, or an analytical model.

A watershed model can be constructed using programming code or modeling environments (Wurbs, 1994). The programme coded models are application files, written in computer languages (e.g., VC++, Basic), in which no further addition or subtraction of routines is possible without getting access to the source code of the model. The structure of these

models is complex and needs a high level of expertise for any modification. HSPF, SWAT, and SHE are key examples of such models. Modeling environments are flexible tools for simulation in which the system under consideration is modeled using a conceptual description of the system. This type of modeling approach gives users and developers an advantage in that model structure can be easily modified according to varying needs and the geographic locations. Wurbs (1998) also suggested that models should be classified on the basis of usefulness to stakeholders and divided watershed models into seven categories: (1) runoff models, (2) river hydraulic models, (3) water quality models, (4) reservoir/river operation models, (5) groundwater models, (6) water distribution models and, (7) demand forecasting models.

2.2 Basic Components of Watershed Models

The above mentioned categories and classifications of watershed models helps to identify where a particular model fits in the field of hydrology. Principally, all watershed models tend to satisfy the water balance equation,

$$P = R + D + ET \pm \Delta S \qquad [2.1]$$

where P is precipitation; ΔS is soil moisture storage change; I and D are infiltration and deep percolation; and ET is evapotranspiration. All models compute and uphold the basic law of mass conservation. Accordingly, an ideal watershed model should address all of the processes mentioned in equation 2.1. Hence, the basic components of a process-based watershed runoff model include: (1) precipitation, (2) infiltration and percolation, (3) evapotranspiration, and (4) runoff. The following discussion gives a brief overview of how the various different components of watershed (rainfall-runoff) models may be represented.

2.2.1 Precipitation Component

The precipitation component serves as the driving force in a watershed model. Outputs from the model are largely dependent on the input accuracy of this component (Osborn and Lane, 1982). Precipitation input to the model, in the form of rain or snow, can be on an hourly, daily or monthly time scale. The precipitation component is also required for quantifying snow dynamics. The role of a snow component could be of special importance in models that are explicitly used in cold regions where the snowpack defines the subsurface and surface hydrology (Faria et al., 2000). For the hydrologic modeling of watersheds, the water content in the snowpack is more important than the depth and other properties of the pack (Osborn and Lane, 1982). Melt from the snowpack is usually modeled using energy balance or temperature index methods (Shook and Gray, 1997). The energy budget for the snowpack is given as

$$Q_m = Q_n + Q_h + Q_e + Q_g + Q_a - \Delta U \qquad [2.2]$$

where Q_m is the amount of energy available for melt (W/m^2/day); Q_n is the net radiation at the surface due to the exchange of radiation (W/m^2/day); Q_h is the sensible energy due to the turbulent flux of energy exchanged at the surface in response to the difference in temperature between the surface and the overlying air (W/m^2/day); Q_e is the latent energy representing

evaporation (W/m^2/day); Q_g is the ground heat flux (W/m^2/day); Q_a is advective energy derived from external sources (W/m^2/day); ΔU is the change of internal energy (Shook and Gray, 1997).

Melt rate is usually calculated using empirical relationships such as:

$$M = a Q_m \qquad [2.3]$$

where M is the melt rate (mm/day), and a is a coefficient derived from the calibration process (Maidment, 1993). Although the above-mentioned method gives a physical basis for calculating the melt rate of a snowpack, the method is data intensive. Moreover, the accurate measurement of all of the necessary parameters for quantifying snowmelt is not feasible at all places (Maidment, 1993). Temperature index methods give a reasonably accurate means for calculating the melt rate from a snowpack. The daily snowmelt can be represented mathematically as:

$$M = D_f (T_i - T_b) \qquad [2.4]$$

where M is daily melt rate (mm/day), T_i is the index air temperature (^{0}C), T_B is the base melt temperature (^{0}C), and D_f is the degree-day melt factor (Anderson, 1976). Anderson (1968), McKay and Thompson (1968) and Haupt (1967) have used the temperature-based degree day methods for the calculation of snowmelt.

2.2.2 Infiltration Component

Infiltration can be defined as the downward movement of water into the soil. Infiltration constitutes the major source of water for sustaining the growth of vegetation, and it helps to sustain the ground water supply to wells, springs, and streams. The rate of infiltration is influenced by the physical characteristics of the soil, soil cover (i.e., plants), water content of the soil, soil temperature, and rainfall intensity or rate of snowmelt. The infiltration module in watershed models is one of the most important and complex components, which simulates the infiltration rate and soil water dynamics. This module may use relatively simple empirical infiltration equations or it may require solving one to two-dimensional flow equations. This section addresses how the infiltration is simulated in watershed models.

2.2.2.1 Empirical infiltration equations

Empirical infiltration equations are the result of curve fitting exercises of observed infiltration rate with time-dependent functions or water storage characteristics of the soil. Some of the important empirical equations for infiltration are given in Table 2.1. Kostiakov (1932) proposed a simple infiltration equation based on curve fitting from field data (Eq. 2.5). The equation predicts an infiltration rate approaching zero at long times. Israelson and Hansen (1967) modified Kostiakov`s equation by adding a constant in the equation that represents the final infiltration rate, which is reached once the soil gets saturated after the

prolonged infiltration of water into the soil (Eq. 2.6). Horton (1940) proposed a three-parameter equation (Eq. 2.7) using an exponential function. The equation takes into account of the infiltration happening during ponding stage; however, the parameters in the equation need to be determined from experimental data.

Table 2.1: Empirical Equations for Infiltration Estimation.

Author	Equation (s)	Eq. No.
Kostiakov (1932)	$f = k.t^{-\lambda}$	2.5
Israelson and Hansen (1967)	$f = f_0 + k.t^{\lambda}$	2.6
Horton (1940)	$f = f_0 + (f_i - f_0)exp^{-Bt}$	2.7
Holtan (1961)	$f = f_0 + d_2 D^h (S - F)^h$	2.8
Huggins and Monke (1966)	$f = f_0 + d_3 D^h \left(\frac{S - F}{S_C} \right)^h$	2.9
Smith (1972)	$f = f_0 + d_1(t - t_0)^h$	2.10

where

f	= *infiltration rate of the soil,*	t	= *time, sec*
k, λ	= *empirical parameters obtained from infiltration tests on a given soil,*	f_0	= *some value representing the equilibrium infiltration rate as t becomes large,*
B	= *empirical parameter,*	f_i	= *initial infiltration rate, mm/day*
t_0	= *initial time, sec*	S	= *initial available storage in a given depth of the soil (%),*
d_1 & d_2	= *constants,*	F	= *total infiltration volume (%),*
d_3 & h	= *constants determined as the intercept and slope, respectively of log-log plot of $(f-f_0)$ vs $(S-F)$,*	S_C	= *storage capacity (%).*
D	= *surface layer depth (control depth)*		

Holtan (1961) suggested an infiltration equation (Eq. 2.8), which is independent of time, where infiltration is considered to be a function of the available water storage in a given depth of soil. Huggins and Monke (1966) modified Holtan's equation to account for the storage capacity of the soil, which is equal to the product of total porosity and control depth (Eq. 2.9). Holtan's equation is independent of time and hence is easy to apply to all types of soil. The drawback in Holtan's model was the control depth, which is treated as a fitted parameter that is dependent on the surface soil conditions. It is difficult to determine the control depth on which to base the initial available storage. According to Smith (1976), the infiltration curves for all soils are physically more related to moisture gradients and hydraulic conductivity than to the soil porosity; hence, Holtan's model cannot be expected to adequately describe the infiltration process.

Smith (1972) conducted laboratory experiments and developed a time-dependent model (Eq. 2.10), which requires determination of four parameters. The parameter accounting for the equilibrium infiltration rate (f_0) is set equal to the saturated hydraulic conductivity, while the rest of the parameters are unique to the soil type, initial moisture content, and rainfall rate.

2.2.2.2 Physically-based infiltration models

Physically-based infiltration models have been developed by solving the governing equations for basic soil water movement. Several examples are shown in Table 2.2. The driving principle of these equations is Darcy's law and the mass conservation equation (Smith, 1981). Green and Ampt (1911) developed the approximate physical model represented by Eq 2.11 which is based on the above-mentioned two principles. The Green-Ampt model is based on the following assumptions: (1) there is a defined wetting front, (2) the soil surface is ponded with negligible depth, and (3) the wetting front can be seen as the plane separating a uniformly wetted infiltrated zone from a totally uninfiltrated zone. Mein and Larson (1973) improved the Green-Ampt model for steady state rainfall conditions to determine cumulative infiltration at the time of surface ponding (Eq. 2.12). The Mein and Larson model assumes that rainfall occurs at a uniform rate, saturates the surface and then produces runoff. Mein and Larson (1973) modified the Green-Ampt model and made it applicable to post-surface ponding conditions while accounting for the volume of water infiltrated before the ponding began (Eq. 2.12-2.14). Skaggs (1982) suggested that the Green-Ampt model provides good approximation of infiltration for unsteady rainfall provided that the rainfall distribution does not include relatively long periods of low intensity or zero rainfall, which may result in redistribution of soil moisture.

Philip (1957) made assumptions of the flow velocity and the water content profiles and developed a model for homogeneous soil and homogeneous initial moisture content. Equation (2.15) is based upon two soil parameters, the sorptivity (S), which defines the movement of water to the soil at a particular time, and transmissivity (A), which is the parameter responsible for water movement into the soil under near-saturated conditions. The main disadvantage of Philip's equation is its inaccuracy for long duration rainfall events as there is no parameter in the equation that can account for the equilibrium infiltration rate.

Table 2.2: Physically Based Equations for Infiltration Estimation.

Author	Equation (s)	Eq. No.
Green and Ampt (1911)	$f = K_s(1 + Mh / F_p)$	2.11
Mein and Larson (1973)	$f = I$; $t < t_p$	2.12
	$f = K_s(1 + M_{av} h / F_p)$; $t > t_p$	2.13
	$F_p = \frac{h.M_{av}}{\left(\frac{I}{K_s}\right) - 1}$; $t_p = \frac{F_p}{I}$; $M_{av} = \int \frac{h_i K(h)}{K_s}$;	
	$K_s(t - t_p + t'_p) = F_p - M_{av}.h \ln\left(1 + \frac{F_p}{M_{av}.h}\right)$	2.14
Philip (1957)	$f = S t^{0.5} + A$	2.15
	$S \alpha (\theta_i - \theta_s)$	2.16
Richards (1931)	$C(h)\frac{\partial h}{\partial t} - \nabla.K(h)\nabla h - \frac{\partial K}{\partial Z} = 0$	2.17
	$\frac{\partial \theta}{\partial t} - \nabla.D(\theta)\nabla \theta - \frac{\partial K}{\partial Z} = 0$	2.18

where

θ = *volumetric moisture content, cc/cc*

h = *pressure head, m*

K = *hydraulic conductivity of soil, m/sec,*

Z = *vertical downward distance from soil surface, +ve downward, m,*

K_s = *saturated hydraulic conductivity of soil, m/sec,*

M_{av} = *average head at wetting front*

C = *soil water capacity, 1/m*

D = *soil water diffusivity, m^2/sec*

S = *sorptivity, cm/sec,*

A = *transmissivity, cm/sec,*

θ_i = *initial moisture content, cc/cc,*

θ_s = *volumetric saturated moisture content, cc/cc,*

M = *(θ_s-θ_i) moisture deficit*

T = *time, sec*

Ks = *saturated hydraulic conductivity, m/sec,*

t_p = *time to ponding, sec,*

F_p = *cumulative infiltration at time of ponding,m,*

I = *rainfall intensity,mm/day,*

t'_p = *equivalent time to infiltrate volume Fp under ponded surface condition, sec,*

f = *infiltration rate, mm/day*

h_i = *pressure head at initial moisture*

$K(h)$ = *hydraulic conductivity as*

Richards (1931) derived an equation of flow in unsaturated soil in two forms: (1) based on moisture content (θ), and (2) based on pressure head (h) (Eqs. 2.17 and 2.18). The moisture-based equation contains diffusivity, D(θ), and hydraulic conductivity, K(θ), whereas the pressure head based equation contains soil water capacity, C(h), and hydraulic conductivity, K(h).The relationship between the above-mentioned parameters can be related through the following equation:

$$D(h \text{ or } \theta) = \frac{K(h \text{ or } \theta)}{C(h \text{ or } \theta)} \qquad [2.19]$$

where *D* has units of length squared per unit time, *K* has units of length per unit time, and *C* has units of inverse length. The three parameters vary non-linearly and markedly with water content and pressure head. Skaggs (1982) concluded that the moisture-based models do not perform well for saturated conditions since the diffusivity term tends to infinity. The pressure-head based equation performs well in both saturated and unsaturated conditions but generally yields poor results, characterized by large mass balance errors and erroneous estimations of infiltration depth. The prime source of difficulty in solving the Richards equations is their hyperbolic nature and the strong non-linearity of the parameters subjected to boundary conditions pertinent to infiltration (Skaggs, 1982; van Dam and Feddes, 2000).

2.2.2.3 Unsaturated Soil Hydraulic Properties

The unsaturated soil hydraulic properties, namely soil moisture (θ) and hydraulic conductivity (K), are in general non-linear functions of the pressure head. The equations developed by various scientists for these parameters are presented in Table 2.3. The models presented in Table 2.3 are commonly known as Soil Water Characteristic Curves (SWCC), which describe a soil's ability to store and release water from the soil matrix. The power relationships between soil moisture content and pressure head, given by Brooks and Corey (1964) (Eq. 2.20), have been used to predict the soil water retention curve and unsaturated hydraulic conductivity. Campbell (1974) proposed a simpler model (Eq. 2.21) than that introduced by Brooks and Corey (1964), which eliminates the need to find the residual pore water pressure. Both equations have been widely used in the hydrologic literature. The above-mentioned equations have a limitation; both describe only a portion of the SWCC. The pressure head and soil moisture relationships for pressure heads less than the bubbling pressure or the pressure at which air is able to enter the soil matrix is not explicitly described by either of these two equations.

van Genuchten (1980) used the pore size distribution model of Mualem (1976) to obtain a better predictive model (Eq. 2.22) for computing the unsaturated hydraulic conductivity in terms of soil water retention parameters. The equation uses five independent parameters: θ_r, θ_s, α, n and K_s, which have been mentioned in Table 2.3. These parameters can be calculated using the equations given by Vereecken (1989) and Schaap and Leij (2000), which are based on the percentage of clay, silt, sand and organic matter present in the soil. The model

proposed by van Genuchten (1980) is widely used in many hydrologic models, essentially due to the ready availability of the five parameters from literature.

The literature suggests that there are numerous other infiltration equations and SWCC models available for application to hydrological models. However, at times, applications of the models are site specific and dependent on the availability of information for the various input parameters. According to Singh (1988), the main advantage of using the Green-Ampt model is that the parameters such as saturated hydraulic conductivity and suction pressures can be measured for a particular soil. Hence, it is widely used in hydrologic models for simulating soil moisture dynamics.

Table 2.3: Equations for Estimating Unsaturated Hydraulic Properties.

Author	Equation(s)	Eq. No.
Brooks and Corey (1964)	$\theta(h) = \theta_r + (\theta_s - \theta_r)\left(\frac{h_b}{h}\right)^{\lambda}$ $K(\theta) = K_s S_e^n;$ $S_e = \frac{\theta - \theta_r}{\theta_s - \theta_r};$ $\quad n = 3 + \frac{2}{\lambda}$	2.20
Campbell (1974)	$\theta(h) = \theta_s \cdot \left(\frac{h_b}{h}\right)^{\lambda}$ $K(\theta) = K_s \cdot \left(\frac{\theta(h)}{\theta_s}\right)^{n}$ $n = 3 + 2b;$	2.21
van Genuchten (1980)	$\theta(h) = \theta_r + \frac{\theta s - \theta r}{\left[1 + \lvert\alpha h\rvert^n\right]^m}$ $K(\theta) = K_s S_e^{0.5}\left[1 - (1 - S_e^{1/m})^m\right]^2$ $m = \frac{\lambda}{1+\lambda};$ $\quad n = \lambda + 1;$ $\quad \alpha = h_b^{-1}$ $S_e = \frac{\theta - \theta_r}{\theta_s - \theta_r};$	2.22

where,

θ_s = *saturated water content, cc/cc,*	θ_r =*volumetric residual water content, cc/cc,*
$\theta(h)$ =*soil moisture as a function of pressure head*	$K(\theta)$ =*hydraulic conductivity as a function of moisture content*
θ =*volumetric moisture contect cc/cc*	K_s = *sat. hydraulic conductivity of soil, m/sec,*
α = *inverse of air entry value, 1/m,*	h = *hydraulic pressure head, m,*
h_b =*air entry capillary head, m*	b,n,m,α =*empirical parameters*
λ =*pore size index*	

2.2.2.4 Infiltration through frozen soils

Early records of snowmelt infiltration are found in the Russian literature. These studies were carried out in the field without knowing the exact phenomena occurring during the snowmelt infiltration. Kuznik and Belzmenov (1964) conducted studies from 1951 to 1956 on clay loams in Russia using crude techniques of locating ice crystals in soil using a hand lens. They drew infiltration curves for the water intake into frozen soils from the collected data, concluding that the shape of the curve can be determined by the nature of the soil moisture distribution and the air temperature.

According to Illangasekare et al., (1990), three major processes must be considered for modeling snowmelt infiltration into frozen soil; (1) water flow through a porous medium under partially saturated conditions, (2) refreezing of meltwater in snow, and (3) heat conduction and convection Granger et al. (1984) reported on the interaction between snow water equivalent (SWE), in mm; relative saturation (S) at the time of melt (volume of water per unit volume of voids; and snowmelt infiltration (INF), in mm, in the form of an infiltration model expressed as

$$INF = 5(1-S)SWE^{0.584} \qquad [2.23]$$

Stadler et al. (1997) and Stahli et al. (1999) proposed that liquid water infiltration into frozen soils can occur in two ways: (1) by adsorption onto the particles occupying the smallest pores (low-flow domain), and (2) by downward movement into the pore spaces, which are filled with air at the start of the infiltration process (high-flow domain). The flow within the low-flow domain is based on Darcy's law assuming the same hydraulic conductivity, K_w, as in the case of the unfrozen conditions. Since K_w decreases by several orders of magnitude when the temperature decreases below the freezing point, this water phase is nearly immobile at only a few degrees below zero. Flow in the high-flow domain is assumed to follow gravitational flow based on hydraulic conductivity of the soil. However, it is appropriate to conclude that there is incomplete understanding of snowmelt infiltration into frozen soil.

2.2.3 Evapotranspiration Component

Evapotranspiration (ET) plays a major role in defining the water balance in arid and semi-arid regions. ET represents two components of the water cycle: (1) evaporation, which is the loss of water from the soil surface and waterbodies, and (2) transpiration, which is the consumptive use of water by plants. ET flux moves large quantities of water from the soil back to the atmosphere. The importance of ET in hydrology has been discussed by Parmele (1972), Saxton (1982), and Burt et al. (2005). Many methods of estimating actual ET for hydrologic models often requires estimation of potential evapotranspiration (PET).

2.2.3.1 Potential evapotranspiration

Potential evapotranspiration (PET) is the rate at which ET occurs from the large area completely and uniformly covered with growing vegetation which has access to an unlimited supply of soil water (Dingman, 2002). Burt et al. (2005) suggested that ET can be estimated using four approaches: (1) water balance method, where ET is calculated as a residual from the water balance equation (Eq 2.1), (2) energy balance method, where ET is estimated by measurement of surface fluxes, (3) coupled water and energy balance methods, and (4) empirical approaches. PET is usually estimated by using pan evaporation or climatological data.

The literature suggests that estimation of PET from pan evaporation data is the oldest and most common estimation method. Standard evaporation pans (US Weather Bureau Class A pan) have been used to determine evaporation. Pan evaporation rates are higher than actual lake evaporation and must be adjusted by a coefficient to account for radiation and heat exchange effects. The adjustment coefficient also represents the effect of many influencing factors such as fetch, surroundings, relative humidity and wind speed (Hanson and Rauzi, 1977). Christiensen (1968) developed an empirical equation to calculate pan evaporation from solar radiation data.

According to Saxton (1982), there is a correlation between the climatic variables affecting PET and the air temperature. Table 2.4 mentions some of the commonly used PET models. Blaney and Criddle (1950) developed a temperature-based formula (Eq. 2.24) to estimate PET, since air temperature was the only readily measurable climatic variable. The underlying assumption in the Blaney and Criddle model is that the heating of the air and evaporation share the heat budget in a fixed proportion (Singh, 1988). The multiplication of an empirical monthly consumptive use coefficient and PET yields a monthly ET value. The consumptive use coefficient depends upon the type of the crop and the geographic location of the region. According to Doorenbos and Pruitt (1975), the Blaney and Criddle formula is not suitable for use in: (1) equatorial regions where the temperature does not vary much, but where other weather parameters change; (2) small islands where the air temperature is affected by the surrounding sea temperature, hence shows little response to the seasonal change in radiation; (3) high altitude locations where the daytime radiation is practically independent of the night temperature; and (4) locations having a climate with a high variability in sunshine hours during changing seasons. Pelton et al. (1960) compared several energy-based methods and

temperature-based methods and concluded that energy-based methods are more reliable and preferred if suitable data are available.

Table 2.4: Equations for Estimating Potential ET Using Climatological Data.

Author	Equation(s)	Eq. No.
Blaney and Criddle (1950)	$UE = k_e p \frac{45.7 t_{sa} + 813}{100}$	2.24
Thornthwaite (1948)	$UE = 1.6\left(\frac{10 t_{sa}}{H_I}\right)^{ay}$	2.25
Penman (1956)	$PET = \frac{(\Delta/\gamma)R_n + \frac{(K_p L_E . d_a . U_a)}{\left[ln\left(\frac{Z_a - d_w}{Z_o}\right)\right]^2}}{1 + (\Delta/\gamma)}$ $K_p = \frac{\rho k^2 \varepsilon}{a_p}$	2.26a
Penman Monteith in Dingman (2002)	$PET = \frac{(\Delta)R_n + \rho_a c_a C_{at} e_a^* (1 - R_H)}{\rho_w L_E [\Delta + \gamma(1 + \frac{C_{at}}{C_{can}})}$	2.26b
Modified Penman Dooronbos and Pruitt (1975)	$PET = C[WR_n + (1\text{-}W)f(u)(e_a\text{-}e_d)]$	2.27

where

UE = estimated monthly evapotranspiration, mm,

k_e = an empirical consumptive use coefficient,

PET = potential evapotranspiration, cm/day,

a_y = an empirical exponent,

Δ = slope of psychrometric saturation line, mbars $^0C^{-1}$,

R_n = net radiation flux, cal cm^{-2} day^{-1}

K = von karman constant

d_a = saturation vapour pressure deficit of air, mbars,

Z_a = anemometer height above the soil,

p = mean monthly % of annual daytime hrs of yr,

t_{sa} = mean monthly air temperature,^0C,

H_I =annual or seasonal heat index,

γ = psychometric constant, m bars/^{0} C,

L_E = latent heat of vaporization, cal gm^{-1},

U_a = wind speed at elevation Za, m/day,

d_w = wind profile displacement height,

cm,	*cm,*
Z_o = *wind profile roughness height, cm,*	ρ = *air density, g* cm^{-3},
a_p = *ambient air pressur, mbars*	C = *an adjustment factor to compensate for the effect of day and night weather conditions.*
W = *temperature and elevation related weighing factor the effect of radiation.*	(e_a-e_d) = *pressure difference between the saturated vapor pressure at the mean air temperature and the mean actual vapor pressure of the air, mbars.*
$f(u)$ = *wind related function.*	ε = *water/air molecular ratio*
S = *sensible heat flux, cal* gm^{-1}	t_a = *mean daily air temperature,* ^0C
C_{at} =*atmospheric conductance*	e^* = *saturated vapor pressure, mbars*
ρ_w = *density of water,* kg/m^3	C_{can} = *canopy conductance*
c_a = *heat capacity of air, MJ/kg/*^0C	

Thornthwaite (1948) suggested that an exponential relationship exists between mean monthly temperature and mean monthly consumptive use (Eq. 2.25). Some of the limitations of the formula are: (1) temperature is not a good indication of the availability of energy for evapotranspiration; (2) the formula does not take into account the wind effect, which might be an important factor in some areas; and (3) it does not consider the effect of warm and cool air on the temperature of a location (Chang, 1968).

PET can also be estimated using mass transfer methods (aerodynamic methods), which involve determination of the transport of water vapour from a water surface to the atmosphere. Temperature, humidity and wind velocity vary approximately linearly with the logarithm of height or elevation. The methods involve evaluation of the turbulent eddies that form in the air above a certain height (usually the height of vegetation). The eddy diffusion is related to the wind velocity. Saxton (1982) indicated that the aerodynamic methods involve measurements of temperature and vapour pressure at two different heights above the crop canopy. Further, he stated that the measurements are quite sensitive and require precise instrumentation for measurement purposes.

Penman (1956) developed a PET model (Eq. 2.26a) based on a combination of the energy budget and aerodynamic methods. The model is known as the Penman equation.. It uses four meteorological variables for the estimation of PET including net radiation, air temperature, air humidity and wind characteristics. Penman's equation is based on Dalton's laws of fusion and a transport function, and defines the relationship between the vertical energy balance and lateral wind speed. Saxton (1982) describes the basic steps in the derivation of the Penman equation which are as follows: (1) define the vertical energy budget; (2) apply the Dalton-type transport function to obtain the Bowen ratio; (3) apply Penman's psychrometric

simplification to eliminate the need for surface temperature; and (4) apply the vertical transport equation obtained from turbulent transport theory.

Dingman (2002) reported the modified form of Penman equation commonly referred to as Penman-Monteith equation (Eq. 2.26b), for estimating PET. The Penman-Moneith equation takes into account the canopy conductance, therefore can be used in vegetated surfaces (Dingman, 2002). Dooronbos and Pruitt (1975) modified Penman's equation to provide empirical adjustments for predicting PET (Eq. 2.27) based on a study conducted by the Food and Agricultural Organization (FAO) group using data from 10 sites with widely varying climates. The combined energy balance and aerodynamic equations, being based upon physical laws and rational relationships, provide more accurate results than empirical or temperature-based equations (Saxton, 1982). The Penman equation is the most widely used PET equation in the hydrological literature. It has gone through several revisions, but the principle on which it is based is still the same (Burt et al., 2005).

Remote sensing is now playing an important role in the estimation of PET in large-scale studies. Bastiaanssen et al. (1997) and Boegh et al. (2002) used data from satellite images to compute the actual and potential evapotranspiration. One consequence of the remote sensing method is that it needs to be updated frequently throughout the growing season, which is expensive both in terms of satellite images and in terms of processing time (Kite, 2000), hence its use is limited accordingly.

2.2.3.2 Actual evapotranspiration (AET) methods

PET methods are based on the assumption that water is freely available, and there is no moisture stress in the soil. PET methods may be successfully applied for estimating the water balance of lakes and other free surface water bodies. However, such methods generally require major calibration and validation in watersheds where soil moisture is the limiting factor for evapotranspiration (Saxton, 1982). Hence, many methods have been developed for estimating AET, which depends on the soil moisture regime, climatic factors and crop growth parameters. A variety of semi-empirical equations is reported in the literature and the key ones are mentioned in Table 2.5.

Saxton (1982) suggested that the vertical energy budget of a vegetated surface limits AET since the available soil moisture governs the vapour transport process. Bowen (1926) proposed that AET equations should use sensible heat and net radiation to estimate actual evapotranspiration (Eq 2.28). The ratio of sensible heat to latent heat is commonly referred to as the Bowen ratio (β), which can be calculated from gradients of air temperature and vapor pressure above the evaporating surface (Saxton, 1982). Haan et al. (1982) reported that Bair and Robertson model estimated AET by dividing the total available soil moisture in the soil profile into several zones of different available water capacities. They assumed that water is withdrawn simultaneously from the various depths of the crop root zone in relation to the PET rate and the available soil moisture in the root zone (Eq. 2.29). However, their model does not take into account the effect of crop growth stage and various environmental factors, and it needs calibration. Saxton (1982) also expressed that the need for calibration of this model poses difficulty in its application for

Table 2.5: Equations for Estimating Actual Evapotranspiration.

Author	Equation (s)	Eq. No.
Bowen method in Dingman 2002	$\beta = \frac{S}{LE}$	2.28
	$AET = \frac{R_n}{1-\beta}$	
Baier and Robertson in Haan et al, (1982)	$AET = \sum k_j Z_j PET\, e^{-w(PET-PE)} \frac{S_i}{S_j}$	2.29
Holtan et al. (1975)	$AET = G_I . K_r . E_p \left(\frac{S_T - A_{ST}}{S_T} \right)^x$	2.30
Haan (1972)	$AET = PET\left(\frac{A_{ST}}{S_T} \right)$	2.31
Ritchie (1972)	$E_{so} = PET = R_n \exp^{(-0.398LAI)} \left(\frac{\Delta}{\Delta + \gamma} \right)$	2.32
	$E_s = \alpha t^{0.5}$	2.33
	$E_{pt} = PET(-0.21 + 0.70 L_{AI}{}^{0.5})$ $\quad 0.1 < L_{AI} < 2.7$	2.34
	$E_{pt} = PET$ $\quad L_{AI} > 2.7$	2.35
Kristensen and Jensen (1975)	$\left(\frac{AE}{EP} \right) = C + (1-C) \left(\frac{A_{ST} - F_C + C_1}{C_1} \right)$	2.36
Granger (1989)	$\text{AET} = \frac{\Delta G R_n}{\Delta G + \gamma} + \frac{\gamma R_n f(u)}{\Delta G + \gamma}$	2.37

where

AET = *actual evapotranspiration, mm/day,*

β = *Bowen ratio*

k_j = *coefficient for soil and plant characteristics in the* j^{th} *soil layer,*

S_i = *available soil moisture on* i^{th} *day, mm,*

PET = *potential evapotranspiration, mm* day^{-1},

S_j = *capacity of available moisture in* j^{th} *layer, mm,*

PE = *average PET for month or season, mm/day,*

W = *factor for varying PET rates.*

E_s = *Soil evaporation, mm/day*

E_p = *Plant transpiration*

Δ = *slope of saturation vapor pressure curve,*

E_{so} = *potential soil evaporation, mm/day*

L_{AI} = *leaf area index,*

G_I = *growth index of crop, %,*

K_r = *ratio of ET to pan evaporation for full*

canopy,

S_T = total soil porosity, %, A_{ST} = available soil porosity, %,

x = an exponent estimated to be 0.10,

Z_j = factor for different types of soil dryness curves, Rn = Net radiation, cal/cm^2/day

T = time, days, α = coefficient to be determined experimentally,

γ = psychrometric constant, (mbars/^{0} C), C ,C_1 = calibration constants

EP = Pan evaporation, mm/day, F_C = field capacity of soil, mm

ΔG = relative evaporation

---

those who do not have expertise in handling the equation. Saxton proposed a simple model relating the soil moisture index to a coefficient. However, there is no use of Saxton's equation reported in the literature.

Holtan et al. (1975) used a parameter called the crop growth index that varies with the stage of the crop growth (Eq. 2.30). In their work, the soil moisture was related to pan evaporation measurements. This model estimates AET based on soil moisture stress, which means that AET will be reduced as moisture is depleted from the soil.

Haan (1972) simulated the daily AET in the estimation of monthly streamflow from daily precipitation (Eq. 2.31) by dividing the moisture holding capacity of the soil into two parts: (1) free soil water that is available without any stress, and (2) limited soil water, which is dependent on soil properties such as porosity and moisture index. The model has been developed assuming that the moisture holding and transmitting characteristics of the soil along with the amount of rainfall are the factors governing AET. The model does not consider the effect of climatic and crop factors on the ET process.

A comprehensive work on the estimation of AET is reported by Ritchie (1972) who gave a set of equations (Eqs. 2.32 to 2.35) to estimate AET, beginning with the Penman equation to define PET and then separately calculating the soil evaporation and plant transpiration. Ritchie's model for estimating AET followed the same two-step procedure laid out by Haan (1972). When there is free availability of water, the potential soil evaporation below the plant canopy has been computed by ignoring the aerodynamic term in the Penman equation, and by approximating the net radiation flux using an exponential relationship taking the leaf area index into consideration (Eq 2.32). Under limited water availability, soil evaporation and plant transpiration are calculated using equations 2.34 and 2.34, respectively.
Kristensen and Jensen (1975) developed a model based on available soil moisture (2.36). Their model was applied to fallow and cropped areas. Coefficients were estimated using calibration procedures and were based on the leaf area index and the fraction of the incoming radiation that reaches the soil surface. They also suggested that soil moisture based methods for estimating AET can be used in lumped models because such equations are easily calibrated. Granger (1989) used the concept of relative evaporation and modified the Penman

equation for non-saturated surfaces under varying crop conditions (Eq 2.37) to estimate AET. Granger suggested that, with the inclusion of a relative evaporation term, which is the ratio of actual to potential evapotranspiration, the combination equation becomes sensitive to vegetation.

The literature presented in this chapter suggests that AET is always computed using available soil moisture. Plants cannot take water at a constant rate. The uptake of water by plants for their consumptive use depends on the stage of plant growth and moisture availability. Only the freely available water which is present between the field capacity of a soil and the permanent wilting point is available for consumptive use by plants (Dingman, 2002). Hence, the role of soil moisture cannot be neglected while calculating AET. Moreover, Singh (1988) emphasizes on the fact that soil moisture remains an integral part in calculation of AET. Saxton et al. (1974) suggested that, for a small watershed, there should be a method that accounts for climatic, crop and soil variables under suitable ranges of soil moisture regime.

2.2.4 Runoff Component

According to Horton (1933), runoff is generated when the rainfall rate exceeds the infiltration rate. Overland flow or surface runoff may include thin sheet flow over a plane surface, flow over irregular surfaces or flow in small channels. Overland flow occurs on the sloping land surfaces under two conditions (Dingman, 2002); (1) either the soil surface is saturated from above (Hortonian overland flow) or (2) the soil surface is saturated from below (saturation overland flow). Hortonian overland flow occurs when the water input rate to the soil surface exceeds the saturated hydraulic conductivity of the surface layer. This type of flow plays an important role in semi-arid to arid region; areas where soil frost has reduced the surface conductivity, and permeable areas. Saturation overland flow is the overland flow due to saturation from below and it consists of direct subsurface water input to the saturated areas. Such type of flow primarily occurs in humid climates and more specifically where (1) subsurface flow lines converge in slope concavities and water arrives faster than it can be transmitted downslope as subsurface flow, (2) concave slope breaks, where the hydraulic gradient of subsurface flow from upslope is greater than that of downslope transmission, (3) soil layers conducting subsurface flow are locally thin, and (4) hydraulic conductivity decreases abruptly or gradually with depth and percolating water accumulates above the low-conductivity layers (Dingman, 2002).

The mathematical routing of unsteady flow in open channels and over the land surface is described by the hydrodynamic equations of continuity and momentum known as the St. Venant equations (Eqs. 2.38- 2.39) (Huggins, 1982), given as

$$\frac{\partial Q}{\partial X} + \frac{\partial A}{\partial t} = q \qquad [2.38]$$

$$\frac{\partial Q}{\partial t} + \frac{\partial (Q/A)^2}{\partial X} + gA\frac{\partial h}{\partial X} = gA(S_o - S_f) \qquad [2.39]$$

where, Q is discharge/unit width (m^2 sec^{-1}), q is lateral inflow rate of water/unit length/unit width of flow plane ($m.sec^{-1}$), A is the area of flow/unit width of the overland flow plane or channel (m), X is the distance in the direction of flow (m), t is time (sec), S_o is bed slope of

the flow plane or channel (m/m), S_f is the friction slope of the flow plane or channel (m/m), g is the acceleration due to gravity (m.sec^{-2}), and h is the depth of flow (m). The first term on the left hand side of the equation (Eq. 2.39) is local inertia, the second term represents convective inertia and the third term pressure is called the differential term. The right hand side of the equation accounts for the bed and friction slope. Since the equations (Eq 2.38-2.39) are nonlinear, the solution to these equations is difficult and some simplifications are recommended for time efficacy (Huggins, 1982).

According to Huggins (1982), overland flow in a lumped model can be simulated using point equations for infiltration. The excess water after satisfying the soil moisture dynamics can be routed as overland flow. In lumped models, overland flow volume is generally dependent on the accuracy and boundary conditions of the infiltration equations. Most lumped models are based on storage concepts. Water in each storage zone is dynamically linked with other storage zones using various empirical or physical equations. In such models, overland flow is generally simulated using threshold principle. For instance, when the soil layer gets saturated then the excess water should be routed as overland flow (Sugawara, 1995; Ye et al., 1997).

Various classifications of watershed model have been mentioned in the previous sections. Watershed models make use of one of the following two approaches to compute runoff from the watershed: (1) transfer functions, and (2) phenomenological relationships. Transfer functions rely on the availability of historical data to develop an empirical equation (Huggins, 1982). The method has limited advantages, which include elimination of the need for modeling all hydrological processes in the watershed. However, this approach requires a long record of rainfall-runoff data, and the approach does not facilitate the assessment of impacts of major land use changes (Huggins, 1982).

The models using phenomenological functions enumerate individual components of the physical hydrologic process, which are known to occur in the watershed. Such an approach relies on observed data for calibration of the parameters that govern the movement of water between the various physical components. In these types of models, there may be a reservoir for groundwater storage and a reservoir for soil moisture storage, with the remaining water being routed as overland flow. The phenomenological relationships yield a range of simple to very complex watershed models. Simple models may make use of the SCS model (explained later), while on the other hand, complex watershed models may require solution of the St Venant equations which utilize the conservation of mass and momentum equations to simulate overland flow. The parameters used in phenomenological models are measurable field quantities or can be derived from surface features such as the soil, vegetation, and topographic conditions, or they can be determined during calibration of the model.

Dingman (2002) described some of the commonly used watershed models for runoff simulation. The Rational method is used to predict the design runoff rate, which is expressed as

$$Q = u_r CIA \qquad [2.40]$$

where, Q is the discharge (m^3/s), u_r is the unit conversion factor (0.278), C is the runoff coefficient, I is the rainfall intensity (mm/hr) and A is the watershed area (km^2). The equation was derived from a conceptual model of travel times in basins having negligible surface storage and is widely used for urban and agricultural watersheds. The assumptions behind this model are that the rainfall occurs at a uniform intensity for a duration at least equal to the time of concentration of the watershed. However, in reality, it is difficult to satisfy such assumptions in a watershed.

The Soil Conservation Service (SCS) model, reported in Schwab et al. (2002), is another method for computing the runoff volume from a watershed. The model has been widely applied in the United States due to its simplicity, and is given as:

$$Q = \frac{(P - I_a)^2}{P - I_a + S} \qquad [2.41]$$

where, Q is the runoff depth from the watershed, S is the maximum potential difference between rainfall and runoff, I_a is the initial abstraction corresponding to the amount of storage that must be satisfied before overland flow can occur, and P is the rainfall depth. In order to take account of the vegetation, land use and soil conservation practices, the factor S is computed as:

$$S = \frac{25400}{N} - 254 \qquad [2.42]$$

where, N is called the curve number. Nomograms are available for estimating curve numbers based on the above-noted factors. The literature reveals that there are numerous other models available for simulating the runoff process.

2.3 Watershed Models

The hydrological processes mentioned in section 2.2 are integrated to form a watershed model. Stanford Watershed Model (Crawford and Linsley, 1966) was the first attempt to assemble all of the above-mentioned processes into one common platform (Singh, 1995). Beven (2000), Singh (1995), and Wurbs (1998) reviewed different watershed models and concluded that all of the models are based on fundamentally the same principles of water balance. Model structure, computational time and the perspective with which the models simulate the different processes are the factor that make one model different from another. Table 2.6 summarizes a number of commonly-used watershed models.

There are many other watershed models cited in the literature for rainfall-runoff modeling. However, the reason for the development of all such models can be attributed to the fact that each model differs in its internal structure for handling the various hydrological processes. The literature also suggests that the watershed models are developed specific to both site and problem, and are then generalized over the entire watershed (Woolhiser and Brakensiek, 1982). However, they suggested that watershed models are developed or chosen for the particular problem based on the following four features: (1) accuracy of the prediction, (2)

simplicity of the model, (3) consistency of parameter estimates, and (4) sensitivity of the results to changes in the parameter values. Woolhiser and Brakensiek concluded that the choice of model is usually made on the basis of the time-frame available for development, input data resources, and various other factors such as the experience of the modeller.

Table 2.6 Common Watershed Models and Their Characteristics

Model	Location of application	Time Scale	Characteristics
Hydrologic Engineering Centre-Hydrologic Modeling System (HEC-HMS)	USA	Event based	Physically based, semi-distributed
National Weather Service (NWS)	USA	Continuous	Process based, lumped parameter
Hydrologic Simulation Package-Fortran (HSPF)	USA	Continuous	Physically based, semi-distributed
University of British Columbia Model (UBC)	Canada	Continuous	Process based, lumped parameter
Waterloo Flood System (WATFLOOD)	Canada	Continuous	Process based, semi-distributed
Simple Lumped Reservoir Parametric (SLURP)	Canada	Continuous	Process based, semi-distributed
Runoff Routing Model (ROBR)	Australia	Event based	Lumped
Watershed Bounded Network Model (WBN)	Australia	Event based	Geomorphology based, lumped
Physically Based Runoff Production Model (TOPMODEL)	Europe	Continuous	Physically based, distributed
Systeme Hydrologique European (SHE)	Europe	Continuous	Physically based, distributed
Xinanjiang Model	China	Continuous	Lumped, process based

Although process-based watershed models are able to capture some of the critical processes and realistic mechanisms involved in the watershed sub-systems, the major disadvantage of these models is that they require large data sets, which are sometimes not available at certain locations. Moreover, they may not be applicable to locations except for those where they were developed, and their development is tedious and can be standardized only after years of application. The hydrologic literature in the late 1990s reveals another type of watershed model called the data-driven model. Data-driven models, also called black box models, estimate the unknown dependency between a system's inputs and its outputs simply based on the available data. These models work by finding complex correlations between various combinations of inputs and outputs. Linear regression models like ARMA or non-linear regression models have been under investigation to determine the nature of correlations for complex processes like rainfall-runoff. Artificial Neural Networks (ANNs) are an example of data-driven models, which have been widely used in hydrological prediction and water resource management for the last decade. The ANN technique has been used for rainfall-

runoff modeling by many authors such as Licznar and Nearing (2003), Rajurkar et al. (2004), Elshorbagy et al. (2000), and others.

2.4 Calibration of Watershed Models

The development of a watershed model follows a sequence of calibration and validation processes. Calibration is defined as the process of improving algorithms, determining parameter values and sequencing hydrological processes so that model represents the real world phenomena (Viessman and Lewis, 2003). Validation can be defined as verification of the parameters obtained through calibration. It is evident from Section 2.2 that some physically-based or empirical equations representing various hydrological processes require tuning of the input parameters or constants so as to provide reliable estimates of the desired outputs. Nash and Sutcliffe (1970) concluded that, although watershed models uphold the requirement for mass balance, the mechanisms describing the relationships among the watershed processes are defined by mathematical transfer functions. Thus, physically-based equations, which describe the system, demonstrate a hidden empirical behavior. Sorooshian (1983) discussed the importance of calibration in watershed modeling and summarized that the purpose of calibration is to get a realistic and unique parameter value set that should help in understanding the watershed processes, and to obtain parameter values so that the observed watershed response (streamflow values) matches the simulated results.

Sorooshian and Gupta (1995) classified model parameters into two groups: (1) physical parameters, and (2) process parameters. Physical parameters are defined as those parameters, which can be measured in-situ in the watershed (e.g., area of the watershed, topographic slope, porosity of the soil). Process parameters symbolize non-measurable properties of the watershed (e.g., soil moisture storage depth, coefficients relating the rate of water extraction from the soil).

Calibration of watershed models is generally done by comparing and analyzing observed and simulated streamflow data (Singh, 1988; Ambroise et al., 1995). Ye et al. (1997) observed that lumped models use different storages for simulating the water balance. Movement of water from one storage to another is usually defined by threshold principles, such as the maximum amount of water that the soil can store. Such models are difficult to calibrate using streamflow data time series alone because the exceedence threshold may not occur for certain conditions, such as soils with high porosity and dry climatic conditions. In such conditions, the model parameters obtained using streamflow data do not necessarily represent the true conditions of the internal watershed processes. Ye et al. (1997) reported that many parameter sets can produce identical streamflow even though the interactions of the internal processes may vary. The hydrologic literature reports a few instances where calibration of watershed models has been done using multiple observed variables (Wooldridge et al., 2003). Feiring and Kuczera (1982) indicated that comparing the simulation results with observed of streamflow data is not enough for parameter estimation. They emphasized the need to use at least three or more variables for estimation of the calibration parameters. Jakeman and Hornberger (1993) concluded that, for robustness of any conceptual watershed model, the output from every hydrologic component in the model needs separate validation. They used the rainfall runoff model that has three storages: rainfall, soil moisture and groundwater.

Their study suggested that the simulated response from rainfall and groundwater storage should be validated in order to decrease the uncertainty in parameters.

While emphasizing the importance of different hydrological variables such as infiltration and evapotranspiration, Johnston and Pilgrim (1976) reported an improvement in the performance of watershed models when using multi-variable hydrologic data for calibration. They used optimization techniques to determine the parameter values required for a watershed model and concluded that soil moisture data, when included in calibration procedures, improves simulation accuracy of watershed models. This is the first kind of study reported in the literature that emphasized the need to use multiple variables (soil moisture and evapotranspiration) in estimating the calibration parameters in a watershed model.

Kuczera (1983) used a nine parameter conceptual rainfall runoff model to simulate streamflow. He calibrated the model based on observed soil moisture, interception and streamflow data and reported that, with the use of three variables in the calibration process, uncertainty in the model was eliminated. A similar observation was made by Alley (1984) while finding parameters for a water balance model using evapotranspiration, soil moisture and groundwater recharge. Ambroise et al. (1995) used multi-response data to validate a semi-distributed model. They indicated that "a good validation procedure should include some test of the internal consistency of the distributed results on the sub-catchments, or even on specific simulation units" (p. 1467). They employed streamflow, point measurements of snowpack water storage, and soil water storage data to validate their model.

More recently, Woolridge et al. (2003) demonstrated the importance of using multivariable data sets for calibration and validation of a hydrologic model for an ephemeral watershed. The authors used a three-parameter Variable Infiltration Capacity (VIC) model with three parameters and used streamflow, soil moisture and evapotranspiration for estimating the model parameters. It was concluded that joint use of streamflow and soil moisture during calibration provided enough information for the model to properly simulate all other processes in the watershed.

2.5 Modeling Approach

Table 2.6 is a brief list of models available for simulating the watershed processes. The hydrologic literature is filled with a plethora of watershed models and it often becomes problematic to choose a particular model or modeling approach. Singh (1995) observed that all watershed models need to be packaged at the level of a user who is not necessarily a hydrologist, and should be integrated with, or at least have the capability of being integrating with, social, economic, and management modules. Furthermore, modellers or users of these models should address the issue of the applicability of the models in data-poor conditions (Elshorbagy et al., 2005), especially when multitudes of field parameters, which are necessary for model calibration, are not measured. There is a strong need to explore simulation tools that can represent complex systems in a realistic way and in such a manner that watershed managers and operators can be involved in model development so as to increase their confidence in the modeling results.

Apparently, a modeling approach with specific characteristics is needed. These characteristics are: (1) watersheds can be described and simulated in a simple fashion, (2) the model should start simple, relying on the available data (similar to data-driven models) and be expandable to benefit from additional data as they become available, (3) it should be dynamic so as to cope with the nature of hydrologic systems, (4) it should have the ability to simulate both linear and nonlinear processes, (5) it should provide a way to represent feedback mechanisms for handling counter-intuitive processes, (6) it should have the ability to model human intervention and any shocks (i.e., exceptional disturbances) that might be encountered in the system, and (7) it should provide the ability to test different policy or management scenarios for better decision-making. Although it might appear difficult to have all of these characteristics embodied in one modeling approach, the emergence of system dynamics modeling has made it possible (Elshorbagy and Ombrsee, 2005). A detailed retrospection of system dynamics is summarized in Chapter 3.

Chapter 3

System Dynamics

This chapter provides a basic understanding of the system dynamics modeling approach, and gives an insight into the difference between the system dynamics and the traditional modeling approaches. The usage of system dynamics modeling in water resources engineering is also presented.

3.1 System Dynamics: Definition and Scope

System dynamics (SD) can be defined as a way of thinking about a system as a web of interconnected pathways that affect fixed quantities of the system over time. SD works on a feedback principle, which requires an exchange of information between the various components of the system. In other words, SD is a way of conceptualizing the physical world in terms of the interconnection between its various elements. System dynamics as a field of study was proposed by Jay Forrester of the Massachusetts Institute of Technology (MIT) in the 1960s. The field has a long history of being widely used in diverse subjects such as biology, ecology, and business science.

In order to understand the definition and basic concepts of system dynamics, it is imperative to define two separate words: (1) *system,* and (2) *dynamics*. A system is a collection of mutually interacting, consistent, and inter-reliant mechanisms that affect the whole structure of system (Deaton and Winebrake, 2000). Dynamics can be termed as the degree that defines any change over time. For example, in hydrologic systems, water is present in different forms in various components of the hydrologic cycle such as vapour in air, as condensed particulates in clouds and as soil moisture in the soil matrix. The presence of water in various lithospheric and atmospheric components has little meaning if one is concerned only with analyzing the water cycle on the earth's surface (lithoshperic system only). However, if the components of the atmospheric and lithoshperic systems are joined together, it would explain the overall characteristics of the hydrologic cycle. Water from the soil evaporates and gets condensed in the form of clouds. When the clouds become saturated, water returns back to the earth in the form of precipitation. Nonetheless, when the soil is dry, there will be no movement of water from the soil to the atmosphere, which forms a restriction in the hydrologic cycle. The restricting relationship is known as a feedback loop, which governs the simple system; here known as the hydrologic or water cycle. Since the system is changing over time, it is characterized as a dynamic system. Hence, system dynamics is a technique to conceptualize the structure of the system where the components of the system are connected in such a manner that they form feedback loops, thereby representing the overall behavior of the system.

3.2 Feedback and Causal Loops: Essential Components of SD models

Feedback principles require an exchange of information among different components of the system, and therefore determine the overall behaviour of the system and provide a simpler solution to complex non-linear problems (Li and Simonovic, 2002). The simulation of the

system over time helps in understanding the system and its boundaries, identifying the key variables, representing the physical processes or variables through mathematical relationships, and mapping the structure of the model. The concept of feedback underlines the dynamic behavior of the system under consideration. The feedback loops can be considered as the most fundamental decision-making structural feature of a system (Forrester, 1980a). Feedback loops are relationships that generate a goal-seeking behavior. Goal-seeking enables conditions within a system to remain "on course". When deviations occur, feedback relationships inspire, and then direct, corrective actions that bring conditions back into line. An example of feedback in watershed hydrology is having the soil surface saturate, which affects the amount of water able to infiltrate into the soil. This simple conceptualization has been shown to make SD an effective tool for education and learning of watershed hydrology (Elshorbagy, 2005).

The preceding discussion with respect to system dynamics and systems thinking can be summarized as follows, namely that SD: (1) emphasizes the whole rather than the parts, while highlighting the role of interconnections, (2) highlights circular feedback (for example, X leads to Y, which leads to Z, which leads back to X) rather than linear cause and effect (X leads to Y, which leads to Z, which leads to A, . . . and so on), and (3) describes system behavior, such as reinforcing processes (a feedback flow that indicates exponential growth or collapse) and balancing processes (a feedback flow that controls change and helps a system maintain stability).

The realization of the systems thinking and embedded feedback loops for any system is done by using a graphical sketch called a causal loop diagram. This diagram includes elements (system process descriptors) and arrows, which are known as causal links, linking the various elements together in the manner as shown in Figure 3.1. The causal loop diagram also includes a sign (either + or -) on each link. These signs have the following meanings: (1) a causal link from one element *A* to another element *B* is positive (that is, +) if either *A* adds to *B* or a change in *A* produces a change in *B* in the same direction; (2) a causal link from one element *A* to another element *B* is negative (that is, -) if either *A* subtracts from *B* or a change in *A* produces a change in *B* in the opposite direction. In addition to the signs attached to the links, the feedback loops in the system are specified as well. The sign for a particular loop is determined by counting the number of minus (-) signs on all the links that make up the loop. Explicitly, a feedback loop is considered positive, indicated by a (+) sign in parentheses, if it contains an even number of negative causal links, while a feedback loop is considered negative, indicated by a (-) sign in parentheses, if it contains an odd number of negative causal links. Thus, the sign of a loop is the algebraic sum of the signs of its links. Often a small looping arrow is drawn around the feedback loop sign to more clearly indicate that the sign refers to the loop, as is shown in Figure 3.1.

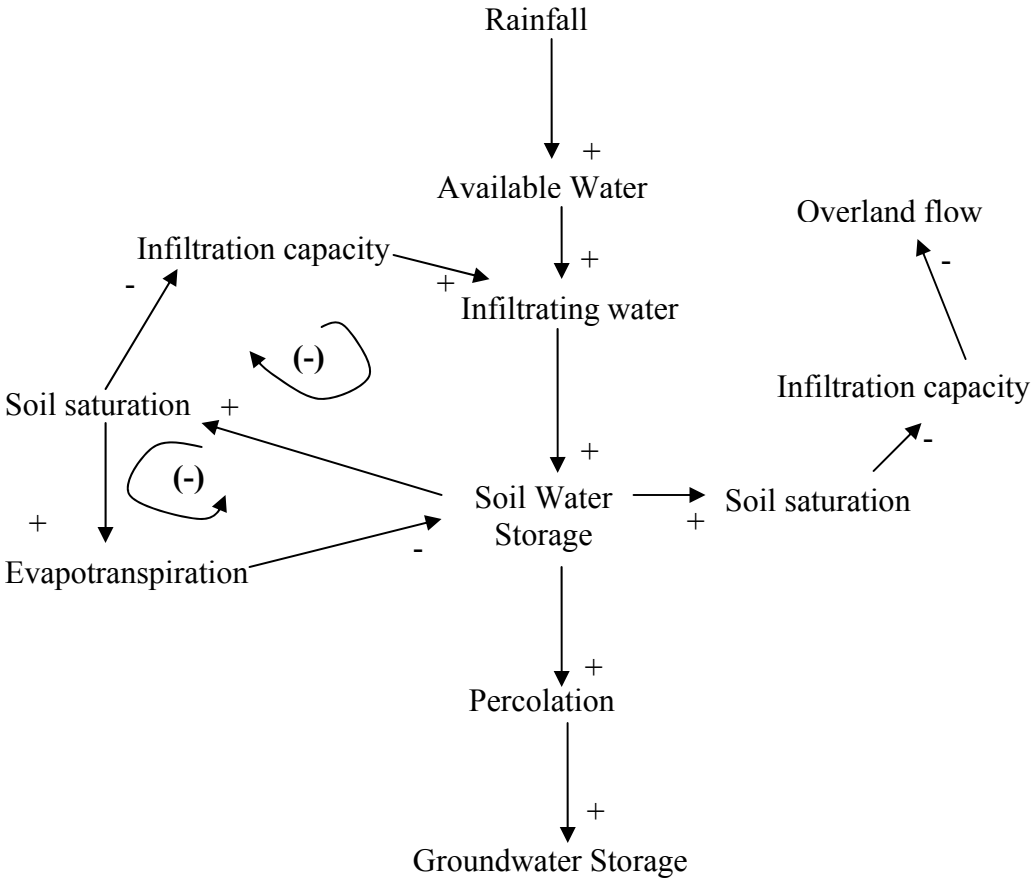

Figure 3.1. Causal-loop Diagram of a Simple Water Balance.

Positive feedback, also referred to as reinforcing feedback, exists whenever changes at one point on a feedback loop work their way back to reinforce or amplify the original change. Systems that have positive feedback loops tend to run out of control. On the other hand, negative feedback, also known as counteracting feedback, exists whenever changes at one point on a feedback loop eventually work their way back through the system to counteract the original change. Systems that have negative feedback loops are self-regulating and are not prone to run out of control. Most natural systems have negative feedback loops (Deaton and Winebrake, 2000).

Figure 3.1 is a classical example of the use of a causal-loop diagram to conceptualize a water balance model in a system dynamics framework. Rainfall is collected in an auxiliary storage called *Available Water*. Water infiltrates into the soil matrix and is then stored in *Soil Water Storage*. It then further percolates into the soil and collects in a storage called *Groundwater Storage*. The increase in the water content in *Soil Water Storage* will increase soil saturation, which will increase evapotranspiration and eventually will tend to decrease the original water content in *Soil Water Storage*. This is a counteracting feedback loop tending to stabilize the *Soil Water Storage*. Also, with an increase in the water content in *Soil Water Storage*, there

will be a decrease in the infiltration capacity of the soil, which implies that a smaller amount of water will go into the soil matrix. Conversely, if the soil matrix is saturated, then there will be more overland flow, which will reduce the water available for infiltrating into the soil. This is an example of an open loop, which operates in the case of system failure. It is interesting to note from this simple model that the open loop is more or less responsible for floods as the water balance system in nature tends to stabilize itself.

3.3 SD-based Modeling Process

3.3.1 Building Blocks of SD Models

SD-based modeling is different from traditional modeling approaches. The focus of SD-based models is more towards a specific and more practical problem (Gillespie et al., 2004). SD models are composed of four fundamental entities or building blocks: (1) stocks, (2) flows, (3) converters, and (4) connectors. These four entities (Table 3.1) are used to build simple as well as complex models using the SD approach.

Table 3.1: Building Blocks of System Dynamics Models (Deaton and Winebrake, 2000)

Name	Description	Symbol
Stock	A component of the system where something is accumulated. The contents of the reservoir or stock may go up or down with time.	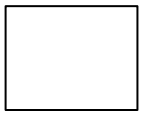
Flows	Activities that determine the values of reservoirs or stocks	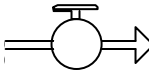
Converters	System quantities that dictate the rates at which processes operate and the reservoirs/stocks change.	
Connecters	Define the cause-effect relationships among the different components of the system	

Stocks are represented by rectangles (Table 3.1) and represent variables that are capable of accumulating a substance over time. These substances can deplete to a minimum value of zero. Stocks can symbolize any physical object, such as the number of citizens or disaster workers in a community, soil moisture, water reservoir, and bank balance (Ford, 1999) or a non-physical stock such as emotions (e.g., anger). In order to decide the variables that can be represented as stocks, it is essential to identify the variables in the system that may contain some value at a given time if the flow is stopped. For instance, at any given moment, there is a certain amount of water in a reservoir. Therefore, a reservoir can be represented by a stock

in an SD model. One property of stocks is that they are more stable than other variables; however, they are responsible for momentum and sluggishness in the system (Ford, 1999). In the simple water balance model shown in Figure 3.2, soil water storage and groundwater storage are represented as stocks. The stocks are referred to as the state variables for the system since they have the ability reflect the change in the state of the system through time (Gillespie et al., 2004).

Flows (Table 3.1) are shown by circles with a small spigot (cloud) attached to arrows leading into and out of a stock. Flows represent the action of either increasing or decreasing the value of a stock. In other words, flows symbolize some ongoing activity in the system that determines the contents of the stocks over time. If a simulation stops, flows, which represent processes, automatically vanish. A "cloud" in a flow represents a source or a sink. If an arrow points into the cloud, it must be a sink. Conversely, an arrow pointing away from a cloud implies that the cloud must be a source. For instance, in Figure 3.2, if simulation stops, the flows such as *Rainfall, Evapotranspiration, Percolation,* and *Overland Flow* stop. However, there will be certain values in the stocks of *Available Water*, *Soil Water Storage*, and *Groundwater Storage*.

Converters (Table 3.1) are depicted by circles and they explain any modifications or additions done in stocks and flows. They are like adjectives in a sentence, adding further refinement and clarification to the picture. Their most significant role is to state the rates at which the processes in a system operate. Converters are calculation units that can represent any variable as a function of time or can be used to input any value or a logical statement. For instance, Figure 3.2 has one converter, called *Infiltration Capacity,* that helps define the rate of flow between *Available Water* and *Soil Water Storage.*

Connectors (Table 3.1) represent intricate connections among all the components (stocks, flows, and converters) of a system. The relationships are usually expressed in terms of mathematical expressions. The arrowheads indicate the direction of the link. In Figure 3.2, the converter called *Infiltration Capacity* is connected to the flow named *Infiltration* and stock called *Soil Water Storage* by connectors. The direction of the arrowheads indicates that, at any time during simulation, soil water storage affects the infiltration capacity, which in turn affects the infiltration process. Further details about the operations of the functions can be found in Ford (1999).

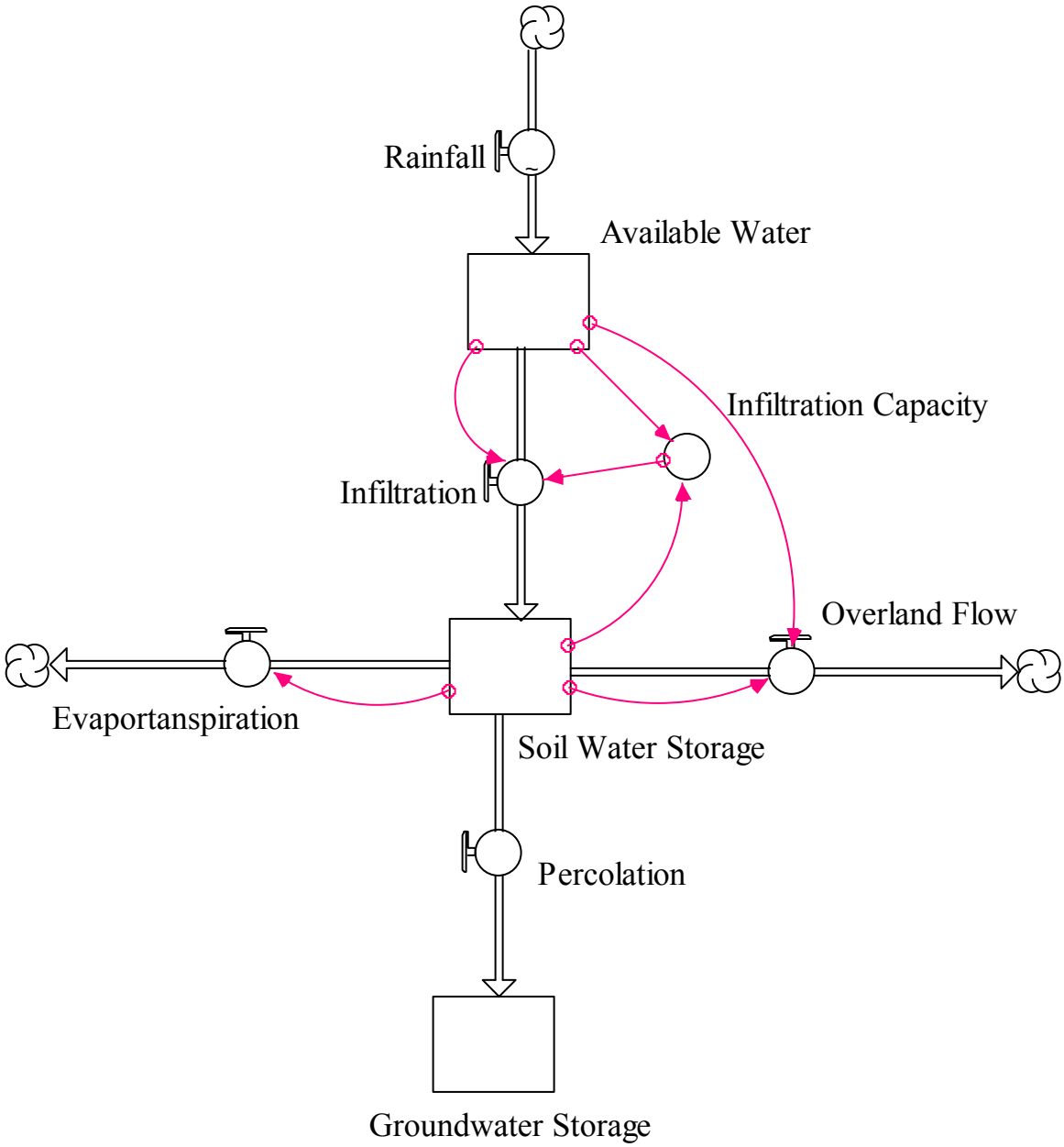

Figure 3.2. Simple System Dynamics Water Balance Model.

All SD models are constructed using the above mentioned four entities. Figure 3.2 is a simplistic water balance model constructed using the STELLA® software, which is explained later. The water balance model in Figure 3.2 was developed utilizing the conceptual causal loop diagram illustrated in Figure 3.1. The model consists of three stocks: *Available Water, Soil Water Storage, and Groundwater Storage*: five flows representing *Rainfall, Infiltration, Overland Flow, Evapotranspiration, and Percolation*; and one connector called *Infiltration*

3.3.2 The Process of Modeling in System Dynamics

The process of building an SD model is an iterative one in which the model is built in steps of increasing complexity until it simulates the actual behaviour of the natural system under

consideration. According to Randers (1996) and Stave (2003), the modeling process in SD can be divided into four stages. Stage (1) is called the conceptualization stage that determines the objective of the problem. The general perspective and time horizon of the problem are established in this stage of model development. In this stage, the modeller attempts to develop the mental models (i.e., a basic understanding of any physical operation in the real world). The mental model is a prerequisite for formulating any formal SD model. The conceptualization stage helps draw the attention of the analyst toward closed loops of cause and effect and stress the distinction between stocks and flows. Causal loops and hence the feedback relationships are determined at this stage. Stage (2), known as the formulation stage, casts the chosen perception of the model into a formal representation. One of the important steps to be followed is to determine the parameters of the model. Some parameters may have fixed measurable or known values in the system while others may vary with time or space. It is essential to identify both types of parameter in the system. For instance, in the hydrologic system, hydraulic conductivity varies with soil moisture at all time steps. Stage (3), called the testing stage, follows after the successful identification of the model parameters. This stage is intended to establish the quality of the model by comparing the results obtained from the model with field or real world data sets. This procedure is also referred to as calibration, which was described in Chapter 2. Also, the goal of this stage is to identify the weak points in the feedback relationships and possible errors in the dynamic theory of the system. Stage (4), called implementation, is directed towards the stakeholders who are intended to use the model. The response of different policies or scenarios of the problem under consideration are tested in this stage.

Figure 3.3 is a diagrammatic representation of the SD modeling approach. It is provided here as a way of illustrating the flow of the basic steps involved in SD modeling. The process of SD modeling starts with specifying the objective. The next step is to make a conceptual model of the problem, which defines the state variables in the system and the boundary of influence of the problem. The state variables are then represented by stocks. The processes influencing the stocks are then connected to the stocks using flows. Converters are then connected to the flows to define the feedback relationships. Various suitable numerical or empirical values or functions are assigned to the flows and converters, using a knowledge-based database or mental models. Each stock is then assigned an initial value. The model parameters are determined after defining the feedback relationships. If the model is found to need refinement, the empirical relationships can be changed, either by using existing data or the perceptions of the modeller. The next step in formulating the model is to initialize it, a process that involves ensuring that the model reproduces acceptable results as defined by a real-time database. The last step includes debugging (i.e., ensuring that there are no mechanical mistakes in the model) and validating the model, which helps to ensure its accuracy and usefulness (Ford, 1999). If the model results do not fall within a reasonable range of acceptance, then the conceptual model is examined and rectified accordingly, thus facilitating a dynamic understanding of the system. However, if the mental model is accurate, then the model parameters are changed, a process called calibration, to get the desired results.

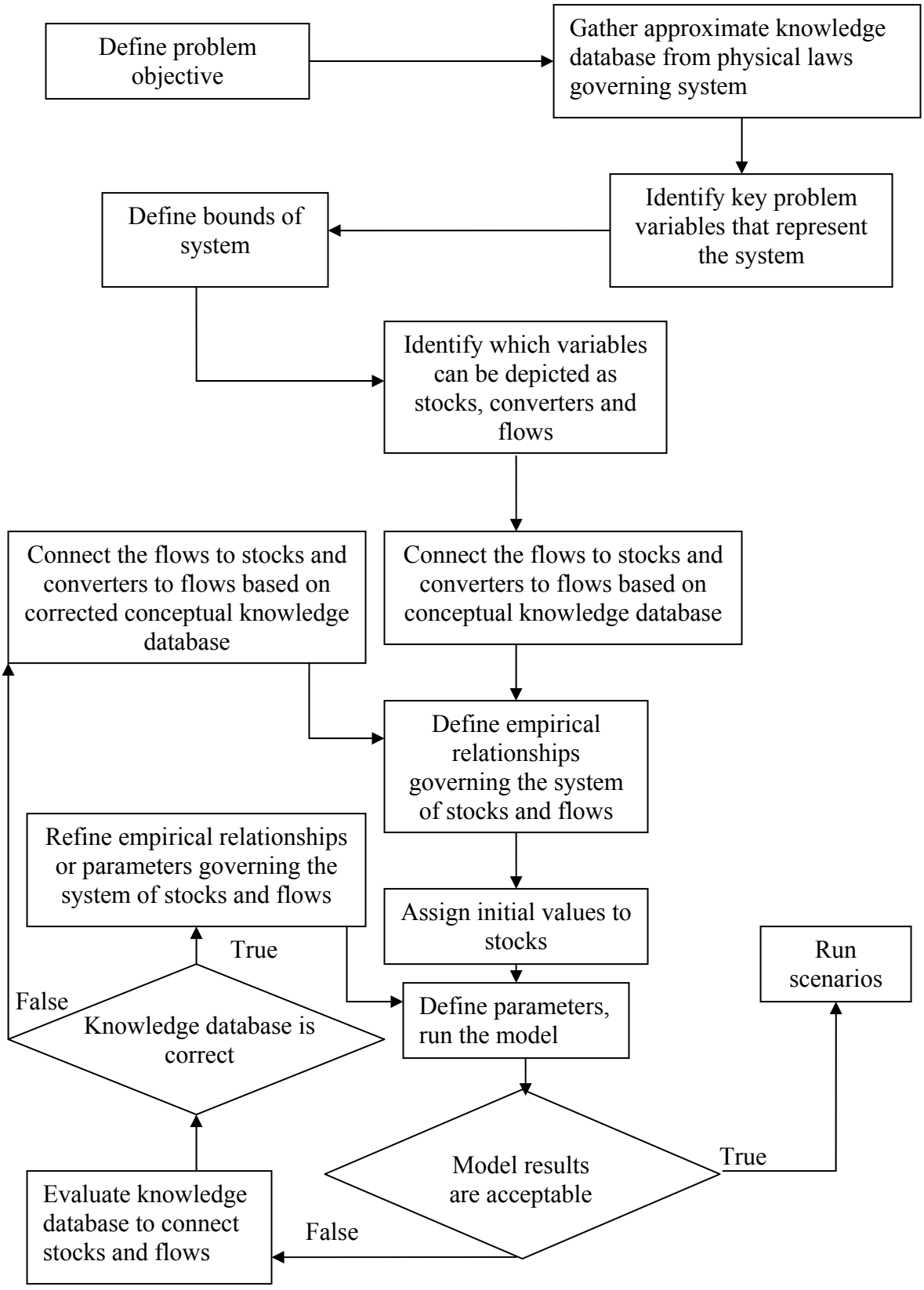

Figure 3.3. Modeling Approach in System Dynamics.

3.4 Simulation Time Interval (Δt)

All SD models are constructed as a combination of various stocks and flows to simulate a system using a specified time step (e.g., day, hour, or year). For example, in the case of a stock, a continuity equation for mass balance is developed considering the inflows and the outflows. The stock, called *Soil Water Storage (SWS)* in Figure 3.2, can be mathematically represented as:

$$\frac{d(SWS)}{dt} = Infiltration - Evapotranspiration - Overland\ Flow - Percolation \qquad [3.1]$$

In SD modeling, all of the governing equations are represented by first order differential equations, such as Equation 3.1. The equations can be solved analytically as well as numerically. However, in a complex system that has many feed-back loops or non-linear relationships, it becomes increasingly difficult to obtain a solution analytically. Numerical methods have proven to be a valuable tool for solving complex non-linear equations in such situations. Hence, in all SD simulation environments, the time-based equations are replaced by difference equations, which are then applied over successive intervals of time. The length of such a time interval is known as solution interval (Δt). In other words, the solution interval is the time interval at which the simulation environment solves the model equations and calculates the value of all variables (Barton and Tobias, 1998).

The solution interval must be short enough so that its value does not affect the computed results. The general requirement that limits the length of the interval arises from the organisation of the equations. Stocks determine flows and vice-versa; however, the system of equations becomes an open system in the sense that all of the information feedback loops are uncoupled during the solution interval. Hence, the interval must be short enough so that the change in the stocks over one solution interval does not lead to unacceptable results. The solution interval must be equal to or less than that of any first order delay. For instance, if a high rate of flow is expected out of a small inventory, the solution interval should be short enough so that only a fraction of the inventory is depleted in one solution interval. Conversely, if the interval is long which will remove the content of the inventory excessively; leading to a negative inventory, or in other words yields absurd result (Forrester, 1964).

Any change in the model takes at least a time period equal to Δt to occur. For instance, if the modeller intends to simulate the SD model on a daily basis, the maximum permissible solution interval is one day. However, if the modeller changes the solution interval to two days, which indicates that the system of equations will be solved every two days, this will cause an error known as Δt error. Before executing an SD model, the modeller should ensure that the solution interval does not introduce Δt error. If Δt error occurs, the modeller should look for the shortest first-order delay in the system and should set the solution interval accordingly. When simulating a model, the modeller should always try to repeatedly cut the Δt in half to check whether the behaviour generated by the model is caused by the model structure or by an error associated with the solution interval (Barton and Tobias, 1998).

3.5 Simulation Environment for SD Modeling

There are many types of simulation environment currently available for building and running models using SD principles. Between the qualitative conceptual model and the computer code, one may utilize a variety of simulation environments that can convert conceptual ideas into operational models. However, there is always a trade-off between universality and user-friendliness. Table 3.3 is a list of various commercial softwares available for implementing the SD modeling approach.

The development of the modeling softwares shown in Table 3.2 has simplified the process of constructing an SD model. However, modeling is still primarily a research process that requires knowledge and understanding of the system to generate more knowledge and more understanding. The simulation environments are indeed helpful if one knows how to build a model. Moreover, no simulation environment is universal. There are always systems that could be better modeled using a different formalism and different mathematics and software. In reality there are numerous different approaches, and all of them may be worth considering when deciding how to model the system of interest.

In the present study, STELLA® software, developed by High Performance Systems (HPS, 2001), has been used to develop the site-specific models. The simulation environment is a user-friendly program that uses an iconographic interface (Figure 3.4) to facilitate construction of an SD model (Costanza and Voinov, 2001**)**. Mathematically, the software solves differential finite difference equations using either Euler's or Runge - Kutta methods. The software allows for choosing the appropriate temporal integration method. While modeling, the modeller places the icons for each of the stocks in the modeling area and then connects them by flows of material or informational relationships . Next, the user defines the functional relationships that correspond to these flows. These relationships can be mathematical, logical, graphical, or numerical. STELLA® represents stocks, flows and converters, respectively, with the icons shown in Table 3.1 and Figure 3.4. The details about the four entities (stocks, flows, converters, and connectors) in the STELLA software are described in Appendix A.

3.6 SD Models versus Traditional Models

This section gives an overview of the basic differences between SD models (SDM) and traditional models (TM). The structural difference in the two modeling approaches is explained using the water balance problem mentioned in Figure 3.1.

3.6.1 Representation of the Water-Balance in SDM

A simulation environment that uses the SD principles enables the mathematical relationships of a model to be expressed without having to program the procedures for numeric integration. The SD-based simulation environments have already been described in Section 3.5.

Table 3.2: Brief Comparison of Some of the Existing SD Modeling Software (Costanza and Voinov, 2001)

Software	Developers	Extendible*	User Friendly**	Learning Curve***
STELLA	High Performance Systems (www.hps-inc.com)	No	5	5
POWERSIM	Powersim (www.powersim.com)	Somewhat	5	4
EXTEND	Imagine That (http://www.ImagineThatInc.com)	Yes	4	3
SIMULINK	Mathworks (http://www.mathworks.com)	Yes	3	2
VENSIM	Ventana (http://www.vensim.com)	No	5	5
MODEL MAKER	CS (http://www.cherwell.com)	No	5	5

*Extendible systems offer tools to incorporate some additional user-defined functionality.
**User-friendliness (max = 5) is a subjective estimate of how easy it is to use the software once you have learned how to use it. Max = 5 means most user-friendly software.
***Learning curve (max = 5) is an estimate of how easy it is to learn to use the software based on the number of hours needed to formulate a simple one-variable model and run it starting from scratch. Learning curve = 5 means a very easy to learn system.

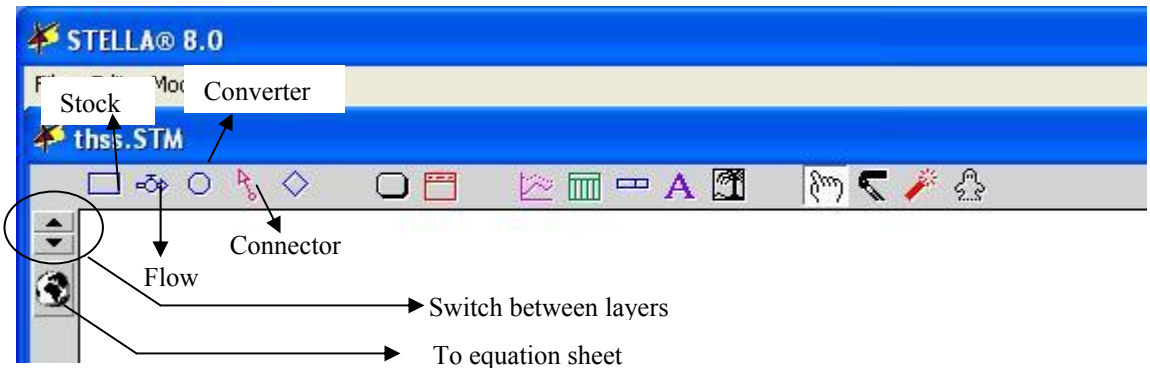

Figure 3.4. Location of Building Blocks in STELLA Software.

Table 3.3 presents a self-explanatory model representing the problem under consideration. The model has been constructed in the STELLA modeling environment. A simulation language like STELLA helps guide the modeller in expressing the mathematical relationships in the model, rather than focussing on the numerical integration part to the software package itself.

Table 3.3: Representation of the Water-Balance in the SD Simulation Environment

Program	Remarks
Available_Water(t) = Available_Water(t - dt) + (Rainfall - Infiltration) * dt	Stock of *Available Water*
INIT Available_Water = 0	Initial value of the stock
INFLOWS:	
Rainfall = GRAPH(time) (0.00, 0.00), (1.00, 0.00), (2.00, 0.00), (3.00, 0.00), (4.00, 0.00), (5.00, 0.00), (6.00, 0.00), (7.00, 0.00), (8.00, 0.00), (9.00, 0.00), (10.0, 0.00), (11.0, 0.00), (12.0, 0.00)	Inflows to the stock *Available Water* by flow called *Rainfall*
OUTFLOWS:	
Infiltration = if Available_Water>0 then Infiltration_Capacity else 0	Outflow from the stock
Groundwater_Storage(t) = Groundwater_Storage(t - dt) + (Percolation) * dt	Stock of *Groundwater Storage*
INIT Groundwater_Storage = 0	Initial value of the stock
INFLOWS: Percolation = 0.35	Inflows to the stock *Available Water* by flow called *Percolation*
Soil_Water_Storage(t) = Soil_Water_Storage(t - dt) + (Infiltration - Evaportanspiration - Overland_Flow - Percolation) * dt	Stock of *Soil Water Storage*
INIT Soil_Water_Storage = 10	Initial value of the stock
INFLOWS: Infiltration = if Available_Water>0 then Infiltration_Capacity else 0	Inflows to the stock *Soil Water Storage* by flow called *Infiltration*
OUTFLOWS: Evaportanspiration = Soil_Water_Storage*0.02 Overland_Flow = if Soil_Water_Storage>200 then Available_Water else 0 Percolation = 0.35 Infiltration_Capacity = if Soil_Water_Storage >200 then 0 else Available_Water	Outflow from the stock

3.6.2 Representation of the Water-Balance in TM

The water balance illustrated in Figure 3.1 can be modeled using any available programming language. For simple models, the solution of the model can be performed analytically, which implies that the solution of the equations provides the value of the soil water content at any point in time. In the case mentioned above, the computer program would consist of equations with inputs of the initial value for soil water content and the rainfall, and the time interval for the intended model simulation. In the vast majority of situations, the modeller needs to solve the equations through simulation (i.e., by numerical integration of the underlying differential equations). In essence, this involves cycling through a loop in which changes are made to the model variables over some small period of time, adding or subtracting these changes to/from

the variables, then repeating the process with the new values for the state variables. Table 3.4 provides a self-explanatory program, written in C++, for simulating the behaviour of the example as shown in Figure 3.2.

The programming done in TM is not the description of the problem under consideration; rather, it is a set of instructions that a computer should follow in order to enable a certain type of inference to be drawn from the model using a particular numerical approach. The inference relates to the future value of soil water given its initial value and the value of parameters. In other words, it is a procedural way to integrate the problem over time.

3.6.3 Comparison of SDM and TM

There are certainly distinctive features that differentiate SDMs and TMs. In TMs, the program statements must be written in an orderly sequence, starting from the first and continuing to the last and in loops. However, in SDMs, the statements can be entered in any order; they are sorted into the right string for evaluation by the simulation environment

Table 3.4: Programming Water Balance in TM

Program in C++

```
#include <iostream.h>
#include <iomanip.h>
#include <math.h>
#include <stdio.h>
#include <fstream.h>
#include <string.h>
#include <stdlib.h>
#include <conio.h>
void main()
{{ifstream in("Rainfall.dat"); //Reads rainfall from test file
  Rainfall.readin(in);
  file>>RR};
.
.Output files programmed here
.
private: double SW, R, OF, i, EVAP, PERC, GW;
//SW = Soil Water Storage, R= Rainfall, OF= Overland Flow, i= time increment,
//EVAP=Evaporation, PERC=Percolation, GW= Groundwater.

for (int i=1; i=365; i++)              //initialization of time loop for a year

if (SW>400)                  //soil water storage is more than 400mm (assumed)
{{ OF[i]=R[i];               // route rainfall as overland flow
OF[i]=OF[i]+R[i]};           // accumulates the overland flow
{if (SW>0)                   // soil water storage is less than 400 but greater than 0
{SW[i]=R[i];                 //route rainfall to soil
 EVAP[i]=SW[i]*0.2;          //calculates evapotranspiration
```

```
PERC[i]=0.25;                    //calculated percolation
GW[i]=GW[i]+PERC[i];             //increases groundwater
SW[i]=SW[i]-EVAP[i]-PERC[i];     //calculates the final amount of soil water available
if (SW[i]<0)                     // checks the soil water for negativity
{{SW[i]=R[i]}; abort ()};        //if soil water is less then zero then abort above calculations
}}                               //and stores all rainfall into soil matrix
}                                //proceed to next time step
```

itself. In TMs, each equation acts as an instruction, which can be called an "assignment statement". The correct way of interpreting it is: *Work out the expression on the right side of the equals sign, then assign this value to the variable on the left side.* In the SD simulation environment, on the other hand, the equation is a statement of the mathematical equality between the left-hand and right-hand sides. Moreover, TMs are difficult to visualize, which is important in understanding any concept. In SD simulation modeling environments, the graphical interface along with its building blocks facilitates the assimilation of the knowledge-based database of the modeller.

In summary, the SD approach differs from traditional hydrologic modeling in three major aspects. First, the SD approach makes the links, including feedback loops, among the different components of the system both visual and explicit. This facilitates the process of verifying individual components and sub-systems, and ensures that all links are reasonable and logical. Second, the SD approach allows for constructing a model that combines process-based and empirical or even qualitative formulations. In the SD approach, it is possible to incorporate a qualitative relationship based on tentative knowledge of the relationship between two parameters. Simulations can be executed and subsequent modifications of the relationships made until the expected behavior of the system is achieved. Third, dynamic (time varying) coefficients and parameters can be easily employed in the SD approach.

3.7 Application of SD Approach to Water Resources

3.7.1 Overview

The SD-based modeling approach has been used in economics, business management, and the social sciences for a long time. However, the potential use of such an approach in water resources has been documented for the first time in Proceedings of the 20th Anniversary Conference on Water Management in 90s, which was held in Seattle in 1993. A conceptualization of hydrological models using SD has been briefly outlined by Lee (1993), who indicated that the SD modeling approach is a candidate to be an excellent tool for teaching hydrological modeling. Lee (1993) emphasized that the model building in hydrology is an art and suggested that models should be built in two stages: (1) model conceptualization, and (2) model programming. These two stages are represented effectively using an SD modeling approach; hence SD is an excellent tool for understanding hydrology. The application areas of SD modeling to water resources issues can be further divided into three categories, which are described in the following sections.

3.7.2 General Water Resources Management

Simonovic (2002) used the SD modeling approach to model world water resources. The research paper focused on prediction of the impacts of various scenarios of water demand

and supply across different continents. The SD approach has also been used in reservoir management by Ahmad and Simonovic (2000), who focused on construction of basic models for reservoir and flood management in the Assiniboine River basin in Canada. The study emphasized that the SD modeling approach is a valuable alternative to the conventional models being used in flood management. Ahmad and Simonovic (2000) reported that the SD models are easy to construct and modify. The SD approach also facilitated the ability to perform sensitivity analysis, rapid development of prototypes, and reduction in programming time and skills. Xu et al. (2002) agreed on the conclusion made by Ahmad and Simonovic (2000) and developed an SD based model for sustainability analysis for the Yellow River in China.

Simonovic and Li (2003) developed models using SD principles for the assessment of climate change and its impact on large-scale flood management systems. Their study emphasized the role of SD in water resource planning and management. Further, the study indicated that Global Circulation Models (GCMs) could be integrated with any hydrological models using SD modeling. Stave (2003) applied the SD modeling approach to understand the water management practices in Las Vegas, Nevada, USA. The case study presented in the study demonstrated the benefits of the SD approach for public participation in water resources management. The ability of the constructed models to rerun several times using the graphical interface of the SD model enabled stakeholders to contribute constructive feedback in providing solutions to various management problems.

3.7.3 Ecological and Environmental Modeling

SD-based models have been used in the evaluation of complex ecological systems. Voinov et al. (2004) constructed a modular ecosystem model using SD for simulating hydrological processes, nutrient cycling and vegetation growth. Their research concluded that SD-based models bridge the gap between the software developers and the researchers. According to them, researchers use models for understanding the systems and not as black boxes, which a software developer perceives. Similar views have been presented by Elshorbagy and Ormsbee (2005), where they used SD models for surface water quality management. Their study also concluded that the SD modeling approach is a good tool and a potential alternative to traditional models in data-poor conditions and hence can be used in the decision-making process. Aassine and El-Jai (2002) constructed SD models to simulate vegetation growth dynamics. Moffatt and Hanley (2001) indicated that population dynamics can be simulated by SD models, and suitable sustainable management schemes can be developed using those models. Three special issues of the Journal of Ecological Modelling have been dedicated to SD modeling use in ecology (Costanza et al., 1998; Costanza and Gottlieb, 1998; Costanza and Voinov, 2001). Although SD has limited spatial-modelling capability, Maxwell and Costanza (1997) have linked SD models to Geographic Information Systems (GIS) using STELLA.

3.7.4 Watershed Modeling

The application of the SD modeling approach in watershed modeling is extremely limited in the literature. Li and Simonovic (2002) successfully adopted SD for predicting floods in two prairie watersheds (Red River and Assiniboine River basins, Canada). Their study concluded that SD-based modeling is a useful tool for understanding complex hydrologic relationships

in the watershed. Their study also concluded that SD-based hydrologic models are easy to calibrate and validate, and on which to perform sensitivity analysis.

The use of SD modeling in watershed modeling has been reported in Elshorbagy et al. (2005). The authors constructed a hydrologic model based on SD principles and used the model for assessment of sustainability of a land reclamation strategy. It was concluded that the flexibility in building models with SD facilitated understanding of the inter-relationships among the various hydrologic processes occurring in the watershed.

Chapter 4

Site Description

4.1 Introduction

Syncrude Canada Limited (SCL) is conducting large-scale experiments to assess the reclamation strategies for reconstructed watersheds. These experiments consist of several integrated hydrological component studies that include determination of the mechanisms of moisture movement, salt transport, evolution of vegetation and performance of wetlands in the reconstructed watersheds.

The present study evaluates the watershed response of one of the reconstructed watersheds, referred to as SW-30 dump (Boese, 2003), located at the Mildred Lake mine, 40 km north of Fort McMurray, Alberta, Canada. The climate of the Fort McMurray region is classified as sub-humid climate. The mean annual precipitation for the region over the past 50 years (1945-1995) has been 442 mm (Boese, 2003)
The SW-30 dump is one of the six shale overburden dumps reclaimed by SCL. A part of the dump (Figure 4.1), which consists of experimental watersheds and wetlands, was reclaimed in 1999. This research focuses only on the hydrology of the soil covers: D1, D2, and D3.

4.2 Reconstructed Watersheds

Figure 4.1 shows the location of the experimental soil covers on the SW-30 overburden dump. The three watersheds, which face in a northerly direction, were constructed to represent three possible cover alternatives, with the purpose of evaluating their performance in terms of holding moisture that can sustain vegetation and minimizing the amount of water that percolates below the root zone. Each of the three watersheds has a 5:1 slope (5 horizontal to 1 vertical) with an area of 1 ha (approximately 200 m long and 50 m wide). Figure 4.2 represents a 3D topographic map of the three watersheds.

Each of the watersheds is treated as a separate sub-watershed in this research. The thickness of the soil layers in each cover is given in Table 4.1. Cover D1 consists of 200 mm of peat/mineral mix on top of 300 mm of till (glacial soil) over the overburden shale. Cover D2 has the thinnest soil layer with 150 mm and 200 mm of peat/mineral mix and till (glacial soil), respectively, which is underlain by the overburden shale. Sub-watershed D3 has the thickest soil layer, having 200 mm and 800 mm of peat/mineral mix and till (glacial soil), respectively, over the overburden shale. Sub-watershed D3 meets the conventional requirements of Alberta Environment, which requires that closure of all mine dumps should be capped with at least 1 m of soil (Alberta Environment, 1995). All three soil covers were seeded with a barley nurse crop, and tree seedlings of spruce and aspen in June 1999 (Boese, 2003).

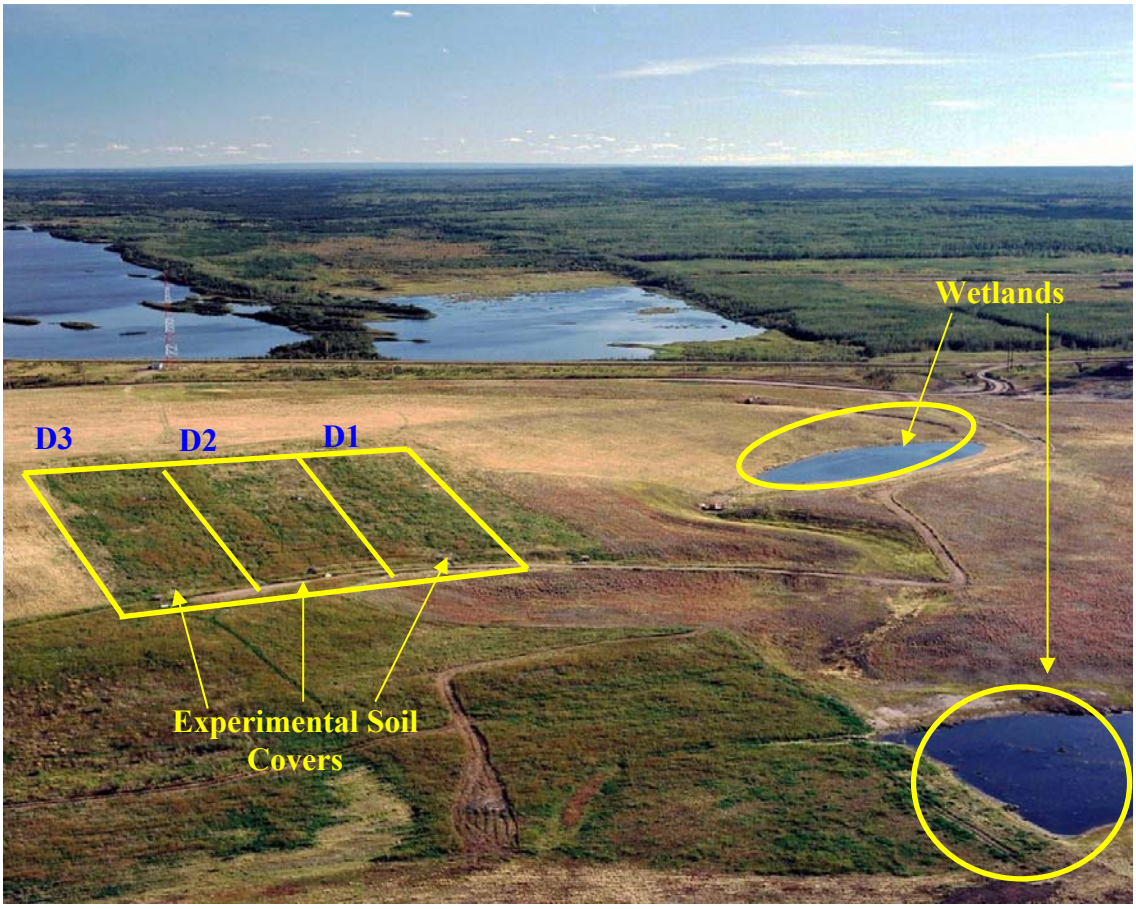

Figure 4.1. Location of Reconstructed Watersheds (D1, D2, and D3) on SW-30 Dump

Table 4.1: Composition of the soil covers

	Reconstructed watershed		
	D1	D2	D3
Peat Layer (mm)	200	150	200
Till Layer (mm)	300	200	800

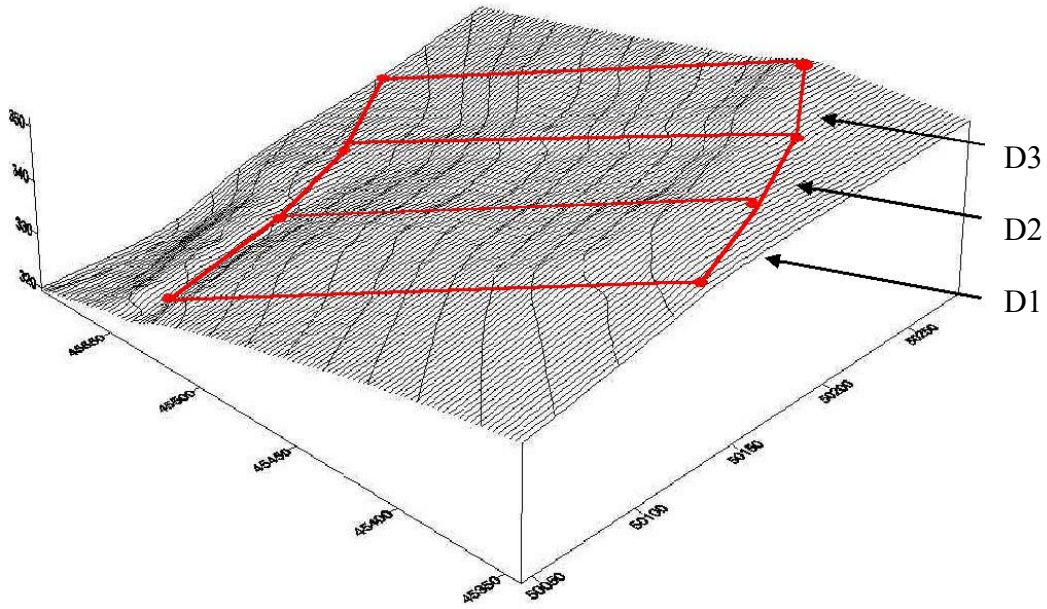

Figure 4.2. Layout of Prototype Covers (Boese, 2003).

4.3 Instrumentation and Field Measurements

The three reconstructed sub-watersheds evaluated in this study were heavily instrumented to permit tracking of hydrologic changes and to allow evaluation of the hydrologic response of each sub-watershed. A summary of the instrumentation sensors installed at the study site is depicted in Table 4.2. The details of the instrumentation programme are described in Boese (2003). A schematic representation of the instrumentation for each soil cover is illustrated in Figure 4.3. The Bowen station is used for measurement of evapotranspiration and is located on the D2 sub-watershed only.

Each sub-watershed has an individual soil station located at the middle of the slope, which measures soil temperature, soil moisture and soil suction at different depths in the peat, till and shale. The soil moisture was measured using Time Domain Reflectometery (TDR) principles using model CS615 (Boese, 2003). The sensors used for the measurement of matric suction, water content and soil temperature were installed laterally into the soil profile. There are eight TDR sensors in sub-watershed D1 for the measurement of soil moisture, installed over a depth range of 0.05 m to 1.00 m. Sub-watershed D2 has seven TDR sensors installed at depths ranging from 0.05 m to 0.80 m. Nine TDR moisture sensors are placed between 0.05 m to 1.70 m in sub-watershed D3. Neutron probes were installed in the soil covers in order to monitor the soil moisture; however, the available data is sporadic, and hence was not used in this study. Matric suction was measured using thermal conductivity principles. The number and depth range of the matric suction sensors coincide with the soil moisture sensors in each sub-watershed. Soil temperature is measured using thermisters buried in each sub watersheds at the depth ranges corresponding to the TDR sensors in each

sub-watershed. Sub-watershed D1, D2, and D3 have eight, eight, and nine sensors, respectively, for the measurement of soil temperature.

Table 4.2: Summary of the Field Instrumentation at the Study Site

Instrumentation	Location	Frequency of measurements	Observations recorded
Weather Station	Mid-slope of sub-watershed D2	Hourly	Relative Humidity, Air Temperature, Wind Speed, Wind Direction, Precipitation
Bowen Station	Mid-slope of sub-watershed D2	20-minute intervals	Dew Point Temperatures, Surface Soil Temperature, Air Temperature Gradient, Net Radiation, Ground Heat flux
Soil Station	Mid-slope of each sub-watershed	Twice a day at 12 h intervals	Soil Moisture, Soil Temperature, Soil Suction
V-Notch Weir	At the toe of each sub-watershed	Five minute intervals	Overland Flow
Interflow System	At the toe of each sub-watershed	Manually after 2-3 days	Amount of water flowing laterally through sub-watershed

Overland flow from each sub-watershed was collected in a swale at the bottom of the slope using a 60-degree V-notch weir constructed in the swale. The weirs were located at the downstream end of each sub-watershed. Depth of water in weir was measured with ultra-sonic sensors.

Interflow at the site was measured using an interflow collection system, which is installed at the toe of each soil cover. The measurement system comprises of a geo-membrane cutoff, located at the cover and shale overburden interface. A weeping tile collection system is then used to gather the interflow water into a barrel at the toe of each sub-watershed. The water in the barrel was pumped out using a pump and a flow meter. After collection of the water in the barrel, the volume of the interflow water was calculated (Boese, 2003). All of the instruments were calibrated in 1999 during installation. The data for this study was available from 1999 to 2004. No data have been collected as part of this research project, rather, the available data from year 2000 to 2004 were used for simulating the watershed response in

this work. The data from year 1999 was not used because it was only a partial year data set. Detailed information on data collection and instrumentation is documented in Boese (2003).

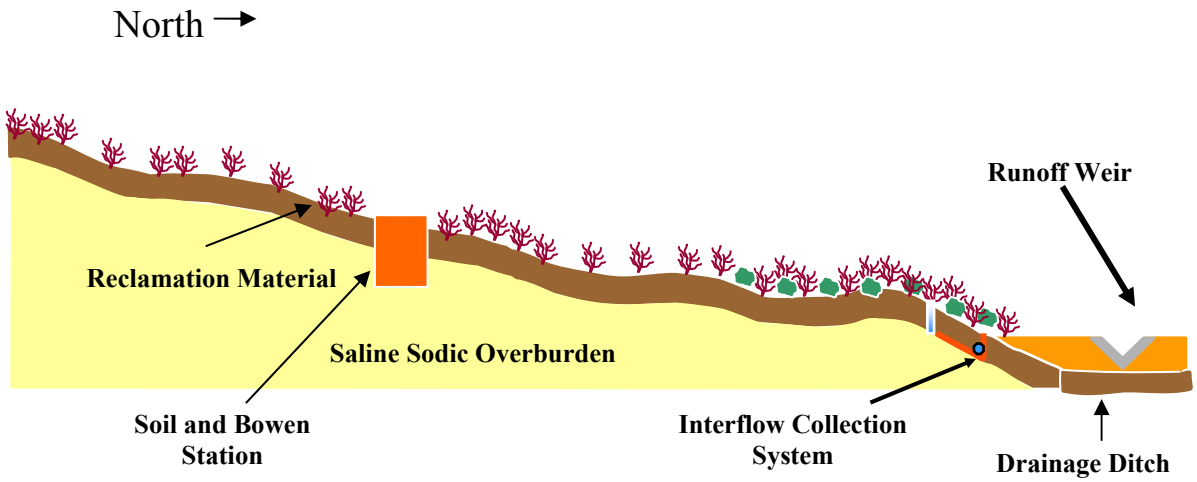

Figure 4.3. Cross Section of Sub-Watershed and Location of Sensors in the Sub-Watersheds (Boese, 2003).

Chapter-5

Model Formulation

This chapter deals with the detailed procedures adopted to construct a hydrologic model for reconstructed watersheds using the system dynamics approach. All formulae and concepts used to develop the model are discussed in this chapter.

5.1 Overview of Research in Reconstructed Watershed Hydrology

A reconstructed watershed generally consists of several soil layers with different physical properties (porosity, hydraulic conductivity, composition, etc.). It is important to evaluate the hydrologic processes within the soil layers in the watershed since these layers have to sustain vegetation for long time periods. The water content of the soil layer in contact with the waste (overburden shale layer) should be minimal in order to prevent hazardous contaminants from leaching out of the soil layer. There is a need for quantitative research for long term evaluation of any reclamation strategy (Khire et al., 1997). As an example, a compacted clay layer placed immediately over the waste may develop cracks if the wilting point moisture content is not maintained within the clay layer. An ideal water balance should allow the soil layer to retain an adequate moisture content while limiting the downward flux of water into the buried waste. Therefore, it is important to evaluate the watershed in terms of water balance (moisture dynamics) within the various soil layers.

The literature suggests that there has been limited research work done to assess the long term performance of reconstructed watersheds. One of the primary ways for evaluating the water dynamics in reconstructed watersheds is to use a hydrologic model to simulate the various hydrologic processes within the watershed. However, the literature also reveals that most reconstructed watershed modeling work has been done from a geotechnical engineering point of view, where emphasis has been given to the modeling of the individual components of the hydrologic cycle. For instance, Wilson et al. (1996) studied the effect of soil suction on evaporation from layered soil covers. Bruch (1993) used the SWIM (Soil Water Infiltration and Movement) (CSIRO, 1990) model for the analysis of evaporative fluxes from the various soil layers in reconstructed watersheds. The SWIM model solves Richard's two-dimensional (2D) equation. The model simulates unsaturated and saturated flows. However, the model structure follows a traditional modeling approach, which does not give insight into the interrelationships among the various components of the system. Yanful et al. (2003) used a one-dimensional finite element program called SoilCover (Mend, 1993) to evaluate evapotranspiration in reconstructed watersheds. Fayer et al. (1992) used the UNSAT-H (Fayer and Jones, 1990) model, which solves Richard's 2D equation using finite difference principles to for evaluate evaporation from soil covers. Woyshner and Yanful (1995) used two models, HELP and SEEP/W, for simulating percolation through soil covers. SEEP/W is a finite element-based model that solves Richard's equation. HELP (Schroeder et al., 1994) is based on a water balance methodology. Swanson et al. (2003) used the a finite element model, SoilCover, to evaluate the unsaturated hydrology of the soil layers in a reconstructed watershed in a humid climate. Shurniak (2003) also used Soilcover to simulate soil moisture

fluxes and evaluated various reclamation strategies in terms of thickness of the soil covers based on moisture retention within each cover.

There is a need to have an appropriate model for reconstructed watersheds for simulating the overall hydrologic cycle (water balance). The characteristics of an ideal watershed model have already been mentioned in Chapter 2. In this research, a hydrologic model based on a water balance methodology (Eq. 2.1) has been developed using a system dynamics approach.

5.2 Model Conceptualization

The lumped modeling approach has a long history in hydrologic modeling. The foremost advantage of lumped models is their computational efficiency (Huggins, 1982). The reconstructed watershed model developed in this research is a lumped model, which can be conceptualized in terms of a control volume as shown in Figure 5.1. The control volume diagram illustrates all of the physical processes that are simulated by the developed model. The developed SD watershed model (SDWM) makes optimum use of the extensive monitoring program established for the study site and uses climatic and hydrologic factors to evaluate the hydrologic processes. The simulation of the daily water balance is conducted using four storages representing; (1) surface water, (2) peat layer, (3) till layer, and (4) shale layer. Canopy storage is neglected because the sparse and short nature of the vegetation dominant in the watershed is not considered to intercept significant amounts of precipitation. However, canopy interception will increase over time and should be considered for any future extension of the present work.

Climatological factors (especially temperature and radiation) determine the rate of snowmelt. Rainfall and snowmelt constitute the water available for infiltration and overland flow. Such storage of water is referred to as surface water storage and is a virtual storage used for modeling purposes only. Water from this storage will either infiltrate into the peat layer storage or will be routed as overland flow. Soil moisture affects the amount of infiltrating water. The difference in the form of a feedback between the amount of water available in the surface water storage and infiltrating water comprises overland flow, which discharges to a channel and can be represented in the model as channel storage. Evapotranspiration, interflow, and further infiltration to the till layer are losses from the peat storage.

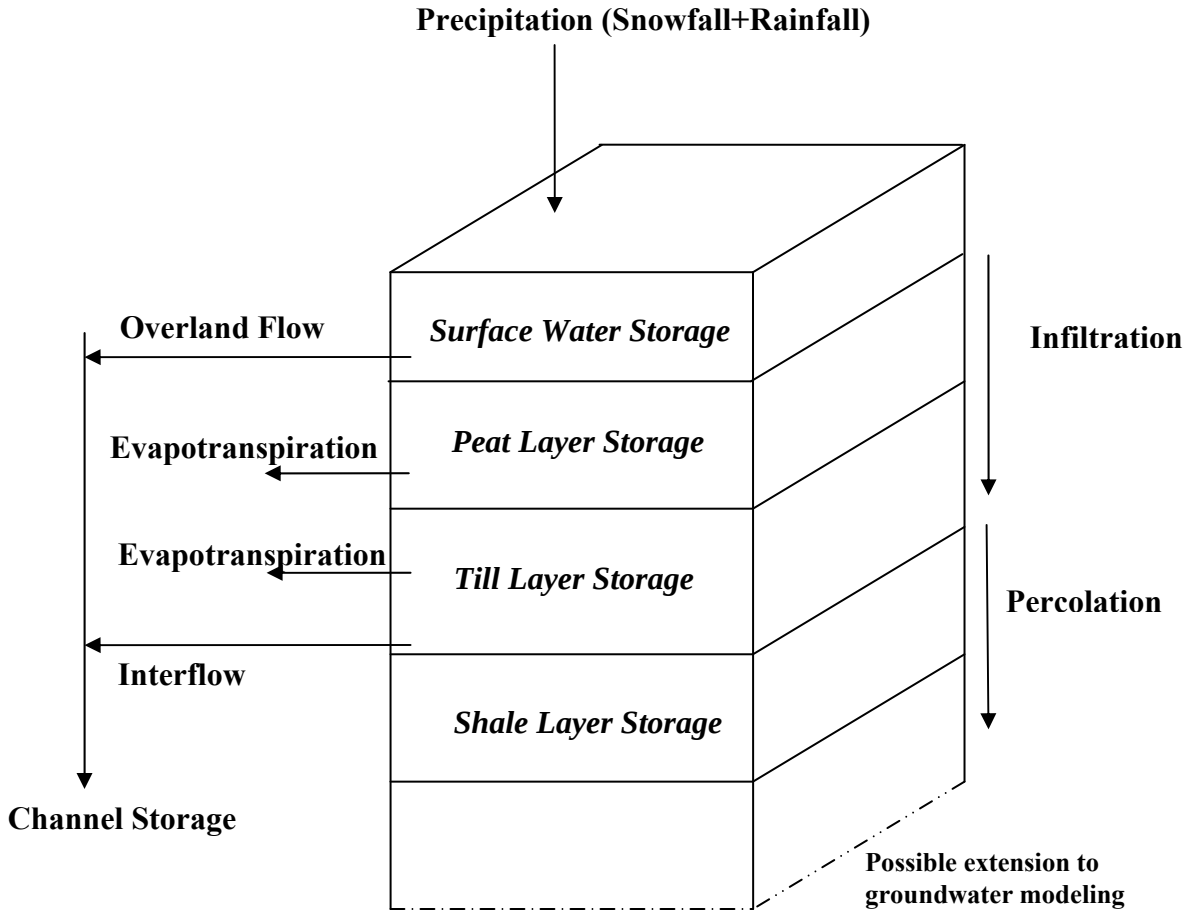

Figure 5.1. Control Volume for the Analysis of Reconstructed Watershed Hydrology.

Evapotranspiration is dependent on moisture and weather conditions. Interflow is a function of the horizontal hydraulic conductivity, water content, and soil temperature. Infiltration into the till layer is dependent on soil temperature, water content within the peat and till layers, and the hydraulic properties of the till layer. Till storage receives water from the peat layer. Losses from the till storage include evapotranspiration, interflow, and percolation to the shale layer (storage). Factors affecting losses from the till storage are similar to those mentioned for the peat storage. In this study, no interflow or base flow from the shale is assumed to be contributing water to the channel. The control volume shown in Figure 5.1 also indicates the possibility for a groundwater modeling component in the SDWM, however, such modeling is not a part of this study.

5.3 Model Realization in System Dynamics: Feedback-loop Diagram

Watershed modeling is a classical application for an SD approach because a watershed can be perceived as an assembly of non-linear dynamic processes controlled by a multiple feedback loop structure. Positive feedback stimulates all factors (or elements) in a loop to

increase or decrease, while a negative feedback loop tends to bring the various elements of the system to an equilibrium state. When any factor (or element) is removed from the system, the negative feedback will work to force the system back into equilibrium (Forrester, 1964). The dynamics (dynamic hypothesis) of the watershed under consideration is sketched as a causal-loop diagram shown in Figure 5.2. External and internal conditions in the watershed influence the various hydrological processes. There are eight feedback loops that govern the entire system (water-balance). Figure 5.2 shows that precipitation in the form of rainfall and snowmelt enters the system and gets stored as surface water storage. In this model, snowmelt rate is accelerated by air temperature. The interactions among the different processes, which are shown in Figure 5.2, are explicitly explained in the following section. The positive and negative signs marked near the arrowheads in Figure 5.2 represent the positive or negative relationships between the first variable and the following one. Table 5.2 mentions the simplified version of Figure 5.2 in order to understand the feedback loops in the reconstructed watersheds.

Loop [1] shows the input of water from surface water storage to the soil system. Water infiltrates to the upper soil layer (peat layer), which increases the amount of water in the layer. With increased soil moisture, the infiltration capacity of the soil decreases, which further limits water entry to the peat layer. During snowmelt, soil thawing results in an increase in the infiltration capacity of the peat layer. Loop [2] describes the evapotranspiration process in the peat layer. An increase in the water content of the peat layer results in increased evapotranspiration, which in turn decreases the peat layer storage. Loop [3] represents the moisture dynamics in the till layer. An increase in peat moisture increases till infiltration. Consequently, an increase in the till moisture content results in decreased infiltration capacity of the till layer, which thereby causes a decrease in the water inflow to the till layer. Loop [4] illustrates the effect of suction in the till layer. An increase in the peat moisture content reduces the suction pressure in the peat layer, which leads to a situation where more water flows into the till layer. However, an increase in the till moisture content reduces the suction pressure in the till layer, which further limits additional water influx. The infiltration capacity of the till layer is also increased when the soil is thawing during the snowmelt process. Loop [5] provides an explanation of the evapotranspiration process in the till layer and is analogous to Loop [2]. Loop [6] explains the interflow from the till layer. Once saturated, the till layer releases excess water as interflow, hence experiences a decrease in its water content. Loop [7] demonstrates the moisture dynamics within the shale layer, which is similar to that of Loop [3]. Loop [8] operates like Loop [4], where the role of suction in the shale layer is highlighted. Loop [7] and Loop [8] are not directly affected by soil defrosting. The whole system has an open loop which ends in overland flow. Any excess water from the system is represented by overland flow or surface runoff, which contributes to channel flow.

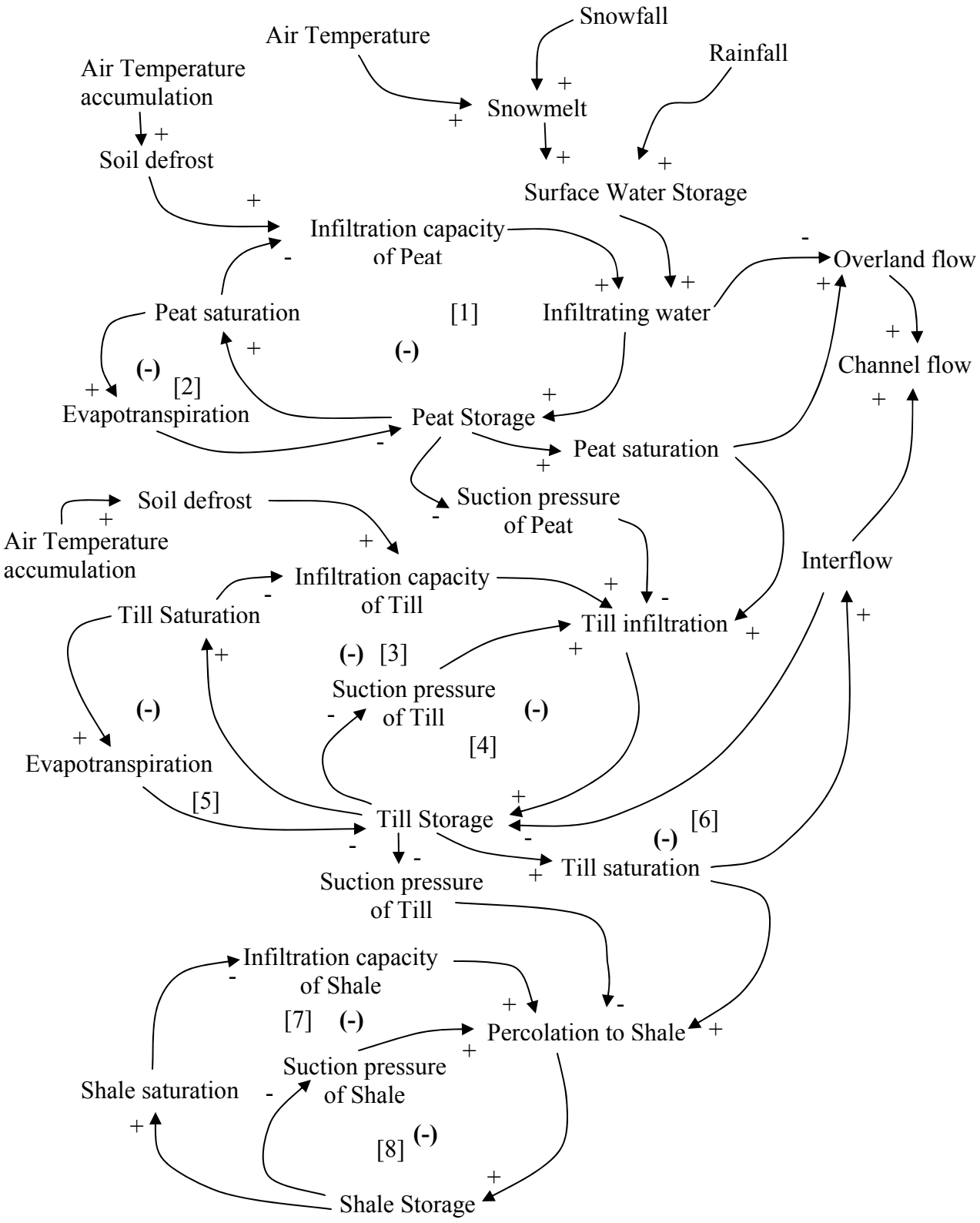

Figure 5.2. Feedback Loop Diagram of the Hydrologic Processes in the Watershed.

Table 5.1: Simplified Notation of Feedback Loops in Reconstructed Watershed

Loop	Description
Loop [1]	Infiltrating water +> Peat Storage +> Peat saturation -> Infiltration capacity of Peat +> Infiltrating water
Loop [2]	Peat Storage +> Peat saturation +> Evapotranspiration -> Peat Storage
Loop [3]	Peat saturation +> Till infiltration +> Till Storage +> Till saturation -> Infiltration capacity of Till +> Till infiltration
Loop [4]	Peat Storage -> Suction pressure of Peat -> Till infiltration +> Till Storage -> Suction Pressure of Till +> Till infiltration
Loop [5]	Till Storage +> Till saturation +> Evapotranspiration -> Till Storage
Loop [6]	Till Storage +> Till saturation +> Interflow -> Till Storage
Loop [7]	Till saturation +> Percolation to shale +> Shale Storage +> Shale saturation-> Infiltration capacity of Shale +> Percolation to shale
Loop [8]	Till Storage -> Suction pressure of Till -> Percolation to shale +> Shale Storage -> Suction Pressure of Shale +> Percolation to Shale

The reconstructed watershed hydrology mentioned in the preceding section through the collection of feedback loops indicates that it is a combination of a closed and an open loop system where each loop adjusts itself according to the effects of other feedback loops. It is worth mentioning here that, in traditional watershed modeling, there is no such formal prior representation of the system structure that helps in understanding the complex interrelationships within the watershed. It is believed that, as a watershed matures over time, the feedback loop structure may require additional loops to enhance the simulation capability of the SDWM, and therefore increase the knowledge base of modelers (hydrologists) as well as designers (geotechnical engineers). For instance, as the watershed evolves, an additional loop will be needed to represent the canopy interception storage. Also, the groundwater table in the waste (overburden) may have some effect on the soil cover and may require an additional feedback loop representing baseflow. However, the scope of this research work is limited to modeling the reconstructed watershed described in Figure 5.2.

5.4 Model formulation

The following sections give an overview of the mathematical formulations of the major hydrologic processes represented in the model. The movement of water in the various layers (storages) of the control volume (Figure 5.1) of the reconstructed watershed is also described.

5.4.1 Surface Water Storage

Precipitation falling as snow accumulates in a storage called surface water storage. In the case of snow, the snowmelt rate is calculated using the degree-day factor (Anderson, 1976). The daily snowmelt can be represented mathematically as:

$$M = D_f\left(T_a - T_b\right) \qquad [5.1]$$

$$D_f = 0.011\rho_s \qquad [5.2]$$

where M is the daily melt (mm/day), T_a is the air temperature (°C), T_b is the base melt temperature (°C), and D_f is the degree-day melt factor in millimetres per degree-day above 0 ^{0}C, and ρ_s is the snow density (kg/m^3). Water accumulated in this storage is released to the peat layer and as overland flow, which are discussed in the following sections.

Mathematically, the change in the surface water storage (S_{SW}) can be expressed as:

$$\frac{dS_{SW}}{dt} = P - f_P - O_F \qquad [5.3]$$

where S_{SW} is the surface water storage (mm), P represents the precipitation (mm/day), which can be in the form of either snow or rainfall, f_P is the infiltration rate to the peat layer (mm/day), and O_F corresponds to overland flow, which is expressed in mm/day.

5.4.2 Peat Layer Storage

Moisture change in the peat storage depends on infiltration from the surface, evapotranspiration, and downward water movement to the underlying till storage. The change of storage in the peat layer can be represented as follows:

$$\frac{dS_P}{dt} = f_P - f_T - ET_P \qquad [5.4]$$

where S_P is the peat storage (mm), f_T is the infiltration rate of the till layer (mm/day), and ET_P is the evapotranspiration rate from the peat layer (mm/day). Before soil saturation occurs, water infiltrates directly through the peat layer (Voinov et al., 2004). In this case, the infiltration rate of the peat layer is equal to the rainfall intensity. If the layer becomes saturated or the rainfall intensity exceeds the saturated hydraulic conductivity of the peat, then the infiltration is governed by the Green–Ampt equation. The infiltration capacity (rate) based on total infiltration volume takes the following form:

$$f_P = K_{sP}\left(1 - \frac{M_P \psi_P}{F_P}\right) \qquad [5.5]$$

$$M_P = \theta_{sP} - \theta_{iP} \qquad [5.6]$$

where K_{sP} is the saturated hydraulic conductivity of the peat layer (mm/day), M_P is the initial moisture deficit (mm), θ_{sP} is the saturated moisture content of the peat layer (%), θ_{iP} is the initial moisture content of the peat layer (%), ψ_P is the suction pressure head at the wetting front in the peat layer (mm), and F_P is the cumulative volume of the infiltration in the peat layer (mm).

There have been attempts by various scientists (Zhao and Gray,1997; Zhao et al., 1997; Zhao and Gray, 1999; Granger et al., 1984; Gray et al., 1985; Gray and Tao, 1994; Gray et al., 2001) to simulate snowmelt infiltration into frozen soils. The literature suggests that some methods are available for quantifying infiltration, however, such methods are data intensive and require much information about the soil properties during frozen conditions. The sensors

used for the measurement of soil moisture at the study research site do not operate at all in frozen conditions (Boese, 2003), hence it was decided to follow a simple parametric approach, which is described in the following section.

Li and Simonovic (2002) used an empirical approach from snowmelt infiltration, which states that the infiltration into frozen soils is affected by the temperature fluctuations and the length of time the temperature stays above and below the active temperature (0 ^{0}C). The phenomenon of temperature fluctuation results in the soil thawing and refreezing. Most hydrologic models either ignore snowmelt infiltration or use a data intensive approach to estimate infiltration into frozen soils. The SDWM assumes that the soil is thawing exponentially with positive air temperature accumulation. However, soil will refreeze if the temperature drops below zero for a number of days. The active temperature accumulation will be lost and will start again from zero (Li and Simonovic, 2002). Snowmelt infiltration is calculated using the set of formulae given in Equation 5.7. Accordingly, the infiltration rate, f_P, is multiplied by a coefficient, C_{tP}, to estimate infiltration into frozen soil.

$$
\begin{aligned}
C_{tP} &= \begin{Bmatrix} (T_I / T_{Imax})^{c_i} & if\ T_I < T_{Imax} \\ 1 & if\ T_I \geq T_{Imax} \end{Bmatrix} \\
T_I &= \begin{Bmatrix} \sum (T_a) & if\ T_a > 0\ and\ N < N_n \\ 0 & if\ N \geq N_n \end{Bmatrix} \\
N &= \begin{Bmatrix} \sum (N_o) & if\ T_a \leq 0 \\ 0 & if\ T_a > 0 \end{Bmatrix} \\
N_o &= \begin{Bmatrix} 1 & if\ T_a \leq 0 \\ 0 & if\ T_a > 0 \end{Bmatrix}
\end{aligned}
\qquad [5.7]
$$

where, T_{Imax} (°C) is a maximum T_I point at which the surface soil is fully thawed, c_i (dimensionless) is an exponent for describing the influence of T_I on soil defrosting, N (days) is the number of continuous days with temperature below the active point, N_n is a maximum N after which T_I will be lost and the surface soil will refreeze again, and N_o is a logical variable to identify the day in which the temperature is higher or lower than the active (positive) air temperature. The two parameters in Equation 5.7, c_i and T_{Imax}, have been estimated during the calibration process in this study.

The actual evapotranspiration from the peat layer is estimated using empirical formulations (Li and Simonovic, 2002) that take into account the available soil moisture and air temperature. These formulations can be expressed as:

$$AET_P = c_P S_{mP}^{\lambda} T_a C_{tP} \qquad [5.8]$$

$$S_{mP} = \frac{\frac{S_P}{S_{nP}} - S_{rP}}{1 - S_{rP}} \qquad [5.9]$$

where AET_P is the actual evapotranspiration rate (mm/day) from the peat layer, c_P is the evaporation constant (mm/^{o}C/day) from the peat layer and is determined during calibration, S_{mP} is the effective moisture saturation in the peat layer (dimensionless), λ is exponential coefficient estimated while calibrating, S_{nP} is the maximum water storage (mm) in the peat layer, and S_{rP} is the minimum storage (wilting point moisture content) that can be attained. S_{rP} and S_{nP} are calculated using the soil water characteristic curve for the peat layer calculated by Boese (2003).

The equations (Eqs. 5.8 and 5.9) used to compute actual evapotranspiration in the developed model take explicit account of the soil moisture and air temperature. Singh (1988) emphasized that soil moisture remains an integral part in the calculation of actual evapotranspiration. Saxton (1982) suggested that, for a small watershed, AET should be calculated using a method that accounts for climatic, crop and soil variables under suitable ranges of soil moisture regimes.

The conventional equations (Penman and Bowen ratio, explained later) for calculating evapotranspiration from the peat layer have also been used. The conventional equations were multiplied by a time varying calibration coefficient to take into account the effect of water uptake by plants during the growing season. However, the empirical formula (Eq. 5.8) for evapotranspiration produced better simulation results. It can be interpreted that the empirical formula takes the available soil moisture into account, which indicates less evapotranspiration when the moisture is low and suction pressure is high. A similar conclusion has been provided by Elshorbagy et al (2005). It was concluded that AET estimation using a parametric equation (Eq. 5.8) is appropriate in sub-humid regions where soil moisture could be a limiting factor for evapotranspiration. This type of approach has been taken by Li and Simonovic (2002), Voinov et al. (2004), and Saysel and Barlas (2001), who used parametric equations to model complex natural systems and obtained encouraging results. Models built within an SD approach work better with empirical formulations since the empirical formulations dynamically link the different components of the system together (e.g., soil moisture and evapotranspiration). Moreover, Forrester (1980b) unambiguously concluded that "empirical evidence is the driving force for delineating the micro-structure of the model and for verifying its behaviour although the information concerning behaviour may reside in historical data and that concerning the micro-structure in experience."

In the developed model, it is assumed that evapotranspiration (ET_P) from the peat layer will occur only if the air temperature is greater than 0°C and the peat layer temperature is greater than 0°C. The peat layer releases water as ET_P when the moisture content in the layer is above the wilting point moisture content.

5.4.3 Till Layer Storage

Moisture movement in the till layer depends on the moisture conditions in the peat layer, soil suction in the peat and till layers, soil temperature of the till layer, evapotranspiration from the till layer and percolation to the shale layer. The mathematical relationship expressing the moisture dynamics of the till layer storage (S_T) is represented as:

$$\frac{dS_T}{dt} = f_T - I_n - f_S - ET_T \quad [5.10]$$

where I_n is the interflow rate (mm/day), f_S is the shale percolation rate (mm/day) and ET_T is the evapotranspiration rate from the till layer (mm/day). There is no movement of water from the peat layer to the till layer if the moisture content in the peat layer is less than the wilting point. In the summer, when the soil temperature of the till layer is greater than zero, water will move down from the peat layer to the till layer following the Green–Ampt equation in the case of a fully saturated soil:

$$f_T = K_{sT}\left(1 - \frac{M_T \psi_T}{F_T}\right) \quad [5.11]$$

$$M_T = \theta_{sT} - \theta_{iT} \quad [5.12]$$

where, f_T is the infiltration rate (capacity) of the till layer (mm/day), K_{sT} is the saturated hydraulic conductivity of till layer (mm/day), M_T is the initial moisture deficit (mm), θ_{sT} is the saturated moisture content of the till layer (%), and θ_{iT} is the initial moisture content of the till layer(%), ψ_T is the pressure head in the till layer (mm) and F_T is the cumulative volume of the infiltration in the till layer.

The peat layer will release water only when the moisture content in the peat layer is greater than the wilting point moisture content. In a case of a saturated till layer, the maximum rate at which water can be absorbed by the till layer will correspond to the saturated hydraulic conductivity of the till layer. Otherwise, the following logic will apply:

if (soil temperature of till greater than 0 °C)
then (if ($\Psi_P > \Psi_T$)
then (no movement of water)
else (if ($\theta_P >$ *wilting point moisture content in peat layer*)
then (if (*peat layer is saturated*)
then (follow Eq. 5.11)
else (follow Equation 5.13))
else (no movement of water))
else (follow the same concept used for frozen peat layer))

where Equation 5.13 is an empirical equation which can be written as:

$$f_T = \frac{\theta_P}{\theta_T}\frac{S_P}{\Delta t} I_{cT} \quad [5.13]$$

where I_{cT} is the coefficient of till infiltration (unitless), which is determined during calibration of the model, and Δt is the solution time interval. The equation works on a simple principle, which states that the moisture redistribution from the peat to the till layer is strongly dependent on the moisture contents in both layers. The simulation results obtained by using the equation are encouraging. Under frozen conditions, the same concept followed in the peat layer (i.e., Eq.5.7) is replicated for the till layer to estimate C_{tT}, the till infiltration coefficient. The only difference is that the air temperature in Equation 5.7 is replaced by the temperature of the peat layer.

Actual evapotranspiration from the till layer is treated in the same way as that in the peat layer and is computed using the following equations:

$$AET_T = c_T S_{mT}^{\lambda} T_{sP} C_{tT} \quad [5.14]$$

$$S_{mT} = \frac{\frac{S_T}{S_{nT}} - S_{rT}}{1 - S_{rT}} \quad [5.15]$$

where AET_T is the actual evapotranspiration rate (mm/day) from till layer, c_T is the evapotranspiration constant (mm/^{o}C/day) from the till layer estimated while calibrating the model, S_{mT} is the effective moisture saturation in the till layer (dimensionless), λ is an exponent determined while calibrating the model, S_{nT} is the maximum water storage (mm) in the till layer, S_{rT} is the minimum storage (wilting point moisture content) that can be attained, and T_{sP} is the temperature of the peat layer (^{0}C). S_{nT} and S_{rT} are determined from the soil water characteristic curve for the till layer mentioned in Boese (2003). There will be no loss of moisture through evapotranspiration if the moisture level in the till layer is below the wilting point moisture content. The evapotranspiration (ET_T) from the till layer is computed only when the soil temperature of the peat and till layers is greater than zero.

Actual evapotranspiration is also calculated using the Bowen Ratio method (Eqs. 5.16 and 5.17). A Bowen ratio station is present at the research site, however, the station occasionally fail to record observations. In that case, Penman`s equations (Eq. 5.18) derived in Mays (2005) is used to compute the potential evapotranspiration

$$AET_B = L_e = \frac{R_n - G}{1 + \beta} \quad [5.16]$$

$$\beta = \frac{H}{L_e} = \frac{PC_p(T_1 - T_2)}{\lambda_{le}\varepsilon(e_1 - e_2)} \quad [5.17]$$

$$PET_{PM} = \frac{R_n 86720}{2.5E^6 - 2370T_a}\left(\frac{\Delta}{\gamma + \Delta}\right) + \frac{0.102u}{77.52}\left(e_s - e_s R_H\right)\left(\frac{\gamma}{\gamma + \Delta}\right)$$

$$\Delta = \frac{2503878e^{\frac{17.27T_a}{237+T_a}}}{(237 + T_a)^2} \quad [5.18]$$

where T_1 (^{0}C), e_1 (mm) and T_2(^{0}C), e_2 (mm) is the temperature and vapour pressure at two different heights, P is the atmospheric pressure, β is the Bowen Ratio, λ_{le} is the latent heat flux density, ε is the ratio of molecular weight of water to molecular weight of dry air, C_p is the specific heat of air, L_e is the latent heat (potential evapotranspiration, PET_B), R_n is the net radiation from the soil surface, H is the sensible heat flux, and G is the total the soil heat flux. The term $\frac{PC_p}{\lambda_{le}\varepsilon}$ is also known as the psychrometric constant and value of 66.9 mm/^{0}C has been used in the model. Penman`s equations take the following form. PET_{PM} is the potential

evapotranspiration using the Penman formulae, Δ is the slope of the psychrometric saturation line (mm/^{0}C), γ is the psychometric constant (mm/^{0}C), u is the wind speed (m/s) at 2 m height, e_s is the saturated vapour pressure (mm) and R_H is the relative humidity (%).

As developed, the model eliminates the possibility of the calculated actual evapotranspiration exceeding the potential evapotranspiration in the case of unlimited soil moisture. At each time step, the model computes the ratio R_a, which is the ratio of calculated actual evapotranspiration from the peat layer to the total actual evapotranspiration from the soil covers (peat and till layers):

$$R_a = \frac{AET_P}{AET_P + AET_T} \qquad [5.19]$$

The ratio, R_a, is then multiplied with the potential evapotranspiration to obtain PET from the peat layer only. If the numerical value is less than the calculated AET_P from the peat layer, then the model uses the product of R_a and potential evapotranspiration to estimate the actual evapotranspiration from the peat layer. Similarly, in the till layer, if the computed AET_T is more than the product of (1-R_a) and the potential evapotranspiration, then the model discards the computed AET_T value and calculates the actual evapotranspiration using the product of (1-R_a) and the potential evapotranspiration.

The till layer is responsible for interflow occurring in the watershed. In this study it is assumed that there is no direct contribution of interflow from the peat layer. Interflow (I_n, *mm/day*) from the till layer is estimated as follows:

$$I_n = \left(\frac{S_T}{\Delta t} - \frac{\theta_{sT} D_T}{\Delta t} \right) C_i \qquad [5.20]$$

where D_T is the depth of the till layer (mm) and C_i is the interflow coefficient determined during the calibration of the model. Interflow in the SDW model will only occur if the temperature of the till layer is greater than 0 °C and the till layer is fully saturated. However, if the temperature of the peat layer is less than 0 ^{0}C and the soil temperature of the till layer is greater than 0^{0}C, then interflow is computed by multiplying the interflow coefficient by the rate of water available in the till storage. When the peat layer freezes in early winter, the moisture content in the till layer may decrease while there is no increase in the moisture content in the lower layer (shale) or upper layer (peat). The only way water can be lost from the till layer is through interflow or seeps into the shale layer. It can be interpreted that the till layer may lose some water as interflow at the onset of the winter season. This postulation has not been verified by the field measurements; hence its validity is arguable at this point. Further field investigations are required to understand the physics of the process.

5.4.4 Shale Layer Storage

Moisture change in the shale storage depends on percolation from the till layer. The moisture movement in the shale storage (S_S) can be represented as:

$$\frac{dS_S}{dt} = f_S \quad [5.21]$$

Water will percolate from the till layer to the shale layer following the Green–Ampt equation in the case of a fully saturated soil, viz.

$$f_S = K_{sS}\left(1 - \frac{M_S \psi_S}{F_S}\right) \quad [5.22]$$

$$M_S = \theta_{sS} - \theta_{iS} \quad [5.23]$$

where f_S is the infiltration rate (capacity) of shale layer in mm/day, K_{sS} is the saturated hydraulic conductivity of the shale layer (mm/day), M_S is the initial moisture deficit in the shale layer(%), θ_{sS} is the saturated moisture content(%) of the shale layer and θ_{iS} is the initial moisture content(%) of the shale layer, Ψs is the suction head of the shale layer (mm) and F_S is the cumulative volume of the percolation in the shale layer.

The till layer will release water only when the moisture content in the till layer is greater than the wilting point moisture content in the till layer. In the case of a saturated shale layer, the maximum rate at which the water can move into the shale layer will correspond to the saturated hydraulic conductivity of the shale layer. Otherwise, the following logic will apply:

if ($\Psi_T > \Psi_S$)
then (no movement of water))
else (if ($\theta_T > \theta_{rT}$ *wilting point moisture content in the till layer*)
then (if (*till layer is saturated*)
then (follow Eq. 5.22)
else (follow Equation 5.24))
else (no movement of water))

Equation 5.24 is similar to equation 5.13 and takes the following form:

$$f_S = \frac{\theta_T}{\theta_S}\frac{S_T}{\Delta t} I_{cS} \quad [5.24]$$

where I_{cS} is the coefficient of till infiltration and is determined during calibration of the model, and θ_S is the moisture content of the shale layer.

5.4.5 Overland Flow

Overland flow is estimated after satisfying the various soil moisture demands. Since the model structure uses reservoir-based mechanisms to simulate the different hydrological processes, water in excess of the infiltration capacity of the peat layer is directed as overland flow (O_F) in the summer. During frozen conditions, part of the available water (AW) from both rainfall and snowmelt infiltrates into the frozen soil (Eq 5.7), while the remaining portion contributes to overland flow. In the summer, the overland flow occurs only when the peat layer becomes saturated and is computed as follows:

$$O_F = \frac{S_{SW}}{\Delta t} - f_P \quad [5.25]$$

where the units of O_F are mm/day.

5.5 Modified Evapotranspiration Equation

It is often argued in the hydrologic literature that radiation plays an important role in calculating evapotranspiration (Saxton, 1982). Equation 5.8, which is used in the model, does not have any radiation term associated with it. The equation makes use of both temperature and soil moisture to compute actual evapotranspiration. However, the literature also suggests that temperature and radiation based potential evapotranspiration models tend to be more efficient than others (Oudin et al., 2005). Based on a survey of the literature and modeling experience gained in this research work, a modified equation for calculating the evapotranspiration is proposed:

$$AET = c\, S_m^{\left\{\frac{\lambda}{T}\right\}} R_n \quad [5.26]$$

$$S_m = \frac{\frac{S_t}{S_n} - S_r}{1 - S_r} \quad [5.27]$$

where AET is the actual evapotranspiration rate (mm/day), c and λ are calibration parameters, S_t is the soil moisture at any time (mm), S_n is the maximum possible soil moisture (mm), S_r is the wilting point moisture content (mm), and T is the temperature of the overlying layer. The above equations (Eqs 5.26-5.27) are combination of radiation, temperature and soil moisture, which goes according to the above proposed hypothesis that the temperature and radiation plays an important role in estimating AET. Since the equation takes into account the soil moisture, it can effectively represent the amount of water to be released by transpiration. The equation was tested against the data available from the Eddy Covariance Method (Oke, 1992). The results obtained from Equation (5.26) are encouraging. However, this equation is not considered for the simulation in the present study as it depletes the moisture levels in the peat and till layers. (More discussion on the results obtained from this equation is mentioned in Chapter 6.)

5.6 Calibration and Validation

The description of the model structure and formulation shows that the developed model (SDWM) is a combination of process-based and empirical formulations, which minimizes the number of parameters that need to be calibrated. Calibration of watershed models is generally done by comparing and analyzing observed and simulated streamflow data (Singh, 1988; Ambroise et al., 1995). Lumped models, such as the SDWM developed in this study, use various storages for simulating the water balance (Ye et al., 1997). Movement of water from one storage to another is usually defined by a threshold principle, such as the maximum amount of water that the soil can store. Such models are difficult to calibrate using streamflow data time series alone because the exceedence of the threshold may not occur for

certain conditions, such as for soils with high porosity or under dry climatic conditions. In such cases, the model parameters obtained using streamflow data do not necessarily represent the true conditions of the internal watershed processes. However, the hydrologic literature reports only a few instances where calibration of watershed models has been done using multiple observed variables (Wooldridge et al., 2003). The developed SDWM is a nine parameter model and has been calibrated using trial and error methodology. Root Mean Square Error (RMSE) and Mean Relative Error (MRE) were the performance indicators of model performance. The equations for estimation of RMSE and MRE are mentioned as:

$$RMSE = \sqrt{\frac{\sum_{i=1}^{n}(O_i - S_i)^2}{n}} \quad [5.28]$$

$$MRE = \frac{\sum \left| \frac{O_i - S_i}{O_i} \right|}{n} \quad [5.29]$$

where O_i is the observed data at each time step, S_i is the simulated value and n is the total number of data points. Overall performance of the model in simulating the peat and till layer moisture is calculated using the following formula

$$OP = \frac{\sum_{i=1}^{n} \left(\left| \frac{(S_{SP_i} + S_{ST_i}) - (O_{SP_i} + O_{ST_i})}{(O_{SP_i} + O_{ST_i})} \right| \right)}{n} \quad [5.30]$$

where OP is the overall performance, S_{SP} and S_{ST} are simulated peat and till layer moisture levels, respectively, and O_{SP} and O_{ST} are observed peat and till layer moisture levels, respectively. Calibration has been done by testing the overall performance of the model based on soil moisture in the various soil layers and overland flow. Details on the calibration and validation of the developed model are discussed in Chapter 6.

Chapter 6

Results and Analysis

This chapter deals with the results obtained from the model developed in this research. Data requirements for the System Dynamics Watershed Model (SDWM) are described, followed by a discussion of the calibration and validation of the model. The subsequent sections are discussion of the results obtained from the simulation of the model for the three sub-watersheds (D1, D2, and D3).

6.1 Data Requirements

The SDWM is developed using a combination of empirical and conceptual equations and requires various input data for simulation of the hydrological processes in the reconstructed watersheds. In general, the developed model uses soil and metrological data for estimation of the watershed response. The input variables required to run the model are listed in Table 6.1. The metrological data are primarily used to estimate potential evapotranspiration. Bowen ratio calculations require net radiation and air temperature, as well as an estimation of the vapour pressure at two different heights (2.00 m and 3.18 m). Alternatively, the combined formula of Penman uses net radiation, saturated vapour pressure, wind speed, and relative humidity. Soil data (soil temperature, porosity) are used to define the feedback loops for moisture movement in the soil layers. Soil water characteristic curves are required to estimate the suction pressures for each time step as a function of the volumetric moisture content. The Green-Ampt formula requires information pertaining to soil moisture, saturated hydraulic conductivity, and suction pressure at every time step to calculate the infiltration rates for the various soil layers. Water from the soil layer cannot evaporate beyond wilting point moisture content of the respective soil layer. Soil temperatures play a major role in determining the frozen status of the soil. If the soil temperature is below 0^0C, then the soil is categorized as frozen. The initial moisture content is required for the soil state variables (Peat Layer Storage, Till Layer Storage, and Shale Layer Storage).

The porosity (saturated moisture content) of the peat layer in all the three sub-watersheds (D1, D2, D3) was taken to be 50% (Shurniak, 2003). The porosity of the till and shale layers in all of the watersheds has a value of 54% and 25%, respectively (Boese, 2003). The saturated hydraulic conductivity for the peat, till and shale layers were taken as 17 cm/hr, 2.1 cm/hr and 0.03 cm/hr, respectively (Shurniak and Barbour, 2002). The wilting point moisture contents for the peat, till and shale layers are 10%, 11%, and 10%, respectively (Boese, 2003). The soil water characteristic curves (SWCC), shown in Figure 6.1, were taken from the work done by Shurniak (2003). The data to create the SWCC was obtained from field measurements of volumetric moisture content and pore pressure at various depths within the soil layer of each sub-watershed

Table 6.1: Data Requirements for the SDWM

Data	Variables
Meteorological Data	Air temperatures at two heights (^{0}C) (2.00 m and 3.18 m)* Vapour pressure at same two heights as for air temperatures (mm)* Mean air temperature (^{0}C) Saturated vapour pressure of air (mm of water) Daily net radiation (W/m^2) Mean daily wind speed at 2 m height (m/s) Mean daily relative humidity (%)
Soil Data **(for Peat, Till, and Shale layers)**	Saturated moisture content (%) Saturated hydraulic conductivity (mm/day) Soil Water Characteristic Curve Mean daily soil temperature (^{0}C) Wilting point moisture content (%) Thickness of soil layer (mm) Initial moisture content (mm)

* Used for calculation of PET using the Bowen Ratio method. Alternatively, the model can be run using the combined equation of Penman.

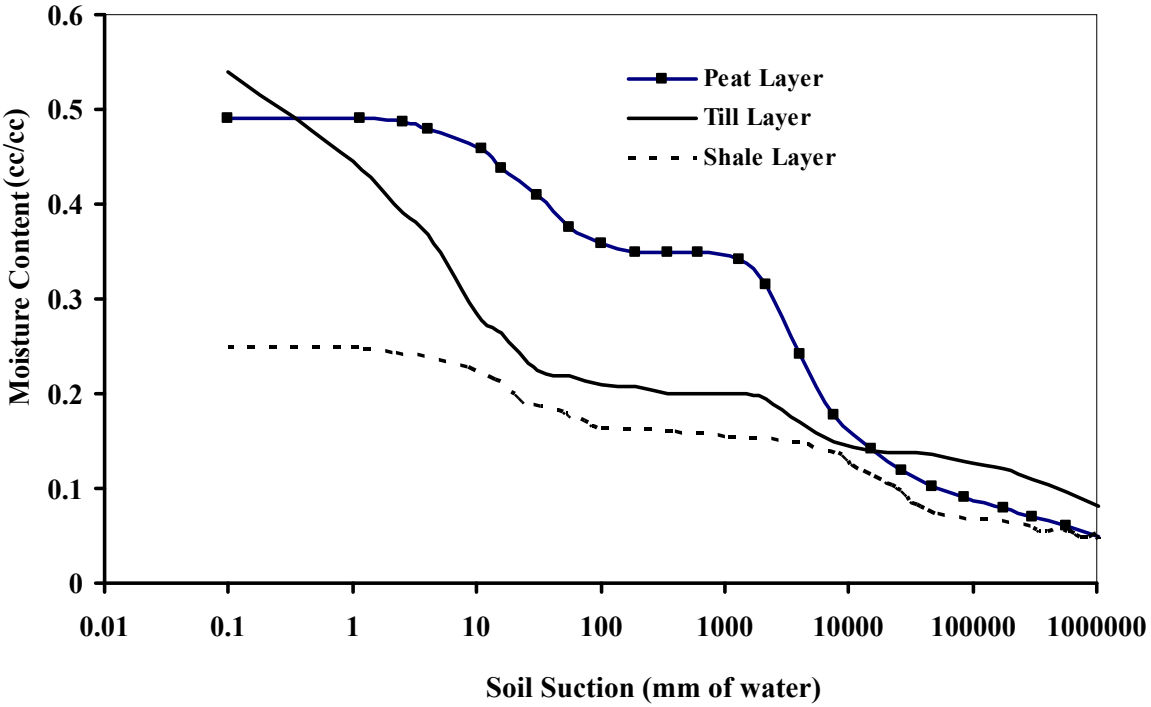

Figure 6.1. SWCC for Peat, Till and Shale Layers (Shurniak, 2003).

6.2 Calibration and Validation of the SDWM

The description of the model structure and formulation shows that the developed model (SDWM) needs to be calibrated and validated before running any possible scenarios for watershed simulation. The reconstructed watersheds are expected to go through a number of changes over time. The probable changes include growth of vegetation, subsidence, and change in hydraulic conductivity. The time needed for the reconstructed watersheds to reach hydrologic stability cannot be estimated with certainty. Such time is dependent on physical changes that occur in the soil cover such as how quickly vegetation develops, natural settlement of the soil matrix owing to subsidence, and so on. The dynamic evolution of reconstructed watersheds makes the exercise of calibrating and validating a mechanistic watershed model a challenging one. The concept of a split sample for the calibration/validation of a model is based on the fact that the data set is stationary over the entire record. However, this is not the case for the dynamic watershed under consideration. Although the watershed is evolving and stable parameters could not be estimated at this stage, yet acceptable values of model parameters is required to be determined so that the structure of the developed model could be evaluated. Hence, the process of calibration and validation of the SDWM in the present study is intended to verify the model construction and formulations used in the model only.

The watersheds were constructed in 1999 (Boese, 2003). Hence, it is expected that large changes in the soil properties will have occurred during year 2000 (porosity, saturated hydraulic conductivity, etc.). Such an expectation is corroborated by the measured field values of saturated hydraulic conductivity, which are presented in Table 6.2 for three years (2000, 2001, and 2002). The saturated hydraulic conductivity for the peat layer increased 400% between years 2000 and 2001. The same type of trend can be seen in the other two soil layers. However, there is relatively less change in the saturated hydraulic conductivity between years 2001 and 2002. Hence, in this study, year 2001 is used for calibrating the model, while year 2002 is used for validation purposes. Sub-watershed D3 was chosen for calibration and validation purposes. Soil cover thickness of sub-watershed D3 meets the requirements of 1m established by the Alberta Government. It is suggested that the soil cover (sub-watershed D3) with 1 m soil capping, will have more moisture holding capacity. Hence in this study, it is assumed that the existing guidelines for reconstructed watersheds design will yield a stabilized watershed. Sub-watershed D3 meets all such requirements, therefore was selected for calibration and validation purposes.

The values of total annual precipitation in 2001 and 2002 are 367 mm and 337 mm, respectively. The precipitation is distributed mainly between soil moisture (peat, till, and shale) storage and evapotranspiration. The model was calibrated and then validated using the parameters listed in Table 6.3, which were obtained by calibrating the model. There is a chance that more than one parameter set can produce the same hydrologic output. This phenomenon is commonly referred to as equifinality of the model parameters (Beven, 2000). However, analysis of equifinality is not a part of this research work. It is recommended that future work should be directed towards a sensitivity and optimality analysis of the parameters of the SDWM

Table 6.2: Average Field Measurements of Saturated Hydraulic Conductivity (cm/s) of the Soil Cover and Waste Materials in the three Sub-watersheds (Meiers, 2002)

Year	Peat	Rate of increase in Peat	Till	Rate of increase in Till	Shale	Rate of increase in Shale
2000	8.0×10^{-4}		3.0×10^{-6}		2.0×10^{-7}	
		400%		6500%		900%
2001	4.0×10^{-3}		2.0×10^{-4}		2.0×10^{-6}	
		5%		100%		200%
2002	6.0×10^{-3}		4.0×10^{-4}		6.0×10^{-6}	

.

Table 6.3: Calibration and Validation Parameter Values (Sub-Watershed D3)

Parameter	Value
Till infiltration (I_{cT}) (dimensionless)	0.05
Shale infiltration (I_{cS}) (dimensionless)	0.60
Exponent describing the influence of T_I on soil defrosting (c_i) (dimensionless)	5
Maximum T_I point at which surface soil is fully defrosted (T_{Imax}) (^{0}C)	50
Interflow coefficient (C_I) (dimensionless)	0.001
Peat evapotranspiration (c_P) (mm/day^{0}C)	7.5
Till evapotranspiration (c_T) (mm/day^{0}C)	4
Lambda (λ) (dimensionless)	4.8
Melt factor (dimensionless)	1.9

A summary of the model performance with regard to the simulated soil moisture is provided in Table 6.4. Calibration of the SDWM was done using a trial and error method to minimize the Mean Relative Error (MRE) and Root Mean Square Error (RMSE) with regard to the soil moisture. Observed and simulated overland flow and soil moisture were used to evaluate the model performance during calibration and validation. The performance of the model, given the dynamic nature of the watershed, indicated by the values of the MRE and RMSE mentioned in Table 6.4, is satisfactory.

Table 6.4: Simulation Accuracy of Soil Moisture during Calibration and Validation

	Year	MRE (%)	RMSE (mm)	Average Moisture (mm)
Peat	2001	12	6	41
	2002	8	5	51
Till	2001	4	10	189
	2002	9	21	186
Overall	2001	7	16	230
	2002	9	21	237
Calibration year: 2001 Validation year: 2002				

The simulated and observed daily soil moisture in the peat layer for year 2001 and 2002 are shown in Figure 6.2 and Figure 6.3, respectively. RMSE and MRE values in calibration year, 2001, are 12% and 6 mm respectively while in validation year, 2002, the respective values are 8% and 5 mm. The figures show a good agreement between the simulated and observed moisture content in the peat layer in both the years. Discontinuities of the observed values in the figures are due to missing data. It should be noted that comparison between the predicted and observed data in the winter season should be done with extreme caution. TDR sensors used to monitor the soil moisture content failed to provide reliable readings under frozen conditions (Boese, 2003). Hence, in this research, it is assumed that the sensors did not work during the entire time that the soil temperature was below 0^0C. The last moisture observation when the soil temperature was positive is taken as the last correct moisture observation recorded by the sensors. The moisture observations on subsequent days were subtracted from the preceding day's moisture content to get an estimate of the net change in moisture content in a day. This difference obtained in the moisture content was then added to the moisture content when the soil temperature was positive. In this way, the moisture content was corrected so that the temporal trend in the moisture data could be saved. Therefore, the simulations start in January using the last moisture reading when the soil temperature was positive, not using the moisture reading of January 1st. Figure 6.4 and Figure 6.5 show the observed and simulated till layer moisture for year 2001 and 2002, respectively. The SDWM satisfactorily simulated the soil moisture within the till layer. MRE and RMSE values for year 2001 in the till layer are 4% and 10 mm, respectively. In the validation year (2002), MRE and RMSE values for till layer moisture are 9% and 21 mm, respectively.

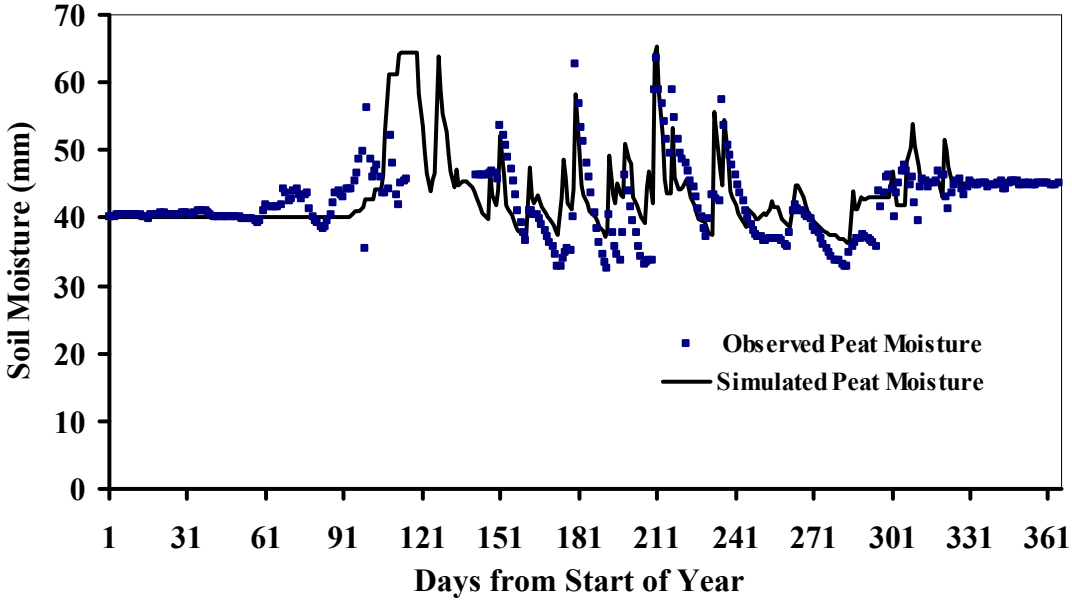

Figure 6.2. Observed and Simulated Soil Moisture in the Peat Layer in Sub-Watershed D3 in Year 2001 (Calibration).

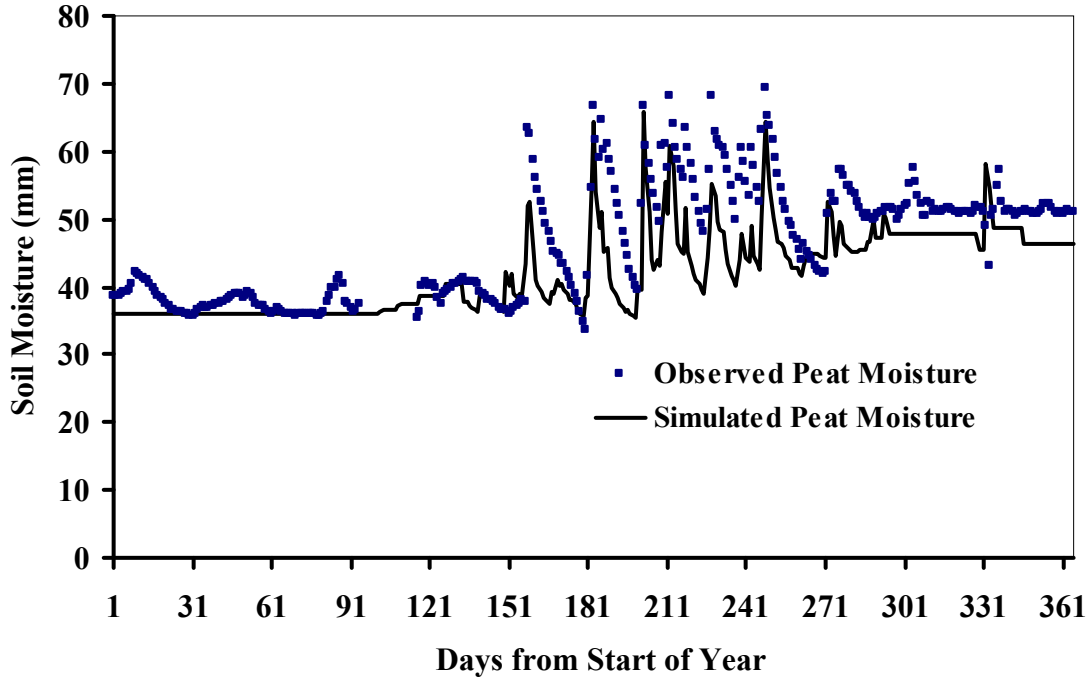

Figure 6.3. Observed and Simulated Soil Moisture in the Peat Layer in Sub-Watershed D3 in Year 2002 (Validation).

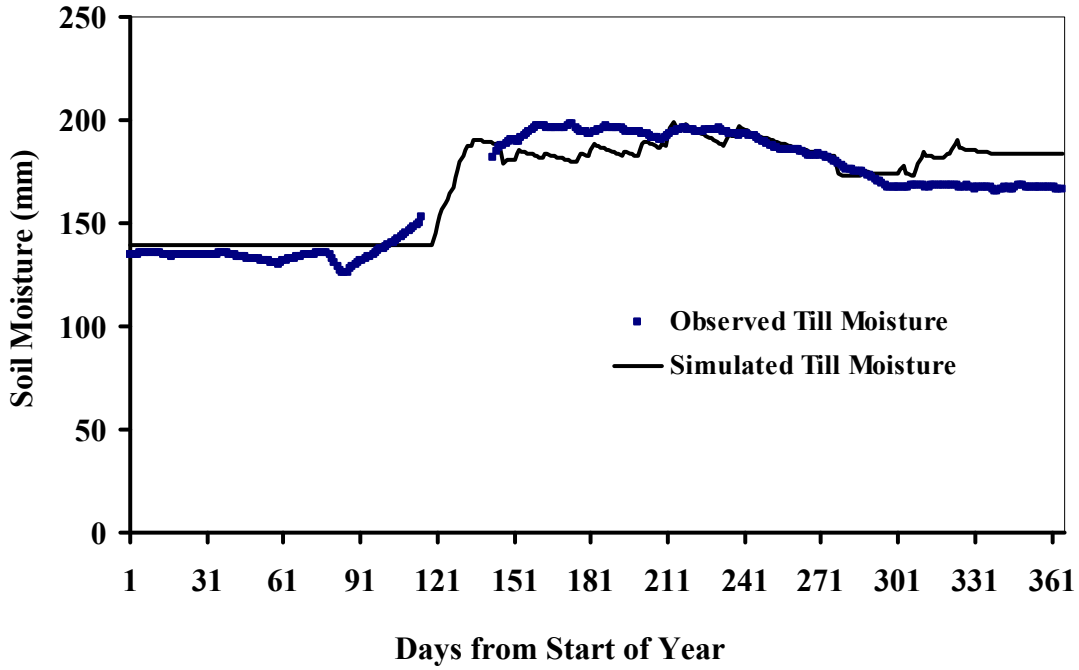

Figure 6.4. Observed and Simulated Soil Moisture in the Till Layer in Sub-Watershed D3 in Year 2001 (Calibration).

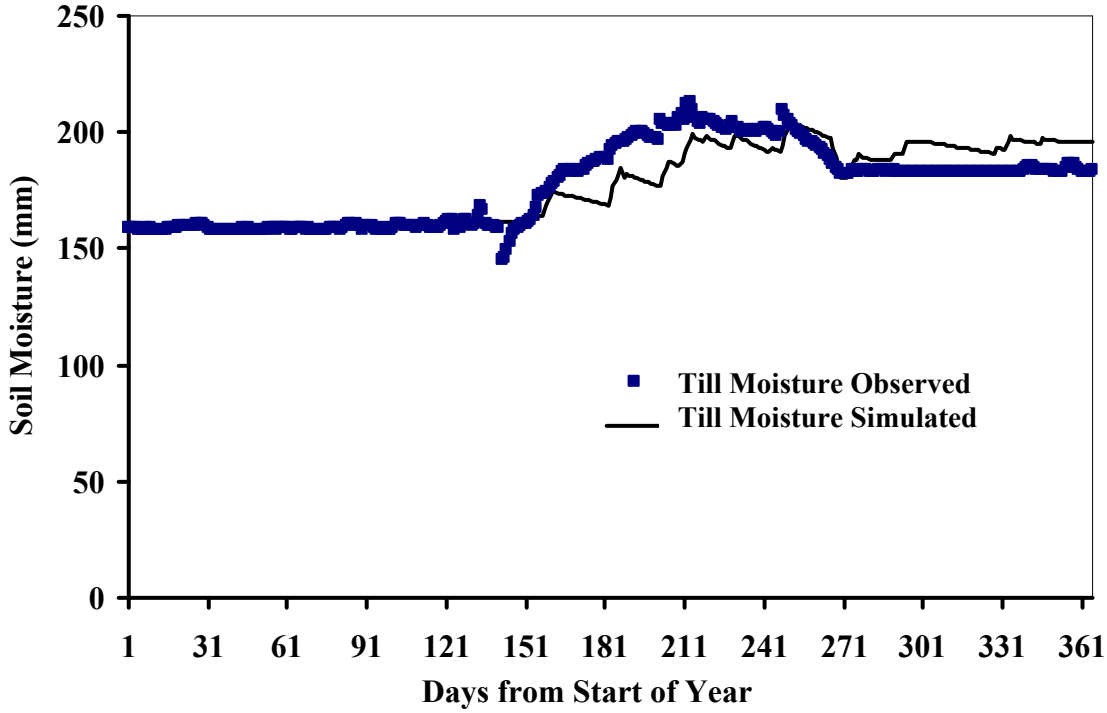

Figure 6.5. Observed and Simulated Soil Moisture in the Till Layer in Sub-Watershed D3 in Year 2002 (Validation).

Moisture observations in the shale layer are available for the top 50 cm of the layer only. Hence, only the top 50 cm of the shale layer is considered for simulating the shale moisture content, which is shown in Figure 6.6 and Figure 6.7. Field personnel have indicated that considerably less reliability can be associated with the moisture readings in the shale layer, especially below the upper 50 cm. The TDR sensors work efficiently when there is a change in moisture content. Simulation results show that water starts to percolate into the shale layer at the start of the winter season, which is close to day 265 as shown in Figure 6.6 and 6.7. However, such increase in water in the shale layer needs to be verified in the field, which is beyond the scope of this research work.

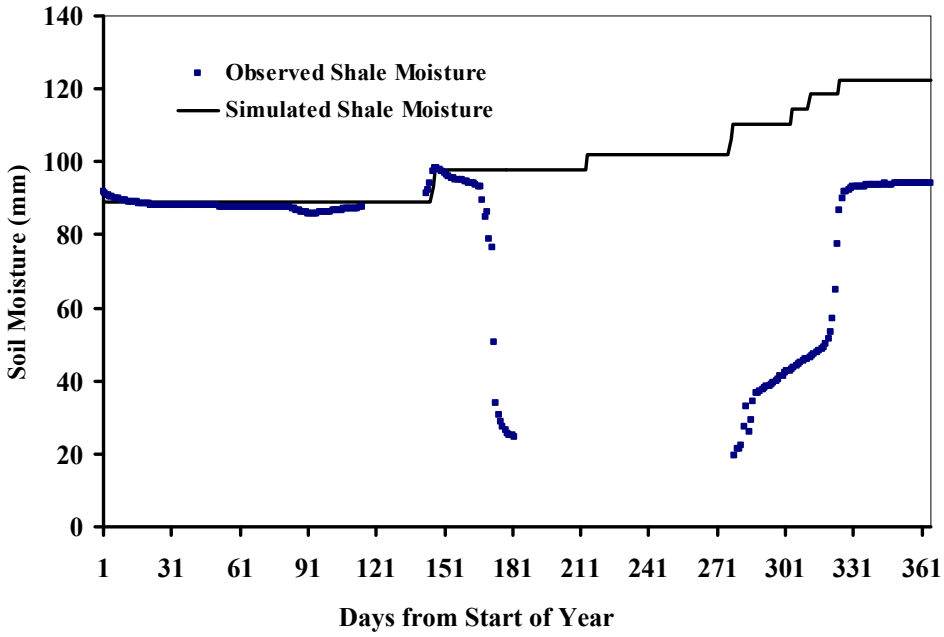

Figure 6.6. Observed and Simulated Soil Moisture in the Shale Layer in Sub-Watershed D3 in Year 2001 (Calibration).

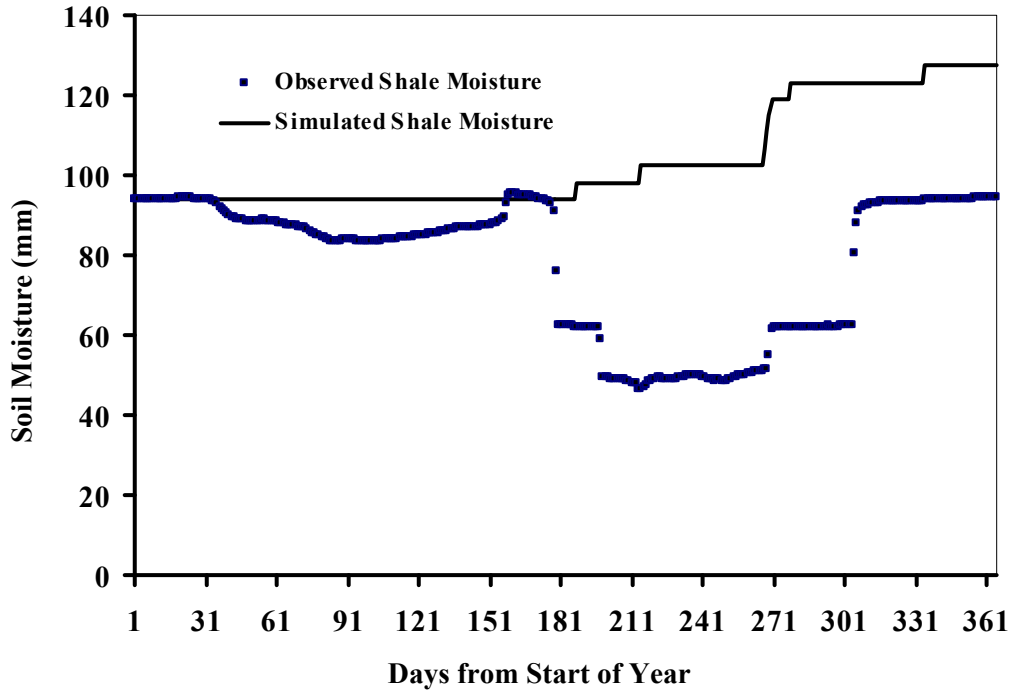

Figure 6.7. Observed and Simulated Soil Moisture in the Shale Layer in Sub-Watershed D3 in Year 2002 (Validation).

Severe drops in the observed shale moisture (Figure 6.6 and Figure 6.7) are impossible to interpret from a physical perspective, knowing that such drops indicate that the shale layer

has been drained to a level much below that of the wilting point moisture. Failure of the moisture sensors can be the only reasonable interpretation, and this is supported by the observations of field personnel.

Figure 6.8 and Figure 6.9 show the observed and simulated overland flow in the calibration and validation years, respectively. The model performance in simulating runoff is less accurate than its performance with regard to soil moisture, however it is plausible given the fact that the reconstructed watersheds are extremely low yielding, and runoff is a sudden event due to snowmelt and may not constitute a significant portion of the water balance. In the calibration year, the model produced an early runoff event due to significant increases in air temperature, which apparently translated into snowmelt. Runoff trapped in small depressions before reaching the swale at the bottom of the sub-watershed and the absence of accurate snow surveys (actual snow depth at the time of melt) could be among the possible reasons for such a discrepancy. It is worth noting that the challenge and the distinctive feature of the case under consideration is that simulation of the soil moisture within the various layers is the main vehicle used to validate the model performance. This differs from the traditional watershed simulation in which runoff is used to judge the performance of the watershed model.

Figure 6.10 is a plot of the cumulative volume of interflow observed in the four years for all of the sub-watersheds. The graph suggests that sub-watershed D3 has yielded a total of 3 mm in four years followed by sub-watershed D2 (1.36 mm) and D1 (0.81 mm). These values reflect the insignificance of interflow with respect to the overall water balance.

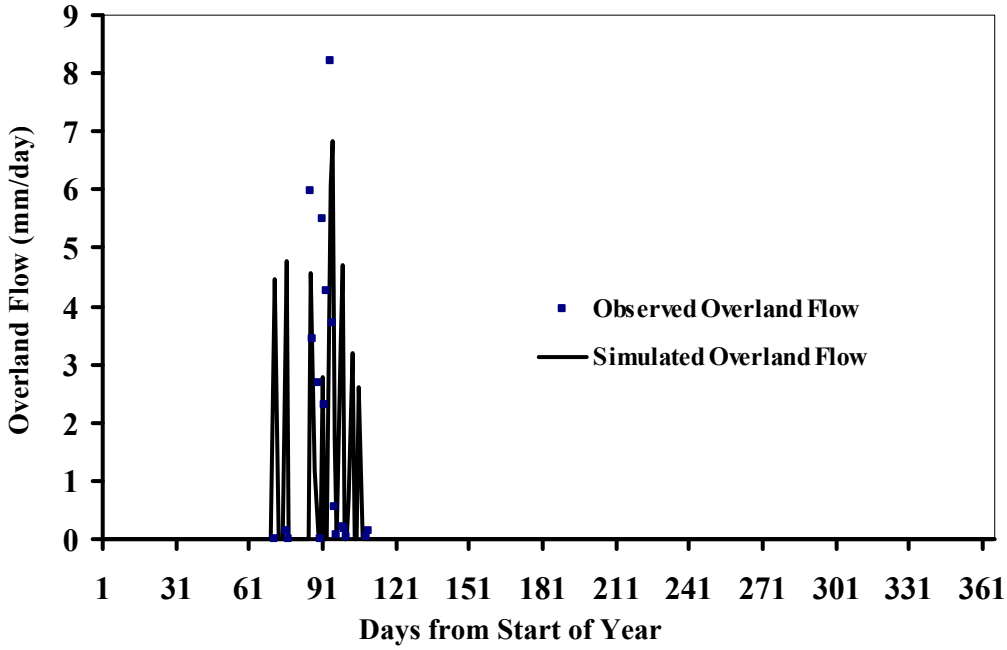

Figure 6.8. Observed and Simulated Overland Flow in Sub-Watershed D3 in Year 2001 (Calibration).

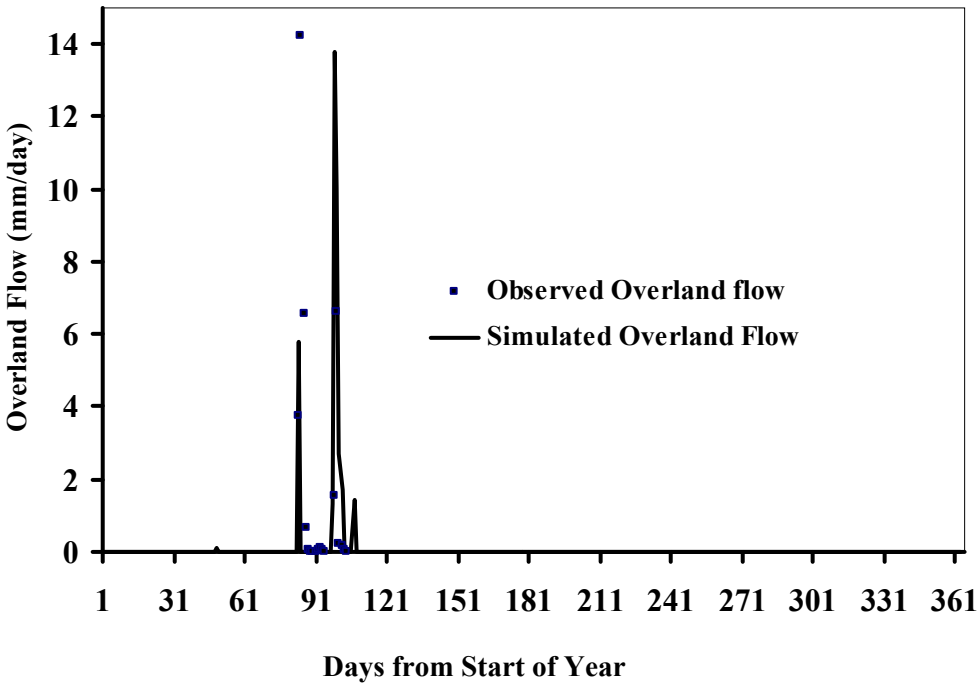

Figure 6.9. Observed and Simulated Overland Flow in Sub-Watershed D3 in Year 2002 (Validation).

The amount of observed interflow in all of the sub-watersheds is very small and ephemeral; it is not possible to capture interflow using the developed SDWM.

6.3 Simulation Results

The hydrologic response of the three sub-watersheds (D1, D2, and D3) is described in this section. Detailed assessment of the watershed response as well as insight into the hydrologic evolution of the watersheds are described.

It has been shown in Table 6.2 that the saturated hydraulic conductivities of the different soil layers in the watershed has been increasing with time. The primary objective behind construction of the reconstructed watersheds is that it should mimic a natural watershed. In that case, the change in the saturated hydraulic conductivity with time is expected to be minimal. With a change in the hydraulic conductivity of the soil layer in the watershed with time, the moisture dynamics between the soil layers also changes over time (Haigh, 2000). It is difficult to estimate the time at which the reconstructed watershed will stabilize. Given the dynamic nature of the watershed, it was not possible to yet determine a set of parameters that could be used for simulating the watershed response for all years i.e., dynamic equilibrium does not yet appear to have been achieved.

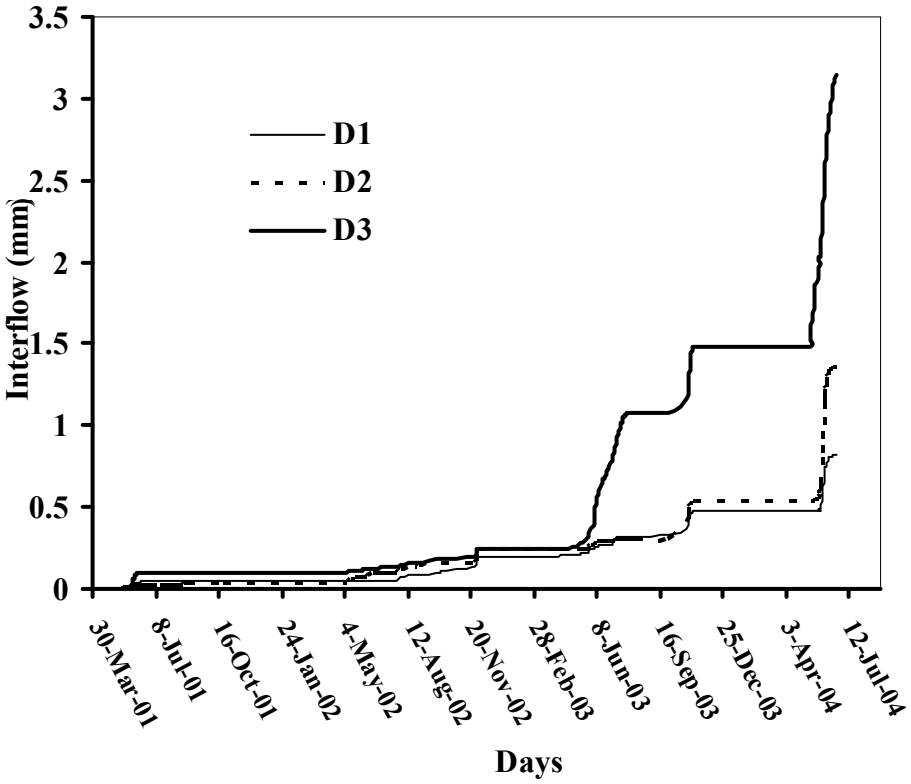

Figure 6.10. Cumulative Interflow Volume per Unit Area in Various Sub-Watersheds in 2001-2004

In this research, a novel approach is proposed and utilized. After finalizing the model structure, as well as the traditional calibration and validation process, the dynamic behavior of the model parameters was analyzed in an attempt to form a dynamic hypothesis with regard to the watershed evolution. The model parameters were fine-tuned every time watershed response for a different year was simulated. The purpose of this procedure was to investigate the existence or absence of trends in the model parameters over time.

6.3.1 Sub-watershed D1

6.3.1.1 Simulation results

Sub-watershed D1 is an intermediate watershed in terms of the thickness of the three existing soil covers (Figure 4.2). The hydrological processes in the watershed were simulated using the developed SDWM for a five year period (2000-2004). Although the watershed was constructed in the summer of 1999, the instrumentation only became fully functional in the late summer of the same year. Hence the incomplete data of year 1999 was not used in the simulation. Since the watershed is evolving over time, the model parameters were changed using a trial and error methodology so as to achieve the minimum possible MRE and RMSE values in each simulation year. The simulated hydrologic response of the watershed was compared with the observed field values. Table 6.5 shows the statistics of the model

performance in the various soil layers and the overall performance (weighted average) for all five years. The overall performance in terms of MRE ranges from 5% to 9%.

Table 6.5: Performance of the Model in Five Years in Sub-Watershed D1.

Year	MRE (%)		RMSE (mm)		Overall Performance
	Peat	Till	Peat	Till	MRE (%)
2000	10	10	6	5	5
2001	6	8	6	4	7
2002	9	11	7	9	9
2003	10	11	8	6	7
2004	17	9	10	6	9

Figure 6.11 presents the observed and simulated moisture contents in the peat layer for year 2000. The figure shows good agreement between the observed and simulated peat moisture content. The MRE for the peat layer is 10% whereas the RMSE for the layer is 6 mm. Visual observation of the simulated and observed moisture contents also demonstrates that the model has satisfactorily simulated the soil moisture dynamics in the peat layer. The soil is recharged during snowmelt (March-April). Since there is very little runoff and interflow in the watershed, most of the water is lost through evapotranspiration from the peat layer. The peat layer moisture is close to the wilting point moisture content (10%) by the end of the summer season due to the absence of rainfall and withdrawal of water by plants in summer season. However, the soil moisture was quickly replenished whenever there was a rainfall event during the summer season. The winter observations are arguable at this stage as the sensors measuring the soil moisture in the winter season failed to provide reliable values of soil moisture. While the summer moisture is adequately simulated by the model, the winter moisture needs further field verification. Such verification work is beyond the scope of this report.

Figures 6.12 to 6.15 presents the simulated and observed results of the soil moisture in the peat layer for years 2001 to 2004. The performance of the model in terms of MRE and RMSE values is shown in Table 6.5. The peat layer moisture in year 2001 shows a similar trend to that of year 2000. However, the average moisture content (60 mm) in the peat layer in year 2001 (Figure 6.12) is more than the moisture in the previous year (45 mm) in the summer season. This could be due to the fact that year 2001 received more rainfall events in the summer season. Figure 6.13 shows the soil moisture status for year 2002. The simulated moisture in the peat layer is responding to the corresponding rainfall events.

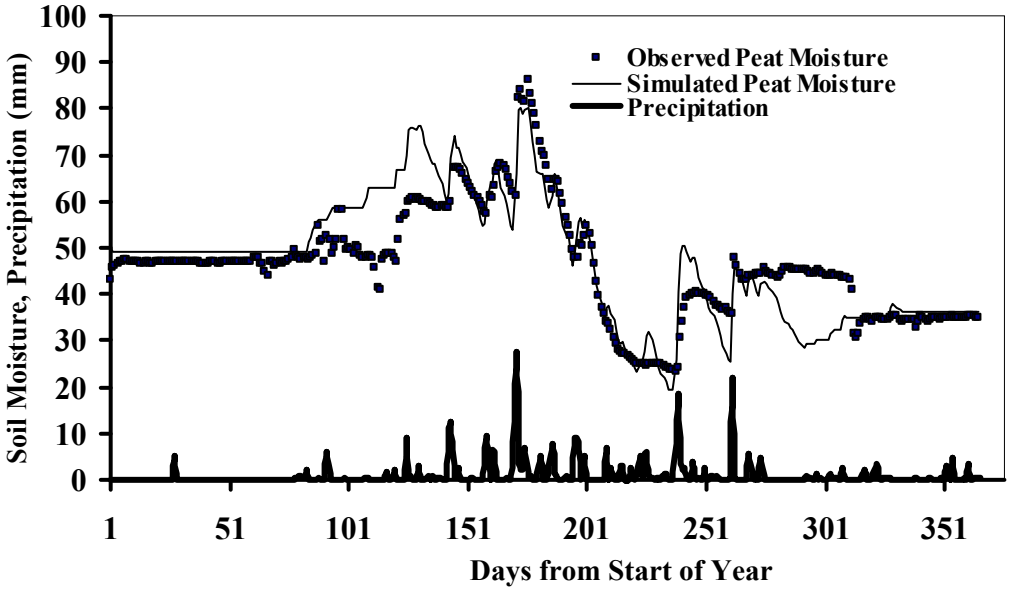

Figure 6.11. Simulated and Observed Moisture Content in the Peat Layer in Sub-Watershed D1 (Year 2000).

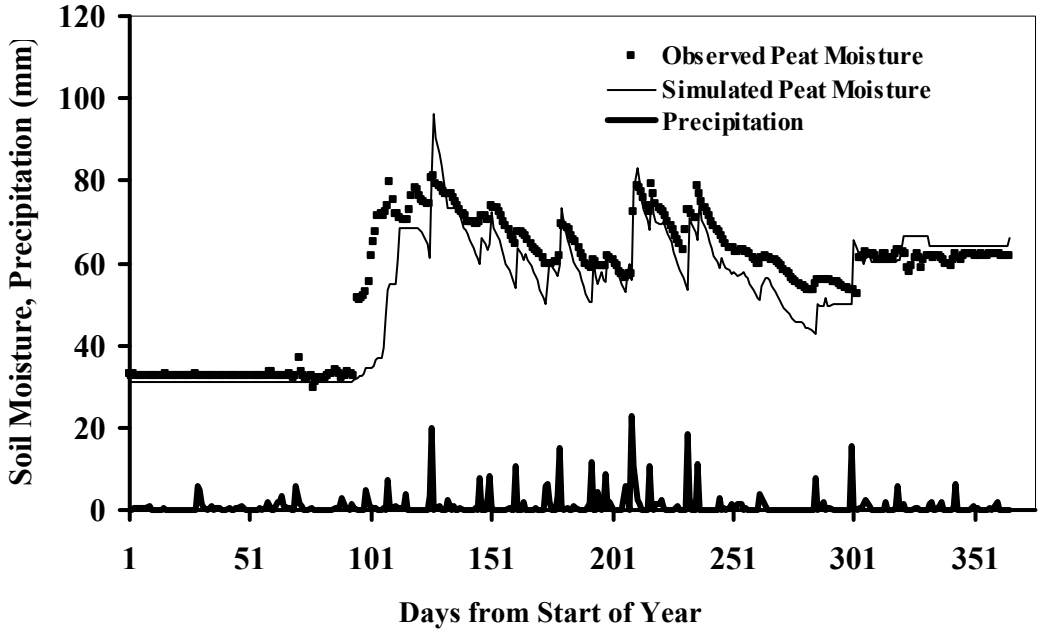

Figure 6.12. Simulated and Observed Moisture in the Peat Layer in Sub-Watershed D1 (Year 2001).

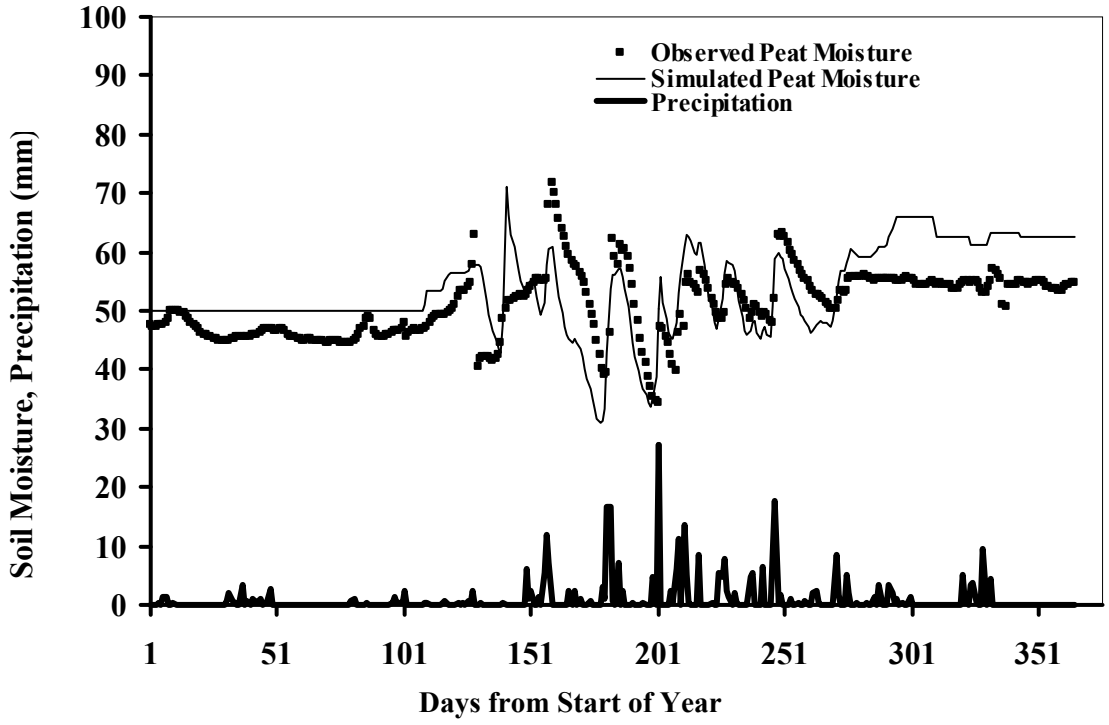

Figure 6.13. Simulated and Observed Moisture in the Peat Layer in Sub-Watershed D1 (Year 2002).

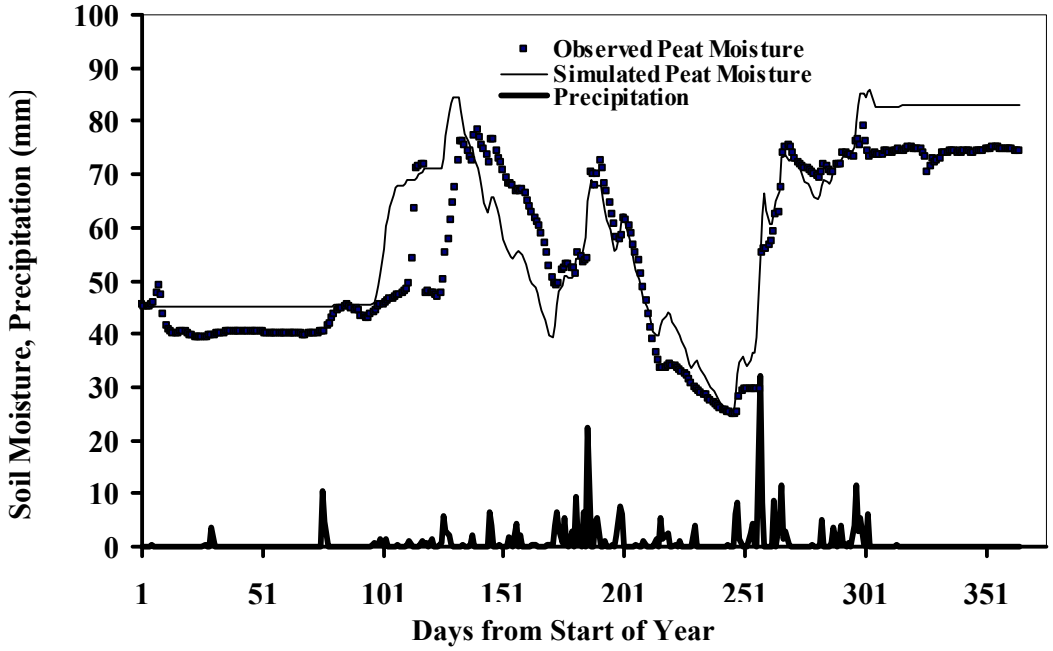

Figure 6.14. Simulated and Observed Moisture in the Peat Layer in Sub-Watershed D1 (Year 2003).

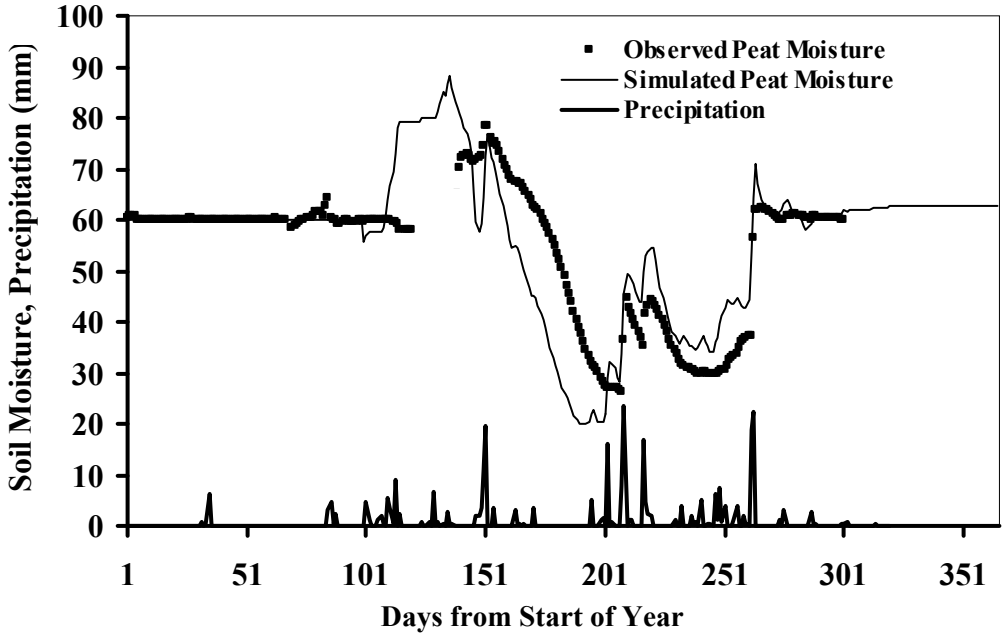

Figure 6.15. Simulated and Observed Moisture in the Peat Layer in Sub-Watershed D1 (Year 2004).

The simulated and observed soil moisture in the peat layer in year 2003 is shown in Figure 6.14. The soil is recharged during snowmelt. The rainfall events in year 2003 kept the soil recharged throughout the whole year. Figure 6.15 shows the simulated and observed peat layer moisture results, which appear to be different from the previous years. The peat layer is recharged during snowmelt but the moisture level decreases continuously as the summer advances. This is due to the fact that the plants may have consumed most of the water. The number of rainfall events also play major role in recharging soil moisture. For instance, a year with four rainfall events of 5 mm/day each would recharge the soil moisture more than a single rainfall event of 20 mm/day. In years 2003 and 2004, the rainfall events are higher in magnitude but less in number. As a result of a lesser number of rainfall events, the soil is not recharged and water is lost by evapotranspiration.

The performance of the model in simulating the till layer moisture in sub-watershed D1 is summarized in Table 6.5. The simulated and observed soil moisture in the till layer for year 2000 is shown in Figure 6.16. The water content in the till layer increases during snowmelt in year 2000 and decreases as the summer advances. The till moisture content in year 2000 is not significantly affected by the variation in the rainfall. In such a sub-humid region like the study area, most of the water is retained within the peat layer (Figure 6.11) during the growing season. However, as the moisture level in the peat layer decreases in the absence of prolonged rainfall, the moisture level in the till may also decrease. This might be due to the fact that water is lost by the evapotranspiration process from the till layer. Again, the winter observations are not reliable.

Figure 6.17 shows the observed and simulated moisture levels in the till layer in the year 2001. The soil is recharged at the onset of the spring season through snowmelt and loses water during the growing season. However, the loss of moisture from the till layer is less than the peat layer in the same year. Since the watershed was constructed in 1999, it is expected that the vegetation may not have a developed deep root system, and therefore there is a possibility that evapotranspiration may occur more in the peat layer.

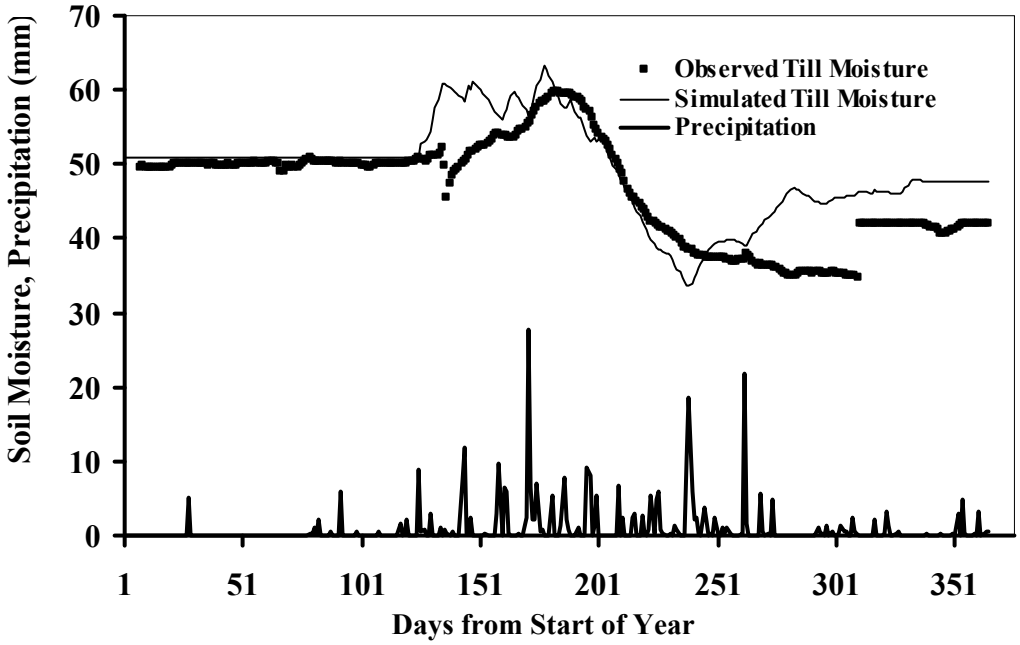

Figure 6.16. Simulated and Observed Moisture in the Till Layer in Sub-Watershed D1 (Year 2000).

The simulated and observed till moisture dynamics for the year 2002 are shown in Figure 6.18. The MRE and RMSE values are 11% and 9 mm, respectively. The model is simulating the increase in the moisture content during snowmelt. During the summer season, soil moisture may be lost through evapotranspiration. There is good possibility that by year 2002 some of the roots of shrubs and grasses may have penetrated into the till layer so as to allow consumption of water for metabolic activities. Explicit account of vegetation and its effects are beyond the scope of this research work.

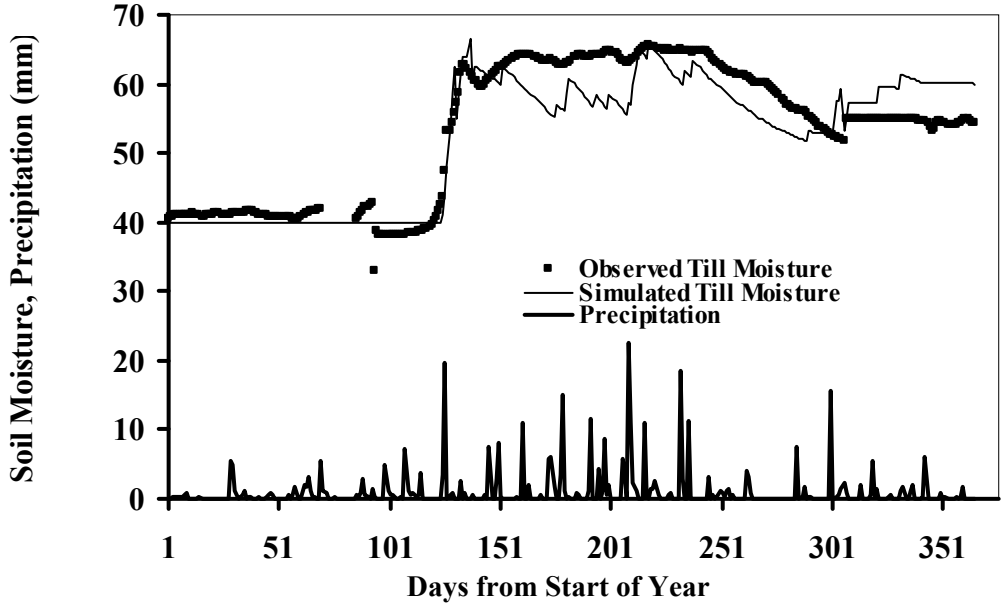

Figure 6.17. Simulated and Observed Moisture in the Till Layer in Sub-Watershed D1 (Year 2001).

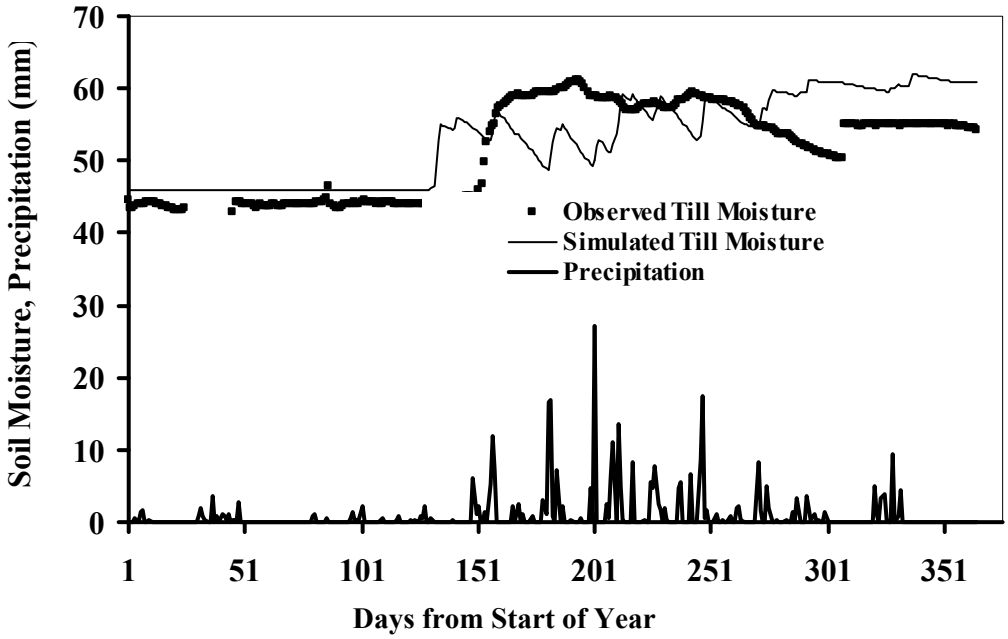

Figure 6.18: Simulated and Observed Moisture in the Till Layer in Sub-Watershed D1 (Year 2002).

Figure 6.19 and Figure 6.20 show the simulated and observed results for years 2003 and 2004, respectively. Both years had relatively fewer rainfall events during the growing season as compared to the other three years (2000-2002). As a result, most of the water from the peat and till layers is depleted through evapotranspiration. Consequently, with any rainfall event, the suction pressure of the peat layer decreases and momentarily the suction pressure in the till layer increases. Hence, water abruptly moves down to the till in the particular time step.

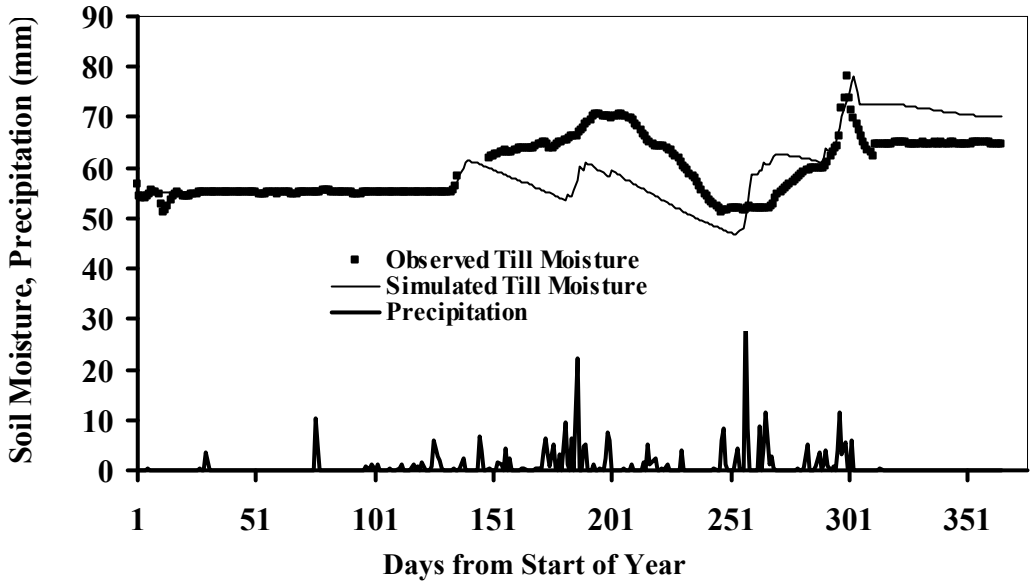

Figure 6.19. Simulated and Observed Moisture in the Till Layer in Sub-Watershed D1 (Year 2003).

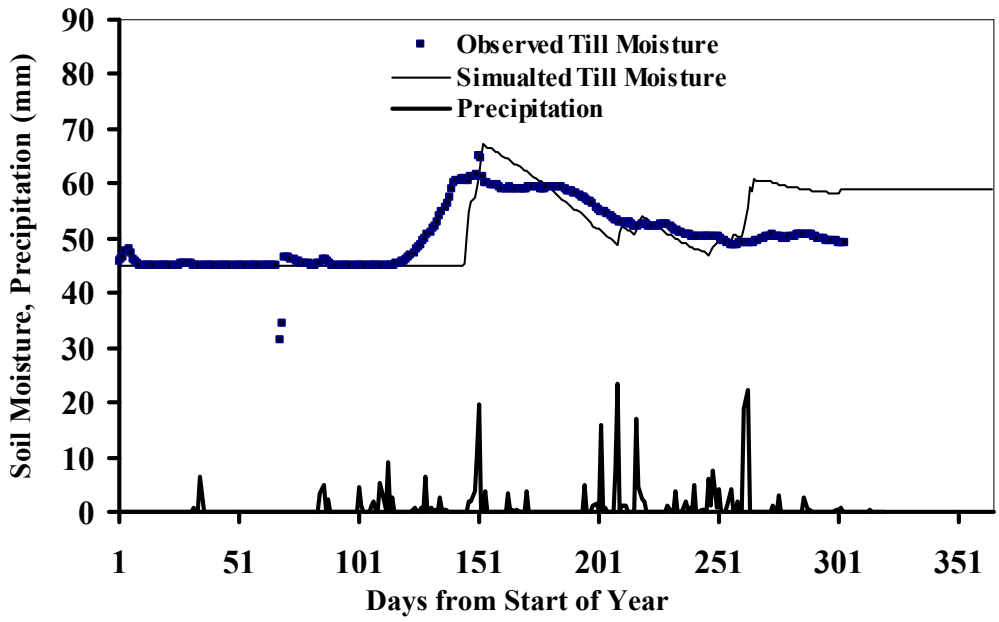

Figure 6.20. Simulated and Observed Moisture in the Till Layer in Sub-Watershed D1 (Year 2004).

Figure 6.21 shows the observed and simulated overland flow in sub-watershed D1 for all five years (2000-2004). The observation with regard to Figure 6.21 is that there is no runoff event in the entire year except during the spring snowmelt. This is due to the fact that the saturated hydraulic conductivity of the peat layer is very high (61200 cm/s). In order to produce runoff during any precipitation event, the intensity of the rainfall must be higher than that of the peat layer or the duration of the rainfall event should be long enough to cause saturation of the peat layer. At the current study site, there was not even a single rainfall event with an intensity higher than that of saturated hydraulic conductivity of the peat layer. Hence for all precipitation events, all of the water was absorbed by the peat layer. However, the situation is different during snowmelt as free water is available on the surface of the frozen peat layer. The free water forms a thin sheet, which flows as overland flow.

The model fails to simulate the peak runoff rates in years 2003 and 2004. This might be due to the location of the weirs that were used to measure overland flow. The overland flow is measured at the toe of the watershed in a swale. This could mean that there is a possibility of formation of ice dams along the slope. The water recorded as overland flow in the swale may have additional water coming from ice dam breaks, which is difficult to quantify and simulate.

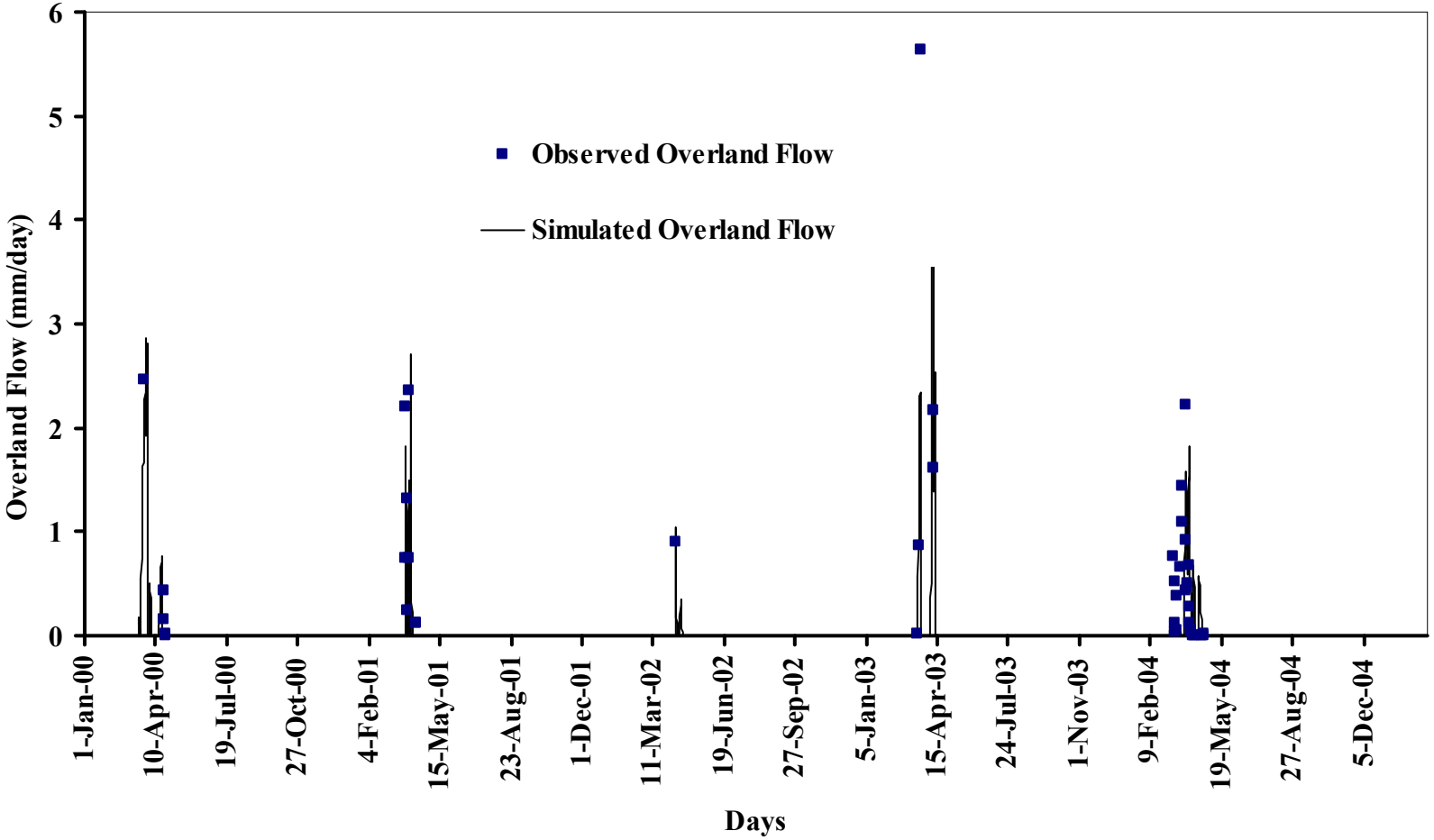

Figure 6.21. Simulated and Observed Overland Flow Measured at the Toe of Sub-Watershed D1.

Figure 6.21 also suggests that the model cannot be validated for any simulation on the basis of overland flow alone. Thus joint validation, as done in this study, with some other hydrologic variable (soil moisture, evapotranspiration) is mandatory. This strengthens the observation made by Wooldridge et al. (2003) that hydrologic models should have more than one checkpoint for validation. The calibration and validation done using two or more hydrologic variables reduces some of the uncertainty frequently encountered in the simulation of hydrologic processes in a watershed (Wooldridge et al., 2003).

The observed and simulated soil moisture in the shale layer is shown in Figure 6.22. According to the field personals, observed shale moisture observations are reliable however the model results indicate, there is not much change in the shale moisture levels in all five years. Therefore, the upper soil layers (peat and till layers) are retaining most of the precipitation. It also suggests that there is very low deep percolation occurring in the watershed. Low percolation to the lower soil (overburden) is one in the primary requirements of the design of reconstructed watersheds. However, with available data of five years, it is difficult to make any conclusions.

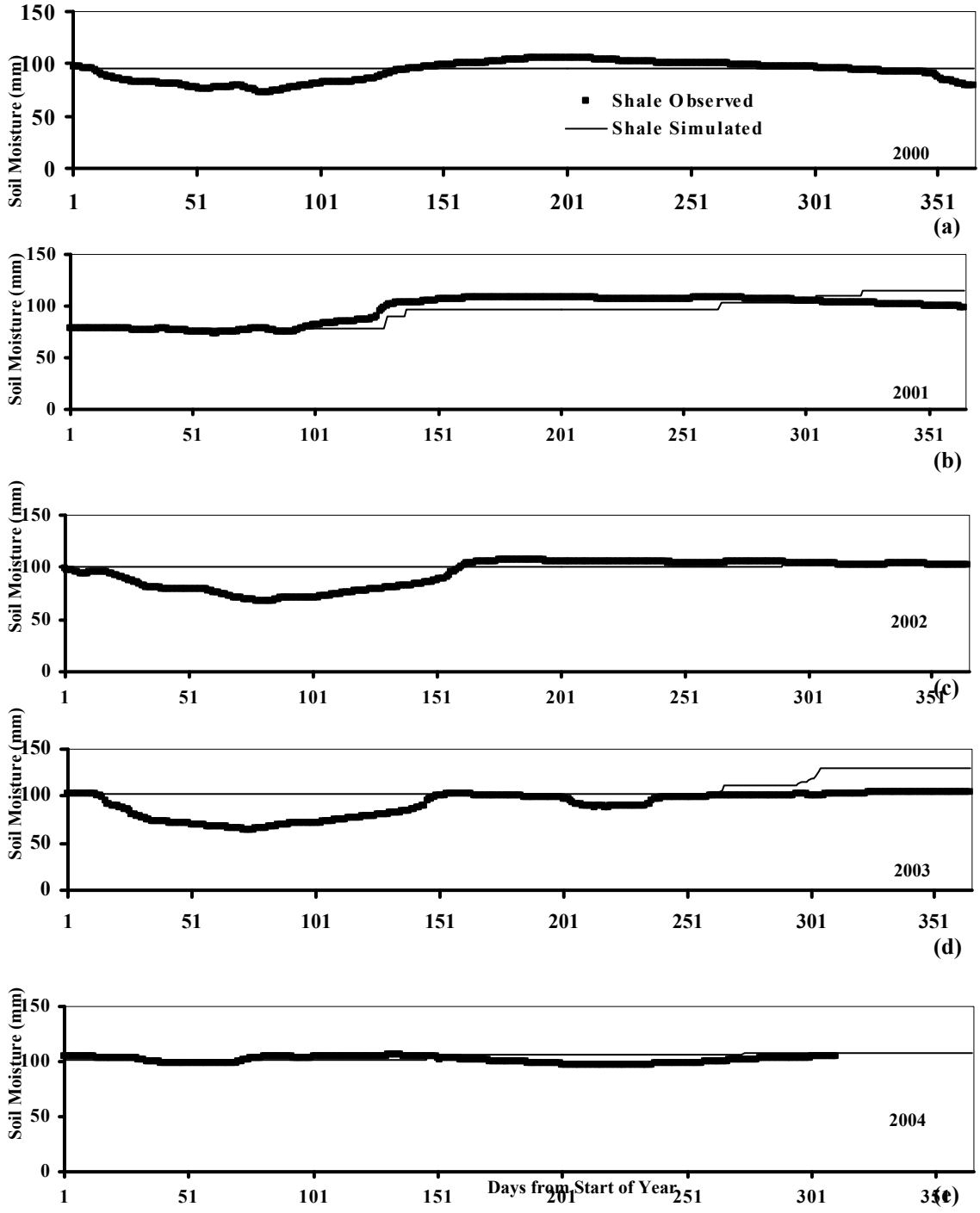

Figure 6.22. Simulated and Observed Moisture in the Shale Layer in Sub-Watershed D1.

6.3.1.2 Watershed evolution

The model parameter values in the developed SDWM, which were obtained using a trial and error methodology, are given in Table 6.6. It is evident from the table that five of the parameters (I_{cS}, c_i, T_{Imax}, m_F, c_T) remained unchanged for all simulation years. The remaining three parameters (I_{cT}, c_P, λ) exhibit dynamic variation over time.

Table 6.6: Model Parameters for Sub-Watershed D1

Year	c_P	c_T	λ	T_{Imax}	m_F	c_i	I_{cT}	I_{cS}
2000	0.18	0.07	0.30	45	0.90	5	0.01	0.9
2001	0.16	0.07	0.90	45	0.90	5	0.02	0.9
2002	0.20	0.07	0.70	45	0.90	5	0.03	0.9
2003	0.20	0.05	0.90	45	0.90	5	0.03	0.9
2004	0.20	0.07	0.70	90	0.90	5	0.04	0.9

In order to analyze the hydrologic evolution of the watershed, the parameters I_{cT}, I_{cS}, c_P, c_T and λ mentioned in Table 6.6 were multiplied by an arbitrarily large number (10000). In order to negate some of the effects of the meteorological variability, the values obtained by multiplying 10000 were normalized using the depth of summer rainfall in each year. The summer rainfall in each of the five model years is 298, 273, 272, 278 and 257 mm, respectively. All the five years have received less rainfall than the mean rainfall in the region. Figure 6.23 shows the trend in the normalized actual evapotranspiration (AET) parameters (c_P, c_T and λ). These results indicate that sub-watershed D1 may still be evolving over time though there is a modest indication that the watershed is trying to stabilize with regards to λ more than the other two parameters. However, no conclusions can be drawn with regard to AET trends from the three parameters as the data are for a short time scale (five years). The increasing trend of c_P may indicate the growth of vegetation, and thereby the need for more water for evapotranspiration. The fact that c_T is nearly constant may indicate that the roots penetrate into the till layer but may not be benefiting from the till moisture except in drier years.

According to the trend in Table 6.6, an increase in the normalized till infiltration parameter value over time should be expected. Figure 6.24 proves the expectation where the normalized till parameter value is plotted over five years. The figure reveals that the watershed is yet evolving over time and that the moisture dynamics in the soil layers is not stabilized. This is possible as the watershed is experiencing freeze-thaw cycles and decomposition of highly organic peat layer, which in turn increases water intake (Haigh, 2000). A similar increasing trend is present in the normalized shale infiltration parameter, which can be attributed to the above mentioned factors.

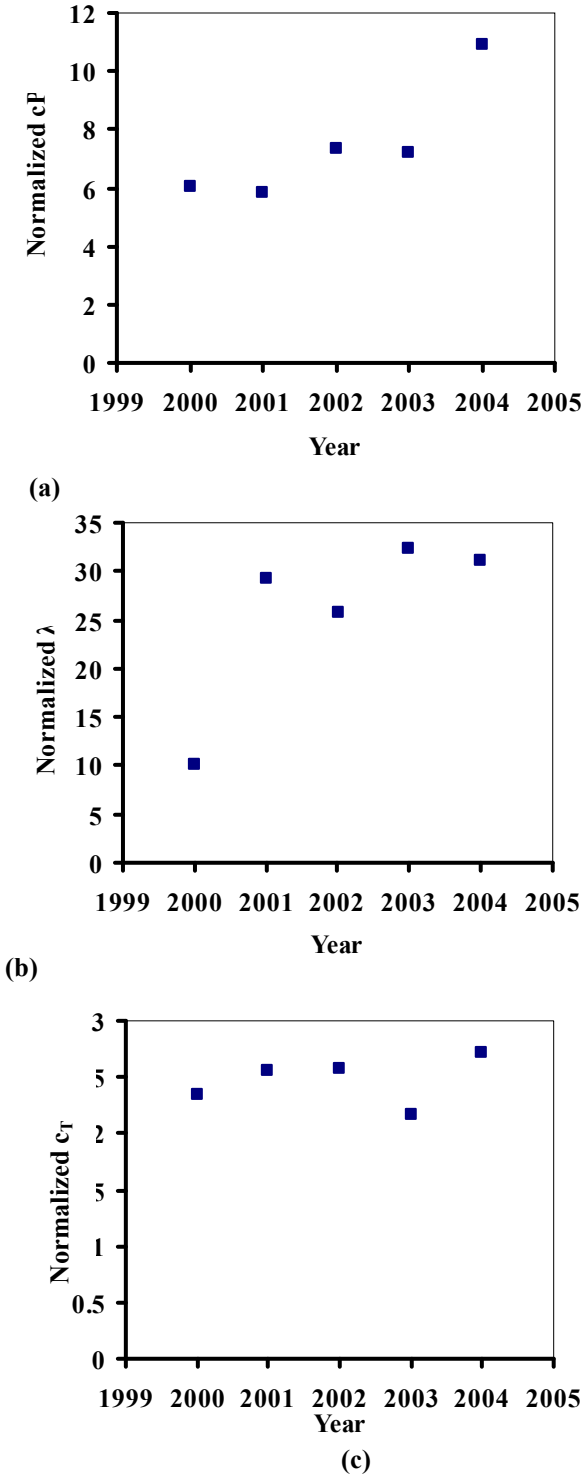

Figure 6.23. Normalized AET parameters over the Study Period in Sub-Watershed D1.

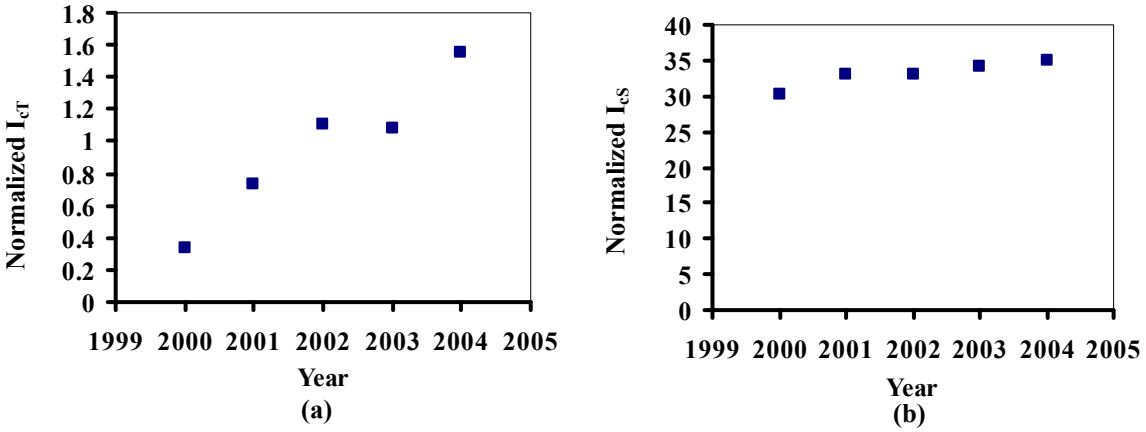

Figure 6.24. Normalized Till and Shale Infiltration Parameter over the Study Period in Sub-Watershed D1.

6.3.2 Sub-watershed D2

6.3.2.1 Simulation results

The watershed response for sub-watershed D2 was simulated using the SDWM for five years (2000-2004). The soil moisture dynamics in the peat, till and shale layers were modeled by changing the parameters in the SDWM to match the observed data. Table 6.7 provides a summary of the model performance for all years in the peat and till layers. The MRE values for the peat layer varied from 17% to 33% whereas in the till layer the values ranged from 10% to 15%. RMSE in the peat layer lies in the range of 7 to 11 mm while it is in range of 5 to 7 mm in the till layer. The overall performance of the model in terms of MRE ranged from 11 to 21%. The MRE and RMSE values are higher in this sub-watershed as compared to those in sub-watershed D1. This may be due to the fact that the D2 cover is thin and thus more dynamic than is the case for sub-watershed D1.

Table 6.7: Performance of the Model in Simulating the Soil Moisture in Five Years in Sub-Watershed D2

Year	MRE (%)		RMSE (mm)		Overall Performance
	Peat	Till	Peat	Till	MRE (%)
2000	25	10	10	6	13
2001	33	12	11	5	21
2002	19	15	10	6	16
2003	17	14	7	7	11
2004	25	12	8	5	18

The simulated and observed soil moisture for year 2000 is illustrated in Figure 6.25. As the results indicate, soil moisture is replenished during the spring snowmelt. The water falling as rainfall is quickly absorbed by the peat layer. The water from the peat layer is lost through evapotranspiration. The rainfall events close to days 230 and 260 replenished some of the moisture in the layer, but it was quickly depleted through evapotranspiration

occurring in the layer. In the late summer (after day 270), there is a discrepancy between the observed and simulated soil moisture. The simulated soil moisture in the peat layer is showing loss of water from the peat layer whereas the observed moisture levels are steady during that time. The precipitation data plotted in Figure 6.25 reveals that there was no rainfall event after day 270 that could generate the trend depicted in the observed data. This increase is possibly due to the lateral flow of water from upslope. Prior to the rainfall event, the peat and till layers had a very low moisture content. This may have resulted in the development of a crack network in the soil layers such that, whenever a rainfall event occurred, water could flow through the crack. Since the locations of the sensors are on relatively mild slope (i.e., relative to the upslope as shown schematically Figure 6.26), the water must have traveled from the upslope end, causing a local increase in the moisture levels in both the peat and till layers around the sensors. In the current set up, the SDWM is not accounting the effects of cracks in the soils.

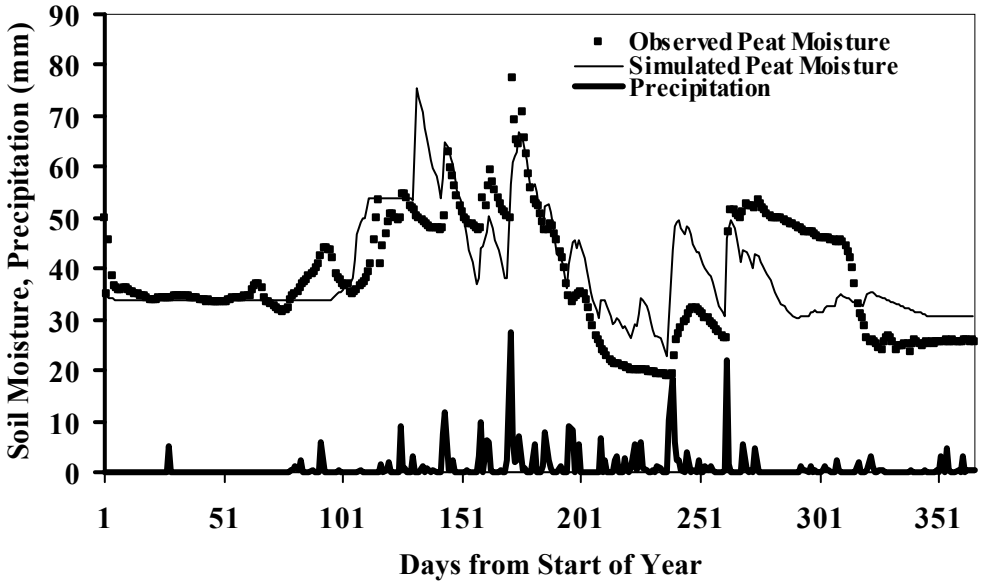

Figure 6.25. Simulated and Observed Moisture in the Peat Layer in Sub-Watershed D2 (Year 2000).

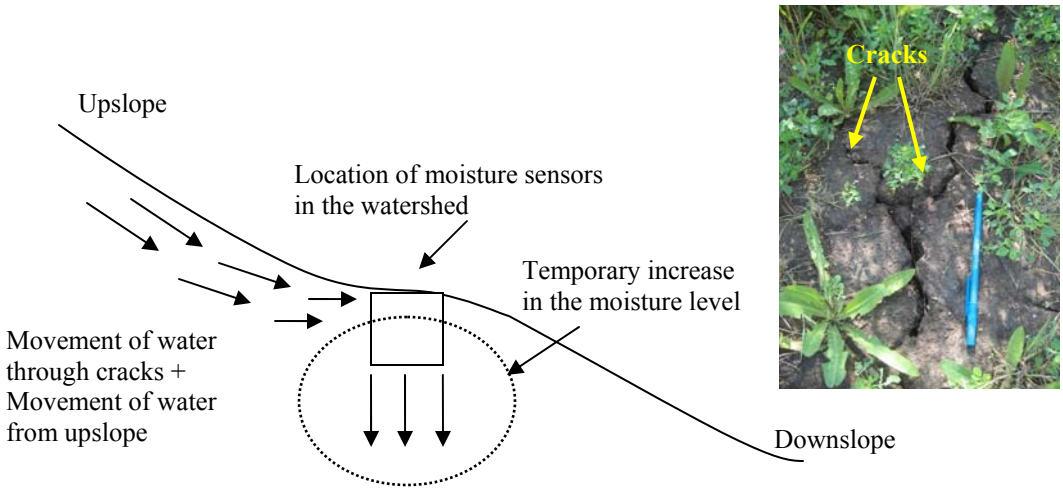

Figure 6.26. Likelihood of Moisture Movement and Entrapment in the Soil Cover.

Figure 6.27, which shows the simulated and observed moisture in year 2001, follows the same explanation as mentioned for year 2000. The MRE and RMSE values for the peat layer in year 2001 are 33% and 11 mm, respectively. The simulated results have deviations in magnitude but not in trend from the observed moisture in the peat layer during the second half of the summer. The discrepancies in the late summer between the simulated and observed soil moisture observations can be explained by the moisture entrapment phenomenon through development of cracks in summer season as explained in the preceding section.

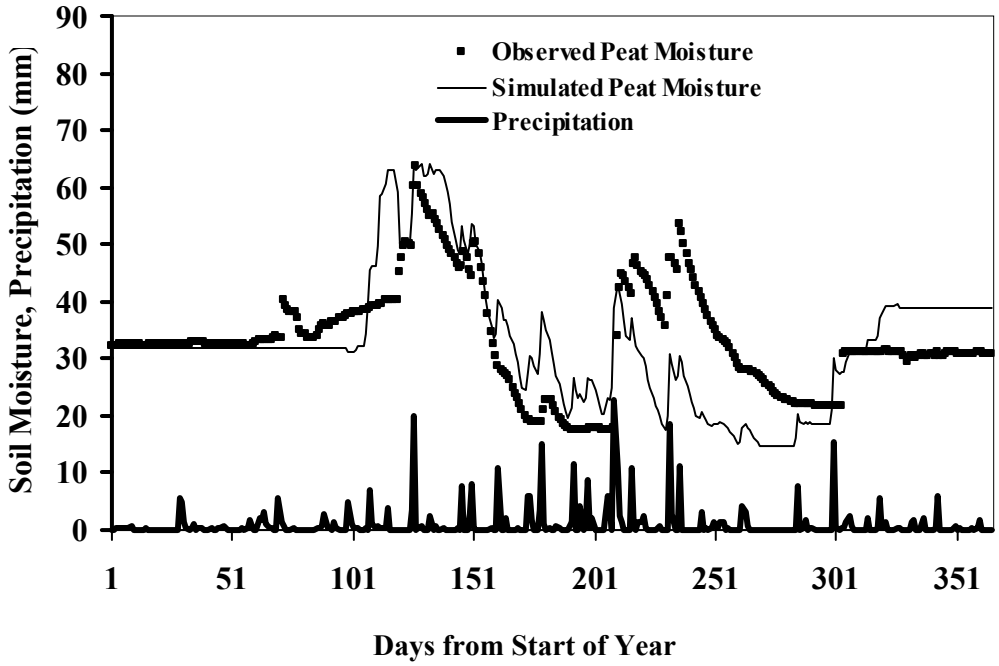

Figure 6.27. Simulated and Observed Moisture in the Peat Layer in Sub-Watershed D2 (Year 2001).

In year 2002 results shown in Figure 6.28, the peat layer is recharged through spring snowmelt but is quickly discharged through evapotranspiration. There are only a few rainfall events which recharge the soil moisture. However, the temporal distribution of the rainfall in year 2002 suggests that the moisture levels in the peat layer are above wilting point moisture contents, which is 10% in the peat layer. The MRE and RMSE values in year 2002 are 19% and 10 mm, respectively.

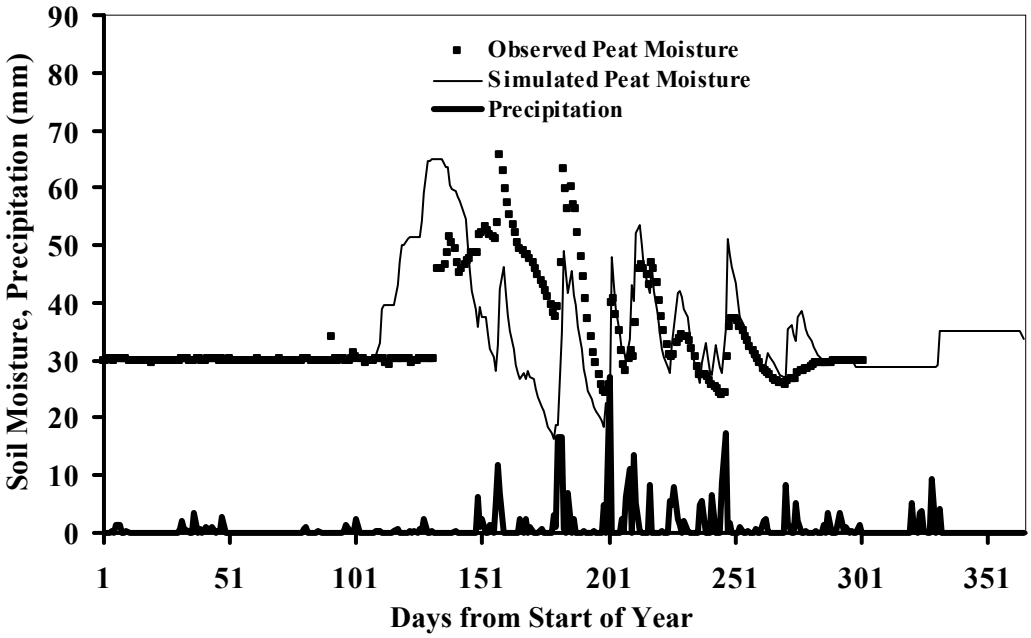

Figure 6.28. Simulated and Observed Moisture in the Peat Layer in Sub-Watershed D2 (Year 2002).

Figure 6.29 and Figure 6.30 show the peat layer moisture in years 2003 and 2004, respectively. Although the rainfall event in the early summer in year 2003 recharged the peat layer, the moisture level nonetheless fell close to the wilting point moisture content (10%) in the late summer season. This may due to the fact that most of the water is absorbed by the plants for their metabolic activities. The same kind of trend is present in year 2004; however, it is evident from Figure 6.30 that the soil remained drier than the preceding year. This may be because of the fewer number of rainfall events in the year 2004 (58 rainfall events) as compared to year 2003 (78 rainfall events).

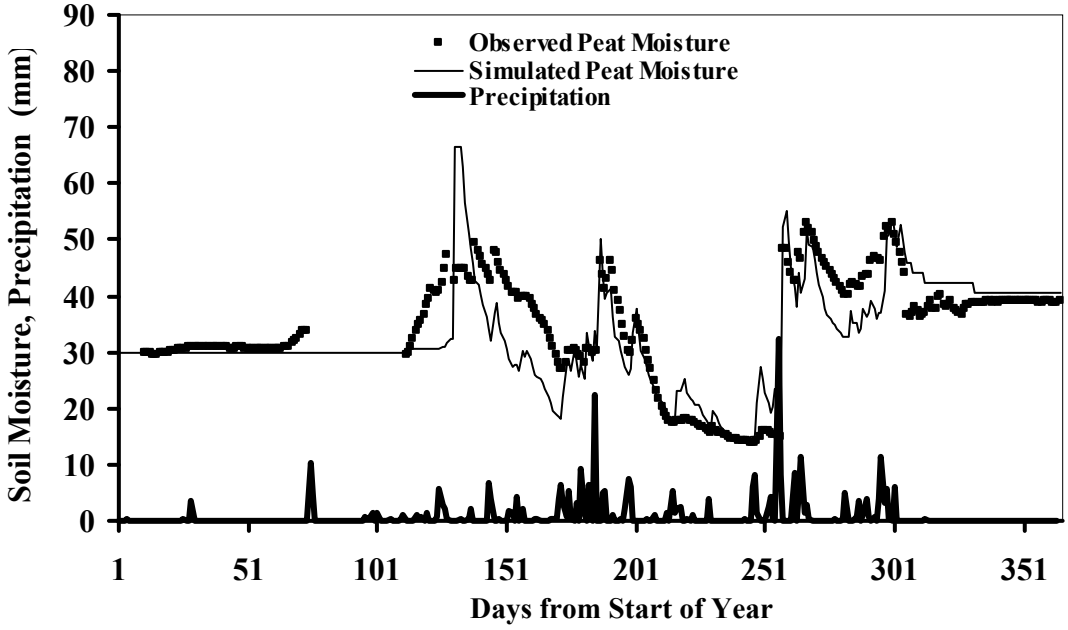

Figure 6.29. Simulated and Observed Moisture in the Peat Layer in Sub-Watershed D2 (Year 2003).

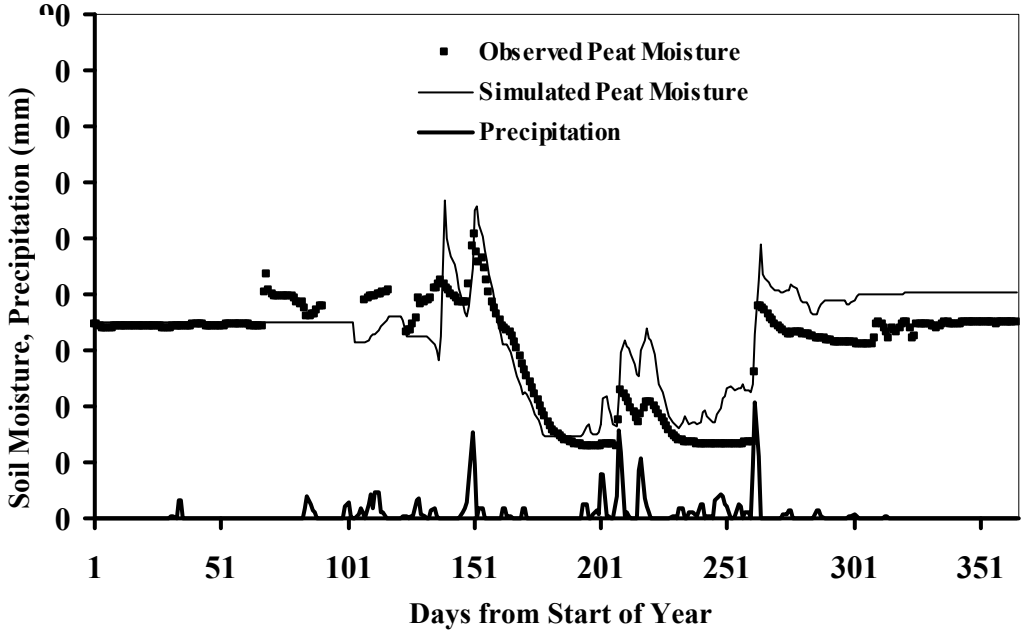

Figure 6.30. Simulated and Observed Moisture in the Peat Layer in Sub-Watershed D2 (Year 2004).

The moisture dynamics in the till layer for all five years are shown in Figure 6.31. It is evident from the figures that the till layer is less susceptible to rainfall fluctuations than is the peat layer. In year 2000 (Figure 6.31a), there is a sudden rise in observed moisture

levels in late summer (close to day 260). However, the model fails to provide a close match to the measured moisture levels. The increase in the observed moisture level in the till layer may be due to the lateral flow of water from upslope or a non-uniform increase of moisture around the sensor due to macropore (cracks) flow. This assumption is reasonable, especially as the rainfall event comes after a dry period, which provides the type of conditions that promote macropore flow.

Till moisture in year 2001 is simulated satisfactorily by the developed SDWM. However, the simulated moisture content in year 2002 deviates from the observed moisture content in the till layer. This may be due to an abrupt change in the suction pressure head that prompts a release of more water from the peat layer to the till layer. The discrepancies in the simulated and observed moisture levels in the till layer in year 2003 can be attributed to the above-mentioned hypothesis. The moisture contents in the till layer in year 2004 is satisfactorily simulated by the watershed model.

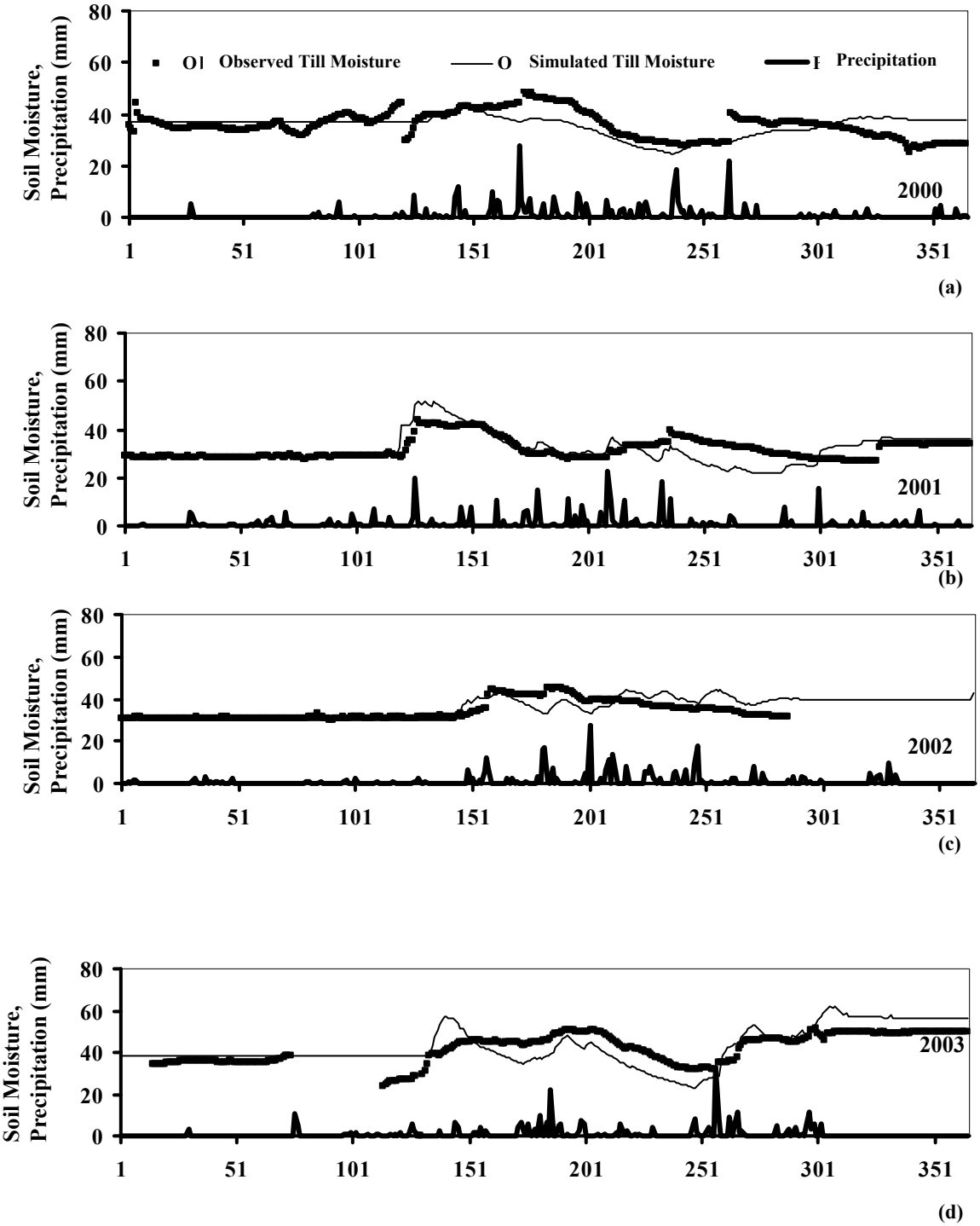
Soil Moisture, Precipitation (mm)
80
60
40
20
0
Observed Till Moisture
Simulated Till Moisture
Precipitation
2000
1
51
101
151
201
251
301
351
(a)
2001
(b)
2002
(c)
2003
(d)

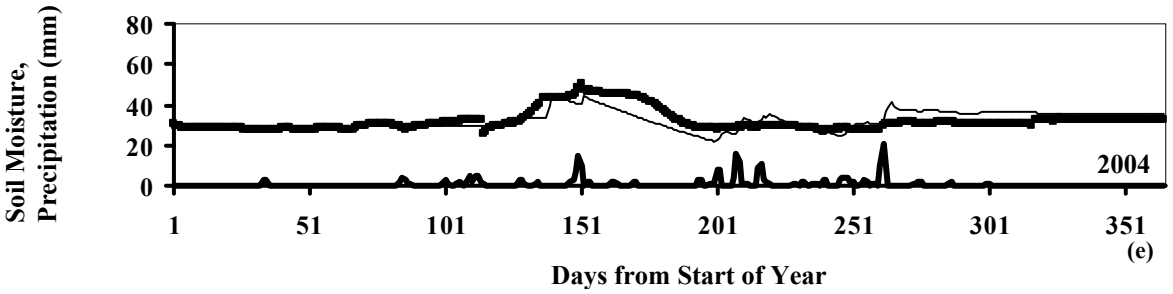

Figure 6.31. Simulated and Observed Moisture in the Till Layer in Sub-Watershed D2.

Figure 6.32 shows the observed and simulated shale moisture contents for five years (2000 to 2004). There is a very less dynamicity in the observed as well as simulated shale moistures for all years relative to that observed in the peat and till layers. The figure also demonstrates that there is not much movement of water to the shale layer and that the SDWM is capturing the behavior shale layer moisture content. However, field personal have expressed concerns about the reliability associated with observed shale moisture. Hence, it is difficult to conclude anything at this juncture. The results from the developed SDWM suggest that the moisture level in the shale layer is not increasing, which means that there is low percolation to the shale layer.

The observed and simulated overland flow for year 2000 is shown in Figure 6.33. The sensors in the sub-watershed recorded unusually high flow rates of overland flow in year 2000. However, the high flow rates are due to ice dam breaks within the drainage collection swale (Boese, 2003). Hence it is not possible to validate the overland flows in the year 2000. The overland flows in years 2001 to 2004 are shown in Figure 6.34. There is a high amount of runoff (26 mm/day) in year 2001, which does not seem to be a plausible rate in one day. This may also be due to the formation of ice dams in the sub-watershed. All other years have very low overland flow, which has been simulated by the SDWM. Figure 6.34 suggests that there is no runoff event during the entire summer season, which clearly emphasizes that the SDW model needs another parameter for validation of the watershed response. Soil moisture has been used as an additional variable for validating watershed response in all of the years.

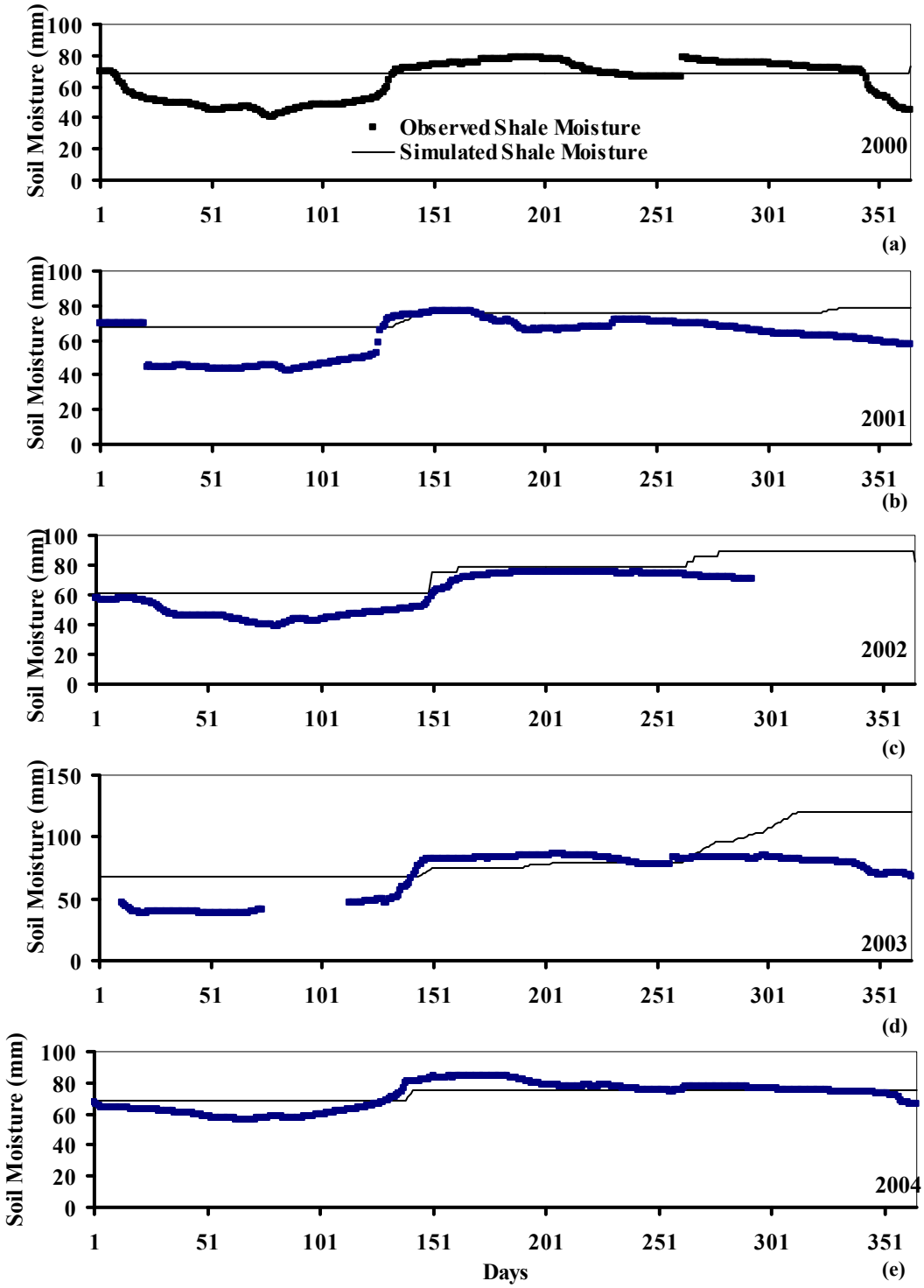

Figure 6.32: Simulated and Observed Moisture in the Shale Layer in the Sub-Watershed D2.

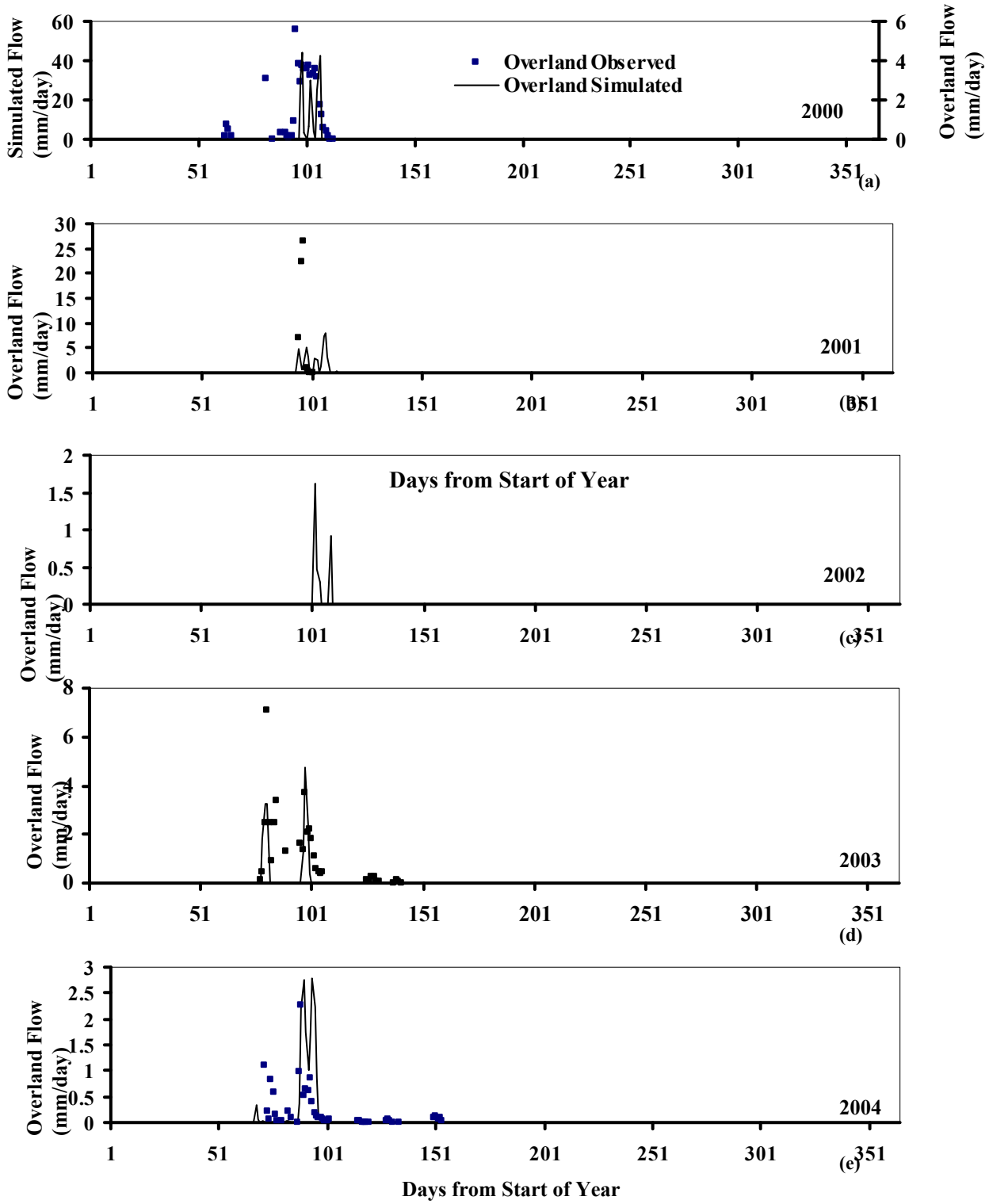

Figure 6.33. Simulated and Observed Overland Flow in Four Years in Sub-Watershed D2 (2000-2004).

6.3.2.2 Watershed evolution

Table 6.8 lists the SDWM parameters for sub-watershed D2 for all five years. As shown, there is some variation in the parameters c_P, I_{cT}, and I_{cS} in the various years. The shale infiltration parameter (I_{cS}) is changing in the sub-watershed D2. The soil cover in sub-watershed D2 is thinner than the soil cover in sub-watershed D1. The thin soil cover in the sub-watershed could imply that there may be a change in moisture dynamics between the shale and till layers while sub-watershed D1 conserves water in the till layer and is not allowing much water to percolate to the shale layer. Hence I_{cS} in sub-watershed D1 is maintaining a constant value over years.

Table 6.8: SDWM Parameters for Sub-Watershed D2

Year	c_P	c_T	λ	T_{Imax}	m_F	c_i	I_{cT}	I_{cS}
2000	0.22	0.16	0.9	45	0.9	5	0.005	0.03
2001	0.25	0.16	0.9	45	0.9	5	0.009	0.09
2002	0.22	0.16	0.9	45	0.9	5	0.022	0.09
2003	0.25	0.16	0.9	45	0.9	5	0.038	0.15
2004	0.35	0.16	0.9	45	0.9	5	0.100	0.20

The parameters (c_P, c_T, λ, I_{cT}, and I_{cS}) in sub-watershed D2 were normalized in a similar way as was done in sub-watershed D1. According to the trends in the saturated hydraulic conductivity shown in Table 6.2, the parameters used to simulate the infiltration processes in the various soil layers in sub-watershed D2 should give indication verifying that the sub-watershed has not yet stabilized. As mentioned in section 6.3.1.2, with a change in the hydraulic conductivity in the watershed soil layers, the moisture dynamics change over time. Normalized till and shale infiltration parameters are shown in Figure 6.35. The till infiltration parameter (I_{cT}), which gives an account of movement of water between the peat and the till layers, verifies the fact that the watershed has not yet

stabilized and that the moisture dynamics is changing over time. A similar type of trend is shown by the normalized shale infiltration parameter (I_{cS}). The results shown in the figure confirm that the watershed has not yet stabilized.

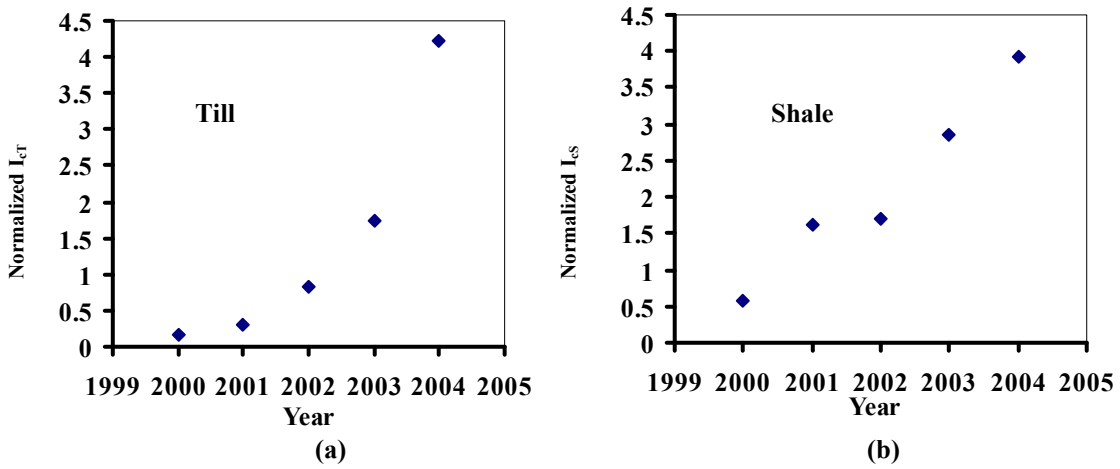

Figure 6.34. Normalized Till and Shale Infiltration Parameter over the Study Period in Sub-Watershed D2.

Figure 6.35 shows the normalized AET parameters over various years in the sub-watershed D2. Figure 6.35 (a) suggests that there has been increase in the evapotranspiration from the peat layer over the study period, which could be due to uptake of water by the shallow rooted vegetation. However, in absence of water during late summer season, the vegetation may suffer water stress. Moreover, the amount of water available for evapotranspiration per unit area from sub-watershed D2 is more because of its thin peat layer. Figure 6.35 (b) shows the plot of normalized parameters associated with the AET from the till layer. There is less variation in the parameter c_T over time. The parameter c_T is the AET parameter associated with the till layer. Less variation in this parameter is reasonable because sub-watershed D2 has the thinnest soil cover, which could mean that there may not be a deep-rooted vegetation network present in the sub-watershed. The variation in the three AET parameters in sub-watershed D2 is an indicator of the fact that watershed is evolving over time.

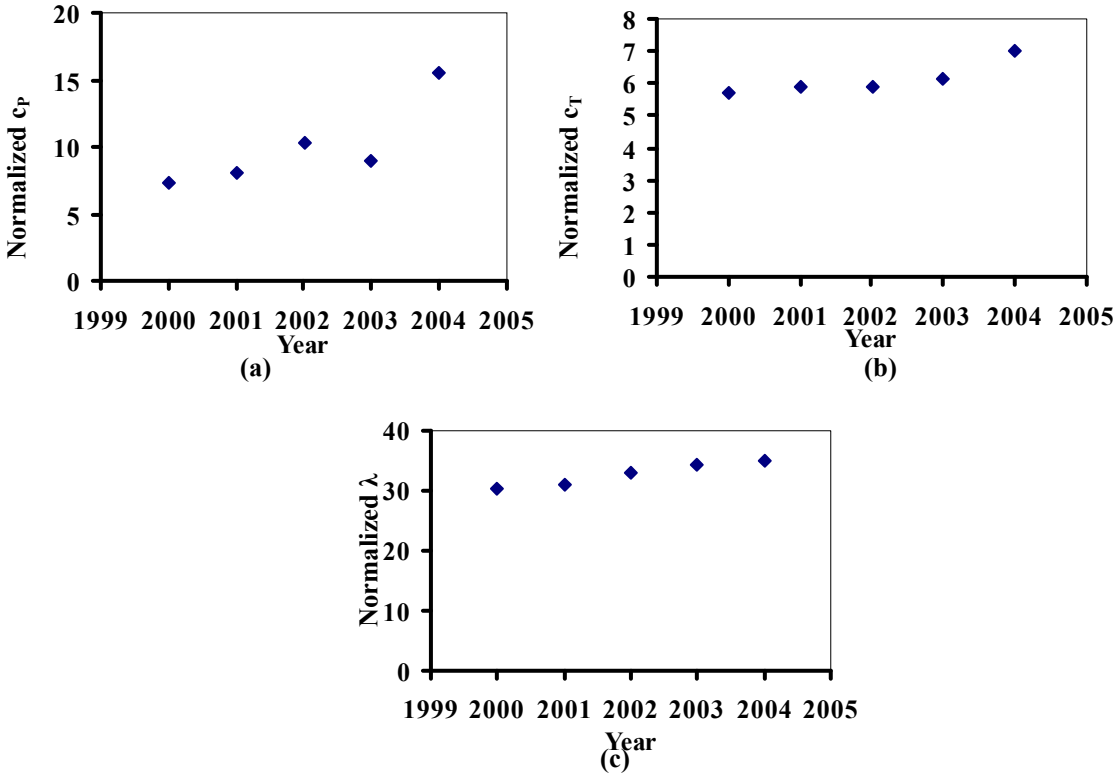

Figure 6.35. Normalized AET Parameters over the Study Period in Sub-watershed D2.

6.3.3 Sub-watershed D3

6.3.3.1 Simulation results

The soil moisture dynamics in the peat, till and shale layers were modeled by changing the parameters in the SDWM to match the observed data. Table 6.9 presents the performance indices of the model in the five years (2000-2004) in the peat and the till layer. The MRE values for the peat layer varied from 9% to 20% whereas in the till layer the values ranged from 3% to 6%. The RMSE in the peat layer lies in the range of 6 to 10 mm and between 5 and 17 mm in the till layer. The overall performance of the model in terms of MRE ranged from 3 to 8%. The MRE and RMSE error values in the watershed are lower than for sub-watersheds D1 and D2.

Table 6.9: Model Performance Accuracy in Simulating Soil Moisture in Sub-Watershed D3

Year	MRE (%)		RMSE (mm)		Overall Performance
	Peat	Till	Peat	Till	MRE (%)
2000	13	6	9	17	7
2001	9	3	7	5	3
2002	14	6	10	14	7
2003	20	6	10	13	8
2004	14	5	6	10	4

Figure 6.36 shows the observed and simulated moisture levels in the peat layer in sub-watershed D3 for all of the years of the study (2000-2004). The figure shows good agreement between the observed and simulated soil moisture in the layer. The peat layer in the sub-watershed is highly dynamic due to rainfall fluctuations. The peat layer in the watershed is able to hold moisture levels well above the wilting point moisture content (10%) in all of the years. The increase in simulated soil moisture in year 2001 (Figure 6.36 b) close to day 120 is due to the snowmelt. The SDWM is producing acceptable temporal trends in the peat layer moisture in all of the years. There is a sharp decrease in the moisture levels after day 175 in year 2004 (Figure 6.36e). This is due to the absence of rainfall in year 2004. Hence the moisture is used by the vegetation and is not replenished in the summer. After day 200, the peat layer has been recharged by the rainfall. Hence, there is a rise of moisture content in the peat layer. The moisture contents fell again sharply at the end of the summer season due to the absence of rainfall.

Figure 6.37 shows the simulated and observed moisture trends in the till layer in all years (2000-2004). There is not much deviation between the simulated and observed moisture contents, which suggests that the model is working satisfactorily to simulate the soil moisture. The till layer is not responsive to rainfall. This may be due to the fact that till layer is below the peat layer hence less variant to atmospheric fluctuations.

Similarly, Figure 6.38 illustrates the observed and simulated soil moisture in the shale layers in each of the five study years in sub-watershed D3. There are sharp drops in the shale moisture during the summer season in all of the years. The sharp drops in the moisture level are beyond explanation and require further field investigation, which is not in the scope of the current study.

The observed and simulated overland flow are shown in Figure 6.39. The watershed is producing overland flow only during the spring snowmelt period, which is satisfactorily captured by the developed SDWM. There were abnormal runoff rates recorded in the field in the year 2000, which are due to ice dam breaks in that year (Boese, 2003).

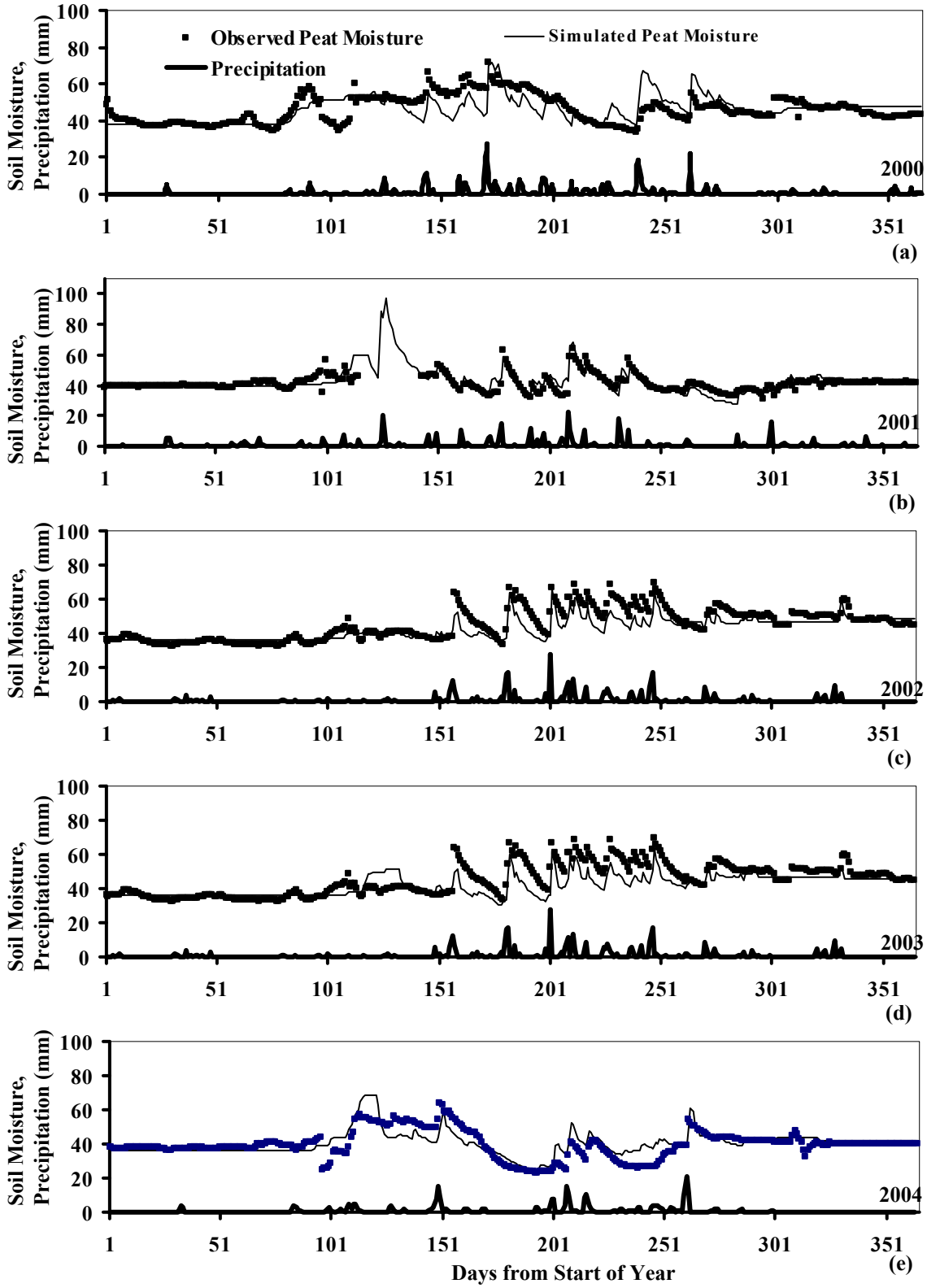

Figure 6.36. Observed and Simulated Moisture in the Peat Layer in Sub-Watershed D3.

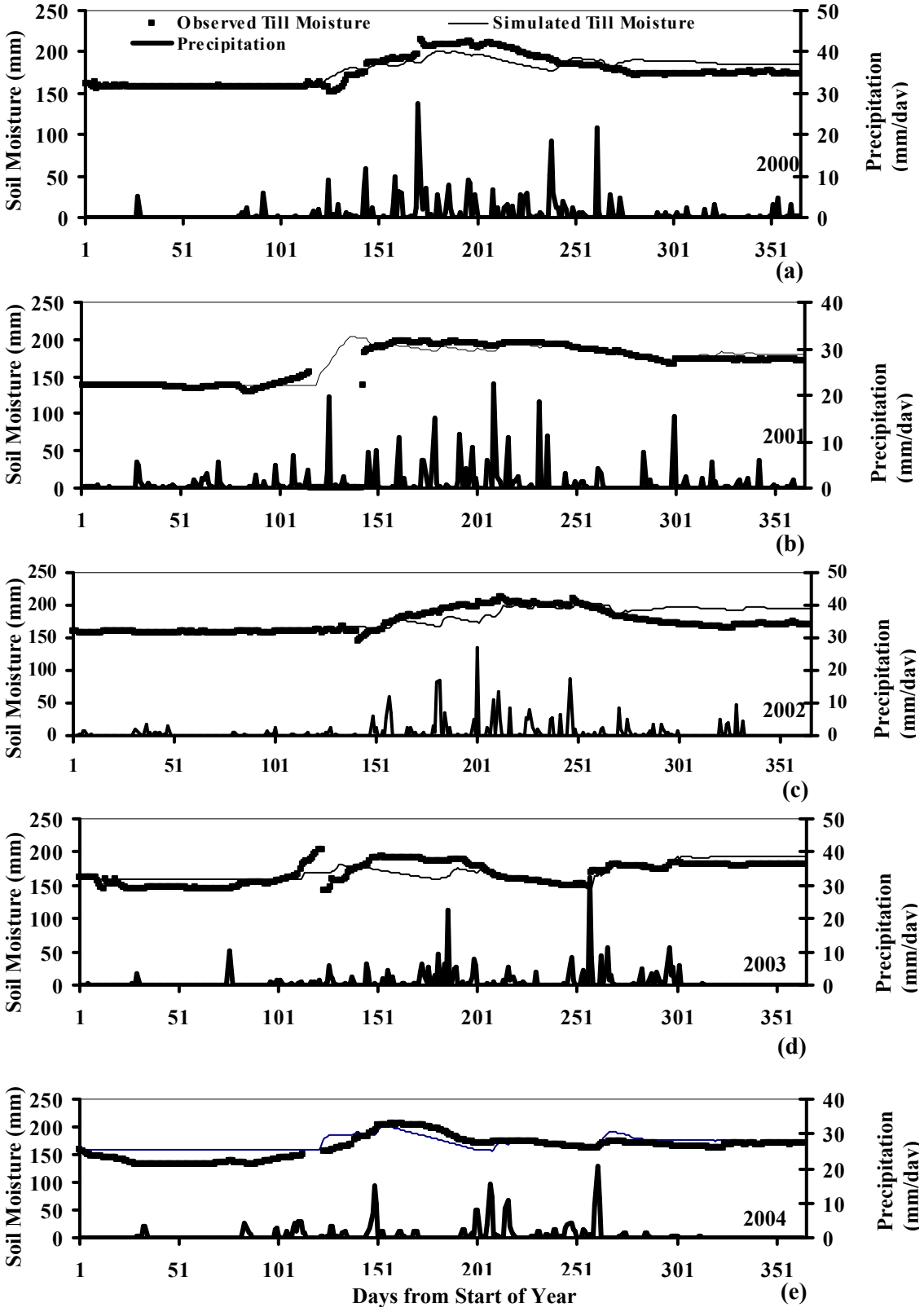

Figure 6.37. Observed and Simulated Moisture in the Till Layer in Sub-Watershed D3.

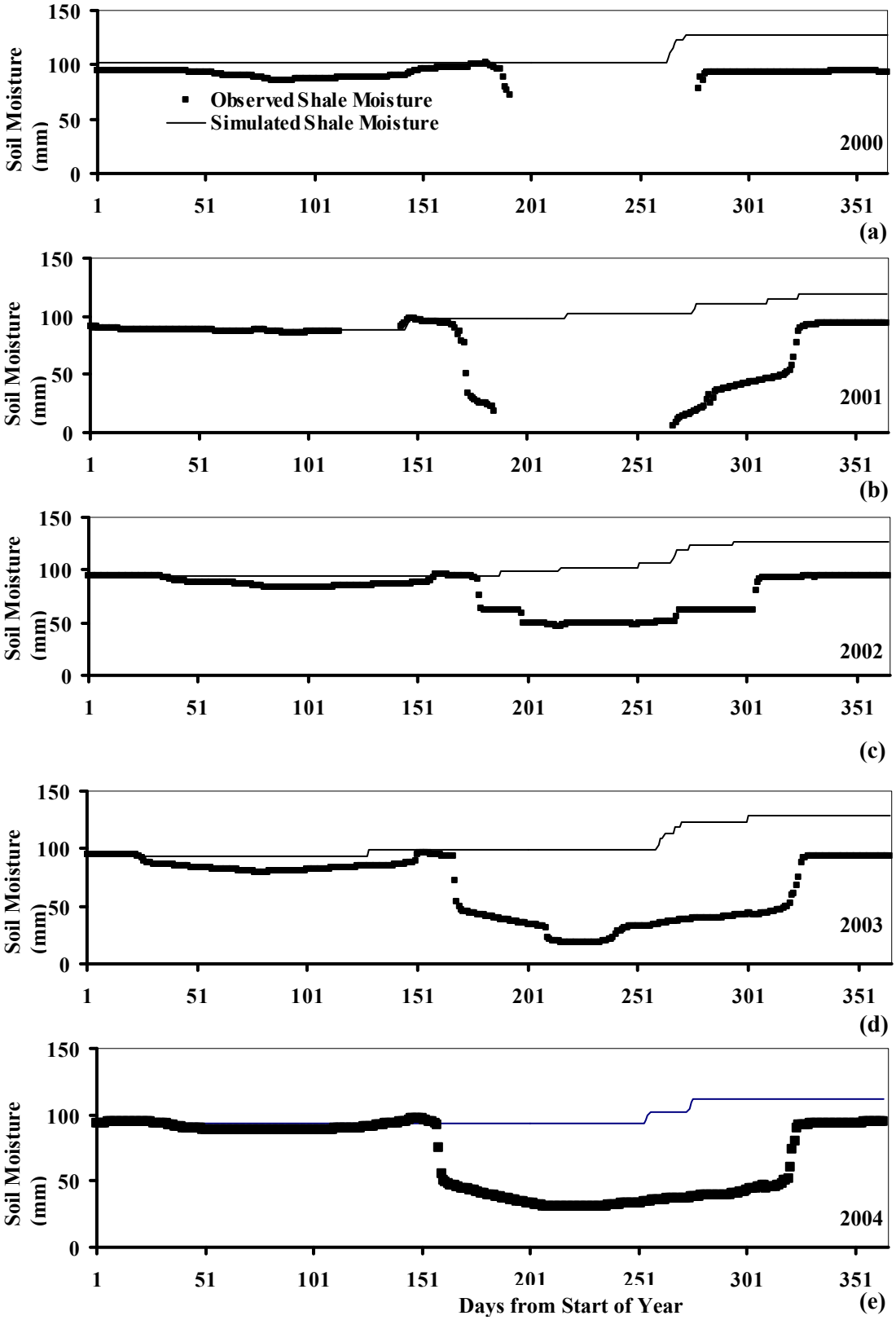

Figure 6.38. Observed and Simulated Moisture in the Shale Layer in Sub-Watershed D3.

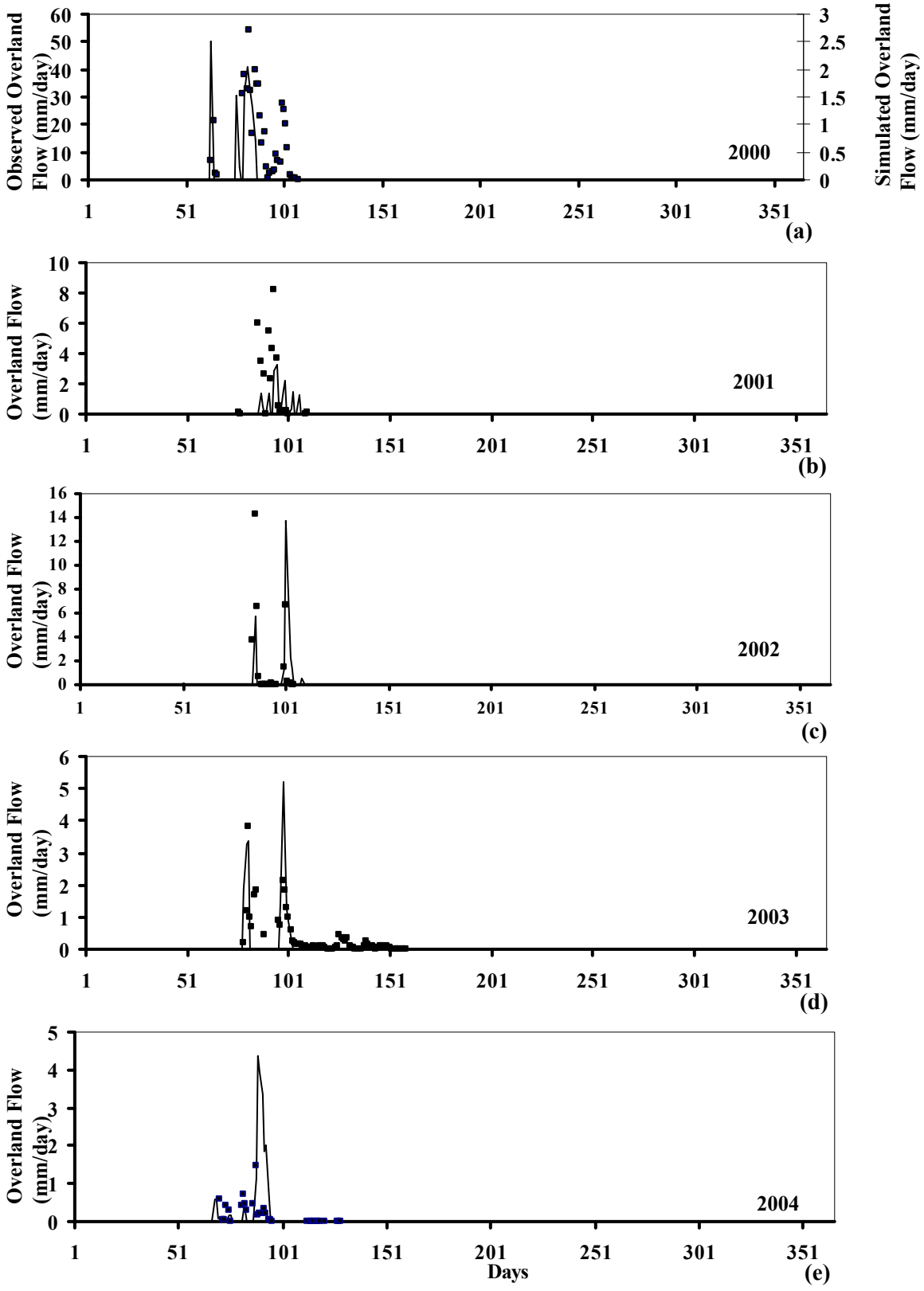

Figure 6.39. Observed and Simulated Overland Flow in Sub-Watershed D3.

6.3.3.2 Watershed evolution

Table 6.9 shows the values of the model parameters over time. Sub-watershed D3 exhibits variation in more of the parameters than the other two sub-watersheds. This may be due to the fact that sub-watershed D3 is conserving more moisture hence is more dynamic throughout the whole year than other two sub-watersheds. The three AET parameters (c_P, c_T and λ) and the till infiltration parameter (I_{cT}) show an increase over the five years of study.

Table 6.9: SDWM Parameters for Sub-Watershed D3

Year	c_P	c_T	λ	T_{Imax}	m_F	c_i	I_{cT}	I_{cS}
2000	0.23	0.08	0.9	50	0.9	5	0.02	0.6
2001	0.31	0.09	1.2	50	0.9	5	0.04	0.6
2002	0.36	0.18	1.6	50	0.9	5	0.06	0.6
2003	0.60	0.50	1.8	50	09	5	0.08	0.6
2004	0.60	0.55	1.9	50	0.9	5	0.10	0.6

The normalized values of the AET parameters are shown in Figure 6.40. The plots show that there is an increasing trend in each parameter value, which supports the fact that the sub-watershed is still evolving in a hydrologic sense. Unlike sub-watershed D2, there is a variation in the AET parameter associated with the till layer. This may be due to the fact that sub-watershed D3 may be sustaining the deep rooted vegetation. Moreover, the soil moisture simulation reveals that the soil cover in the sub-watershed is maintaining the moisture content above the wilting point moisture content throughout the growing season. As a result, the roots will grow deeper and take water from the till layer for metabolic activities. Hence, the observed variation in the parameter associated with the till layer (c_T) is expected.

Similarly, Figure 6.41 indicates that there is an increasing trend in the normalized infiltration parameter for the till and the shale layers (I_{cT} and I_{cS}). This could be due to the thickness of the soil cover. Sub-watershed D3 has thickest soil cover of all of the three sub-watersheds. So, the cumulative effect of subsidence and natural settlement of the soil

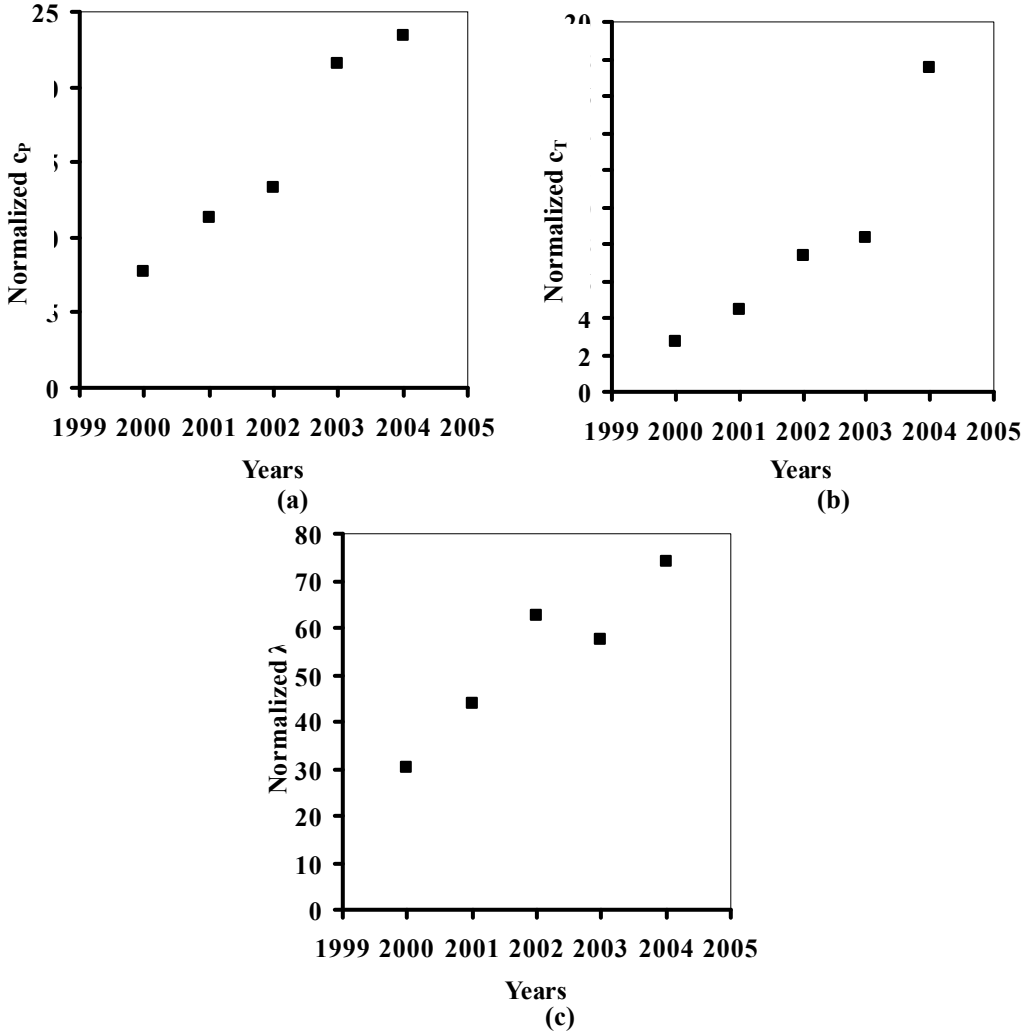

Figure 6.40. Normalized AET Parameters over Various Years in Sub-Watershed D3.

structure might be expected to be most prevalent for the thickest soil cover. Similarly, the normalized shale infiltration parameter shows an increasing trends over the five years of study period. Sub-watershed D1 and D2 exhibited the same trend in the normalized shale infiltration parameter. All the evidence presented above leads to the conclusion that sub-watershed D3 is evolving over time.

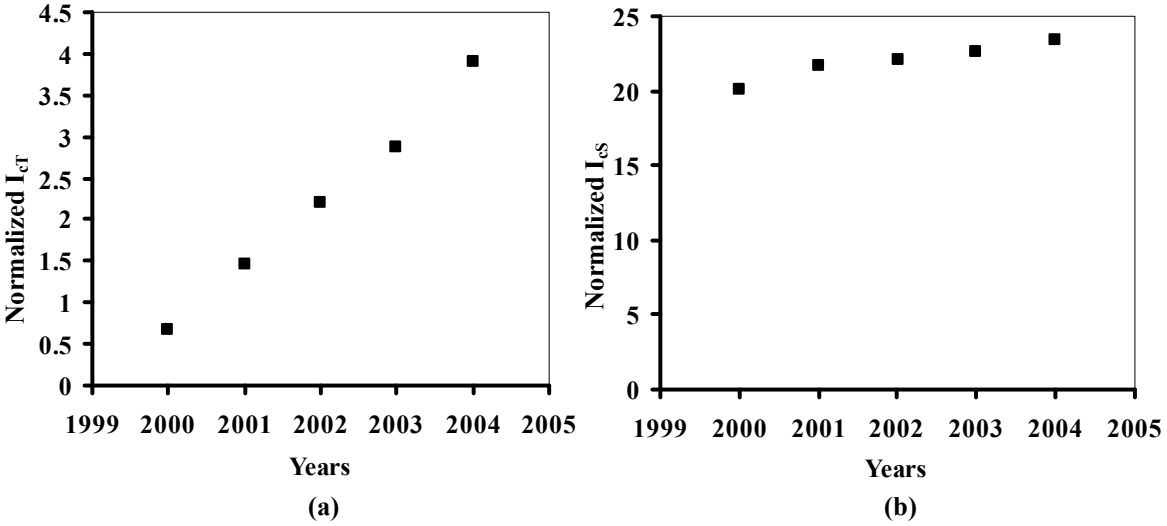

Figure 6.41. Normalized Till and Shale Infiltration Parameter over Various Years in Sub-Watershed D3.

6.4 Results from Improved AET Equation

A modified equation for calculating AET using both a temperature and a radiation term was proposed in Chapter 5 (Eq. 5.26). In order to validate the proposed equation, the simulated AET values were compared with the measured AET. An Eddy covariance system for measuring AET was installed for a separate study in sub-watershed D2. AET data for 74 days in the summer of year 2003 are available for the study site. The original evapotranspiration equation (Eq. 5.8) (originally used in the SDWM) and the modified equation (Eq. 5.26) were first calibrated to produce values of AET as close as possible to the measured values. The results are shown in Figure 6.42. The cumulative AET measured by the eddy covariance system was 187 mm whereas the cumulative AET with the modified equation for 74 days was obtained as 180 mm. The original equation produced a cumulative AET of 155 mm. The MRE value obtained using the modified equation was 37% compared to an 80% value of MRE using the original equation. This shows that the modified equation improves the estimates of AET with regard to both daily trends (represented by MRE) and the seasonal cumulative AET. As the modified equation estimated the AET more correctly, it may be suggested that radiation and temperature play an important role in estimating AET (i.e., both parameters are in the modified equation but not the original equation). Similar type of conclusion has been made by Saxton (1982).

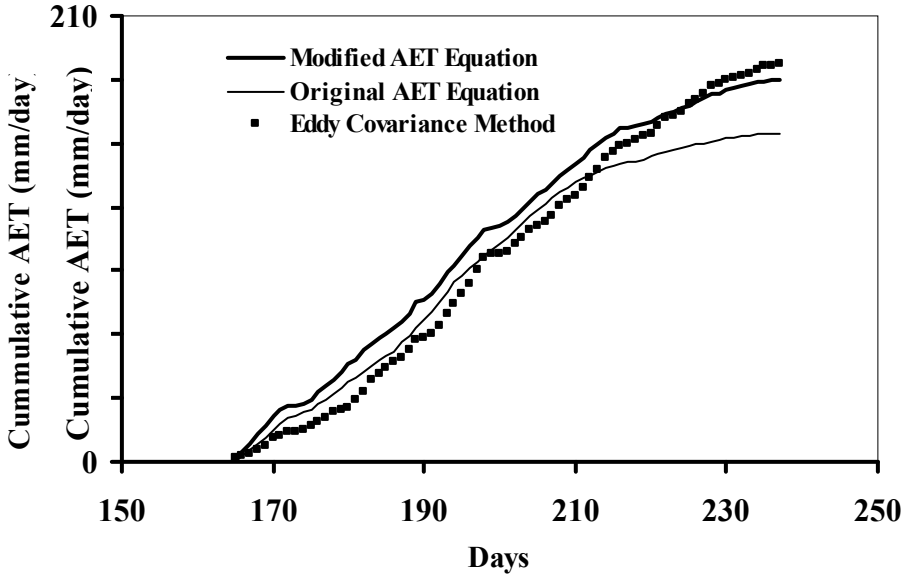

Figure 6.42. Simulated and Eddy Covariance Measured AET in Sub-Watershed D2.

The modified AET equation was not used in the watershed simulation. This is because, during watershed simulation, the modified equation would tend to give higher AET values, which would mean that more moisture from the soil surface would be lost. Figure 6.43 shows the observed and simulated peat layer moisture in sub-watershed D2 and proves the hypothesis. It can be observed that the modified AET equation causes more depletion of the moisture level in the peat layer, and therefore a larger discrepancy between the measured and simulated

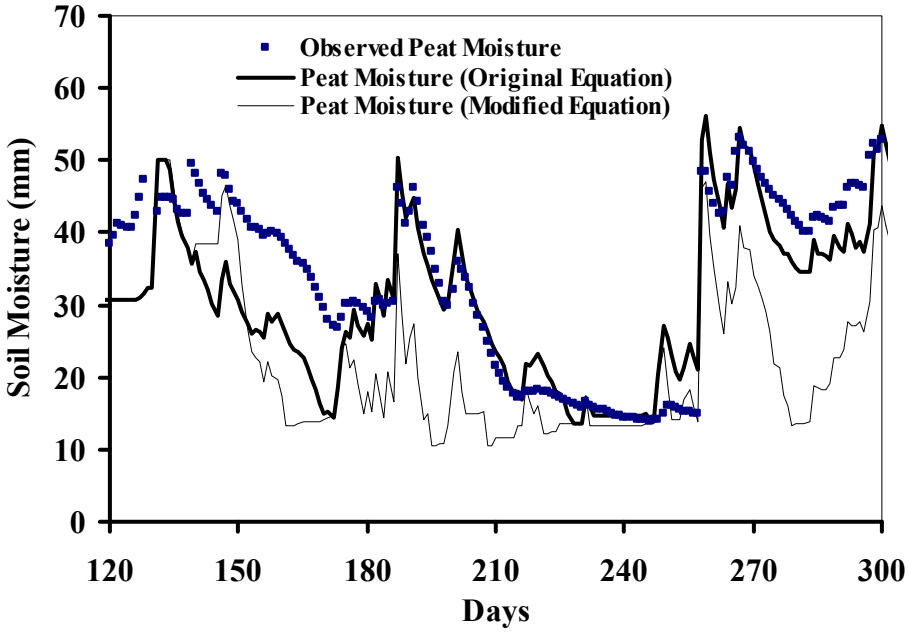

Figure 6.43. Peat Layer Moisture for Sub-Watershed D2 in year 2003.

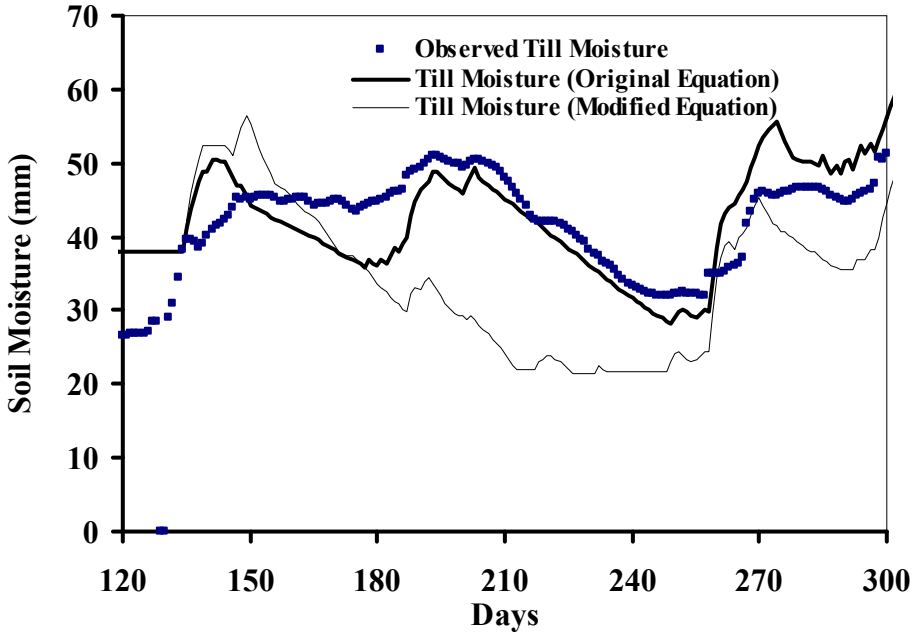

Figure 6.44. Till Layer Moisture for Sub-Watershed D2 in year 2003.

peat moisture. A similar kind of observation can be made from Figure 6.44, which is a graph comparing the simulated and observed moisture content in the till layer using the original and the modified AET equation for the sub-watershed D2 in the year 2003. Figure 6.43 and 6.44 suggest that either the eddy covariance system is estimating more evapotranspiration or the soil moisture sensors need re-calibration. If both the sensors (Eddy covariance and TDR) were working properly, then there should not have excess loss of water from the soil layers when simulated AET tend to get close to the measured AET. The modified AET equation depletes more water; hence, there is not enough moisture available in the soil layers for further AET to occur. Therefore, there is a potential chance that either the eddy covariance system is overestimating AET or the soil moisture sensors need recalibration. Also, there may be an increased possibility that the rain gauges are deteriorating and need attention. It is recommended that the instruments should be tested again before drawing conclusions. The modified AET equation requires additional validation. If the equation gives desirable results, then the originally used AET equation should be discarded and models should be recalibrated using the modified AET equation.

6.5 Discussion of Results

The simulation results indicate that the watersheds are still at an evolution stage. The failure to find a suitable common parameter set for the model simulation for all five years of the study in all three sub-watersheds supports the hypothesis.

The watershed response cannot be properly simulated if one intends to use only runoff as the validation hydrologic variable. The statement is particularly valid if there are no

runoff events in the watershed during the entire summer season. Hence, it is recommended that two or more hydrologic variables should be used for the validation of the watershed parameters (e.g., overland flow and soil moisture). This will help to reduce the uncertainty during predictive modeling of the watershed processes.

The hydrologic processes in the reconstructed watershed have been adequately simulated for five years in all of the sub-watersheds. The increase in the till infiltration parameter and trends in AET further strengthens the point that the watershed is still evolving from a hydrologic point of view. The model performed best in sub-watershed D3 in terms of simulation accuracy, followed by the D1 and D2 sub-watersheds. This may be due to the fact that D3 sub-watershed consists of the thickest soil cover, which is less prone to atmospheric fluctuations. The least optimal model performance has been in the sub-watershed D2. This may be due to the contribution of the upslope water during any rainfall event. Since the model is a lumped watershed model, it is not possible to include the spatial effects in the current setup. However, this is not perceived to be a limiting factor for adopting the model since the area of each sub-watershed is only one hectare. It has been observed that sub-watershed D2 loses most of its water in the summer season, followed by sub-watershed D1 and D3. This is due to the fact that sub-watershed D2 has the thinnest cover. It also appears that the sub-watershed D3 is performing satisfactorily in terms of storing soil moisture in the peat and the till layers during the absence of rainfall in the summer season.

The infiltration to the till layer is increasing in all sub-watersheds over time. This could be a serious threat to the survival of the sub-watersheds in the future. There is an increasing body of evidence suggesting that the soil covers are vulnerable to desiccation and cracking from wet-dry cycles, freeze-thaw cycles, and vegetation (Kim and Daniel, 1992). All of these factors could result in an increase in the hydraulic conductivity of the soil layers, which further facilitates the movement of water into deeper soil layers. Vegetation is expected to further mature in all of the sub-watersheds over the next several years. Vegetal cover is an important component in the design of reconstructed watersheds. The purpose of intentionally planning for plant growth is to control erosion and to reduce the water flux to the overburden by taking up water in the soil through their roots, thereby aiding transpiration. There are also negative effects of plant growth. Of major concern is the possibility that the roots could actually penetrate through to the buried waste. This could result in the roots transporting contaminants to the surface, where undesirable contact with saline salts could occur. Grasses can reach rooting depths of up to eight meters; deciduous trees have a mean rooting depth of 3.3 meters but can root to depths of 30 meters (Suter et al., 1993). These depths are enough to penetrate through any soil cover.

Root growth can change the soil dynamic, and root decay leaves open cavities within the soil profile. Studies by Waugh and Smith (1997) show that unintended plant root growth can increase the hydraulic conductivity of a soil by two orders of magnitude. An increase in the hydraulic conductivity may cause the cover to no longer meet the design criteria. This could mean that the design life of the cover would be compromised, or that more water would infiltrate through the cover, reaching the overburden (shale layer).

Alternately, the roots' uptake of water could dry out soils with high water content potential, such as clay, and then the soil could crack, also resulting in an increase in the hydraulic conductivity (Suter et al., 1993). Plant roots also tend to concentrate in and extract water from compacted clay layers, causing desiccation and cracking. This can occur even when overlying soils are nearly saturated (Hakonson, 1986), indicating that the rate of water extraction by plants may exceed the rehydration rate of the compacted clay. Freezing and thawing cycles can increase the hydraulic conductivity of a soil. A study by Miller and Lee revealed that, in a simulated cover, the water movement through the bottom increased by an order of magnitude after three freeze-thaw cycles. A wet soil shrinks as it dries, and a great water loss can result in cracking. Successive shrink/swell cycles increase the magnitude of the cracks, continually increasing the porosity of the soil (Miller and Lee, 1999). Clay materials are particularly susceptible to cracking. Hence, future field work must be aimed at looking at the hydraulic conductivities of the various soil layers in the three sub-watersheds.

The overall intent of the reconstructed watersheds at the present research site is that it should mimic the natural watersheds present in the local region. This means that the reconstructed watersheds are expected to support forest vegetation, which includes tree species such as pine, spruce and aspen. There is a possibility of having roots deeper than 1 m, which further implies that the model will need modifications to accommodate such changes. In the present model set up, such vegetation effects have not been included. Future work should address required modifications of the model to run both for a developing as well as a fully developed forest.

Chapter 7

Summary, Conclusions and Recommendations

7.1 Summary of the Report

The watershed model (SDWM) developed in this research is a lumped parameter process-based model, which upholds the principle of water-balance on a daily basis. The model was designed and constructed for reconstructed watersheds where the movement of water through various soil layers plays a significant role in defining the overall water balance. The model was developed using on a system dynamics approach, which works using feedback principles. The dynamic hypothesis of the watershed under consideration was perceived in the form of a series of causal-loop (feedback–loop) relationships. Positive feedback stimulates all factors in a loop to either increase or decrease, while negative feedback tends to bring the elements of the system to an equilibrium state. When any of the factors is removed from the system, negative feedback works to force the system back into equilibrium.

The experimental reconstructed watersheds used in this research as the case study, which are located near Fort McMurray, Alberta, Canada, consist of three soil layers (peat, till and shale) of varying depths. In order to examine the hydrologic dynamics of each soil layer, the model utilizes four vertical storages: (i) surface water storage, (ii) peat layer storage, (iii) till layer storage, and (iv) shale layer storage. Soil moisture effects, in the form of a feedback, the amount of infiltrating water. The difference between the amount of water available and the amount of infiltrating water forms the overland flow. Evapotranspiration, interflow, and infiltration to the till layer are losses of water from the peat storage. Evapotranspiration is dependent on soil moisture conditions and weather conditions. Interflow is a function of horizontal hydraulic conductivity, water content, soil type, and hydraulic gradient. Infiltration into the till layer is dependent on soil temperature, water content within both the peat and the till layers, and the hydraulic properties of the till layer. Losses from the till layer storage include evapotranspiration, interflow, and percolation to the shale layer (storage). Factors affecting losses from the till storage are similar to those mentioned for the peat storage. In this study, no base flow is assumed to be contributing water from the shale to the channel storage.

The SDWM was developed using a combination of empirical and physics-based equations. The model requires various input data for simulation of the hydrological processes in the reconstructed watersheds. The model uses soil and metrological data for estimation of the watershed response. Metrological data were primarily used to estimate evapotranspiration via the Bowen ratio and the combined formula of Penman. The model requires various input parameters such as air temperature and vapour pressures at two different heights, net radiation, saturated vapour pressure, wind speed, and relative humidity for estimation of the potential evapotranspiration. Soil moisture-based empirical relationships were used for calculating the actual evapotranspiration in the model. Soil data (temperature, porosity) were used to define the feedback loops that govern the infiltration process in the various soil layers. Soil water characteristic curves were

required to estimate the suction pressures at every time step as a function of the volumetric moisture content. The Green-Ampt formula, which requires information pertaining to soil moisture, saturated hydraulic conductivity, and suction pressure at every time step, was employed to calculate the infiltration rates in the various soil layers. Wilting point moisture levels were used to represent the maximum amount of water that can be evapotranspired from the soil layers. Soil temperatures played a major role in determining the frozen status of the soil. If the soil temperature was below 0^0C, then the soil was categorized as frozen. The initial moisture content was required as an initial value for the state variables (Peat Layer Storage, Till Layer Storage, and Shale Layer Storage).

The model was used to simulate the hydrologic response for five years (2000-2004) in the three reconstructed sub-watersheds comprising soil layers of various depths. In order to validate the structure of the model, calibration and validation of the model were conducted using the data for two years (2001 - calibration year; 2002 - validation year). While simulating the watershed response in each sub-watershed, the model parameters were fine-tuned every year until the output from the model closely matched the observed soil moisture in the different soil layers and the overland flow. This technique of the model tuning parameters helped in understanding the evolution of the reconstructed watershed with time. The outcome of this research work is summarized in following two sections.

7.1.1 Hydrologic Simulation

The model simulated the watershed processes in each of the three reconstructed sub-watersheds (D1, D2, and D3). The model performed best in sub-watershed D3, where the overall MRE varied from 3% to 8%. The result was closely followed by D1, where the MRE value ranged between 5% and 9%. The performance of the model was poorest in sub-watershed D2, where the overall MRE was between 11% and 21%.

The SDWM indicated that all of the sub-watersheds have not stabilized. Failure to determine a unique parameter set for simulating the watershed response for all five years of the study period is a one of the possible arguments that the watersheds are evolving over time. The five years, for which the simulations were done, are characterized as drought years. Hence, the change in parameters can be due to the climate variability itself. Another possibility of change in parameters could be due to the model structure itself. Further research work is required for quantification of the change in parameters. The analysis of the till infiltration parameter (I_{cT}) for all sub-watersheds revealed that there is an increasing trend in the moisture movement from the peat into the till layers in all sub-watersheds. This could be due to the subsidence or biodegradation of the highly organic peat layer. Sub-watershed D3 has the maximum number of varying model parameters. This could be due to the fact that sub-watershed D3 may be experiencing more vegetation growth than the other sub-watersheds (D1 and D2). Also, the shale infiltration parameter (I_{cS}) indicated an increasing trend for all sub-watersheds. This could be due to the fact that the watersheds are experiencing freeze-thaw cycles that cause the saturated hydraulic conductivity to increase.

It appears that sub-watershed D2 is experiencing the highest moisture stress followed by sub-watershed D1, while sub-watershed D3 is experiencing the least moisture stress among the three sub-watersheds.

It is recommended that future monitoring of the sub-watersheds should be carried out in order to establish trends in the SDWM parameters. This would be helpful in designing and planning future reclamation strategies. Once the trends in the parameters are known, suitable nomographs can be made for other watersheds in similar kinds of environment.
The present research emphasised that the watershed models should be calibrated and validated using two or more hydrologic variables. Most watershed models in the hydrologic modeling literature make use of only streamflow or overland flow during model calibration and validation. It is recommended that any watershed yielding only ephemeral overland flow should follow the calibration technique used in this study.

7.1.2 System Dynamics Approach to Watershed Modeling

The model results indicate that system dynamics (SD) is a potential candidate for watershed modeling. The system structure implemented in the SD environment helps to provide for understanding of the system under consideration and gives useful information about the dynamicity of the system. Most hydrological models use metrological and soil data to estimate the watershed response, but such models do not explicitly represent the internal dynamics of the hydrologic processes occurring in the watershed. SD provides insight into the interaction among the various hydrological processes and thus proves to be an effective modelling tool for organizing and integrating the existing information on the hydrologic processes in a watershed. The system dynamics model described in this study is a highly aggregated explanatory model; it is an attempt to simplify reality for the sake of clarity. As a consequence, SD provides much wider scope for expanding a model in accordance with the nature of the circumstances being investigated.

7.2 Research Contributions

The present research work has resulted in the building of a new hydrologic model, the System Dynamics Watershed Model (SDWM), based on the application of water-balance principles by using system dynamics approach. The model is intended to serve as a tool for simulation-for-understanding the evolution of reconstructed watersheds as well as a valuable tool for the prediction of the watershed response to different climatic scenarios. Since the model is specifically designed and coded for reconstructed watersheds, it is expected to give a better understanding of the hydrology of a reconstructed landscape to the stakeholders that primarily include oilsands industry and regulators. It is expected that the SDWM developed in this research will play a vital role in designing and evaluating the long-term performance of reconstructed watersheds.

Simulation of watershed response for each reconstructed sub-watershed gave an indication that the sub-watersheds are evolving with time. The unique methodology of fine tuning the model parameters in order for the simulated results to match the observed data provided an insight into the evolution of the three sub-watersheds used in this study. The dynamic nature of the model parameters helped to conclude that monitoring of the

reconstructed watersheds should be carried out beyond five years or until a modest level of stability in the model parameters is achieved. However, the model has been used for one study area only. It should also be applied to other similar watersheds so that the desired robustness can be infused into the model structure.

7.3 Possible Research Extension

The following section recommends the direction in which future work can be carried out to supplement the research presented in this study.

7.3.1 Advanced Calibration, Sensitivity, and Uncertainty Analyses

The SDWM was calibrated and validated using a trial and error methodology. There is a need to follow a formal and more sophisticated calibration procedure in order to determine the best parameter set for simulating the watershed processes. This would help in eliminating equifinality among the model parameters. The issue of equifinality of parameters needs to be addressed in further studies as well. Future research should be directed towards sound calibration using various advanced calibration techniques.

Mechanistic models (such as SDWM) are often complicated by the presence of uncertainties in the input data, and with the model parameters and structure. A systematic uncertainty analysis provides insight into the level of confidence in model estimates, and can aid in assessing how various possible model estimates should be weighted. Further, such analysis can lead to the identification of the key sources of uncertainty (such as data gaps) as well as the sources of uncertainty that are not important with respect to a given watershed response. The purpose of quantitative uncertainty analysis is to use currently available information to quantify the degree of confidence in the existing data and model parameters. A comprehensive uncertainty analysis of SDWM parameters should be carried out as a part of future research.

7.3.2 Comparison with Other Watershed Models

It has been mentioned in Chapter 1 that this research work is a part of a bigger project that is directed toward developing a sustainable reclamation strategy. It is imperative that the simulated results from any available watershed model (e.g., HSPF, SLURP) should be compared with the results obtained by the developed SDWM. This will help in evaluating the different modeling approaches and their suitability in modeling reconstructed watersheds.

7.3.3 Hybrid Watershed Modeling

Various processes in the watershed (such as interflow) are intermittent but are significant with respect to evaluating the long-term performance of any reclamation strategy. Such minute processes cannot be captured effectively with mechanistic models. However, a data driven model could be useful in capturing such processes. Hence, a data driven model that can be used in conjunction with the SDWM should be developed. The use of such a hybrid model is particularly advantageous in reconstructed watersheds where many minute hydrologic processes can pose a threat to the long-term performance of the watersheds.

7.4 Study Limitations

Although there is a comprehensive amount of data available at the study site, snow depths and soil moisture in the winter season have not yet been recorded. The two missing data sets are a major limitation in simulating the watershed response during the winter season. Snow surveys in the late winter season should be carried out. This, along with continuous records of snowfall, will help in estimating the amount of water available during snowmelt for runoff from and infiltration into the frozen soil. Monitoring of soil moisture in the winter should be carried out in order to simulate the moisture dynamics during winter season. Accurate soil moisture observations during the winter season will enhance the predictive capability of the developed model. The field sensors should be periodically checked in order to ensure their workability and reliability. Shale percolation needs to be measured more accurately to verify the simulated results. The STELLA simulation environment cannot be used for optimization of parameters. It is well equipped to conduct simulation but not optimization. Better SD-based simulation environments should be used in future studies or a link with an appropriate optimization tool should be established.

References

Aassine, S. and El-Jai, M.C. 2002. Vegetation dynamics modeling: a method for coupling local and space dynamics. *Ecological Modeling*, 154:237-249.

Abbott, M.M., Bathurst, J.C., Cunge, J.A., O'Connell, P.E. and Rasmussen, J. 1986. An introduction to the European Hydrologic System-Systeme Hydrologique Europeen, "SHE" 1: history and philosophy of a physically based disturbed system. *Journal of Hydrology,* 87:45-59.

Ahmad, S. and Simonovic, S.P. 2000. System dynamics modeling of reservoir operations for flood management. *Journal of Computing in Civil Engineering,* 14(3):190-198.

Alberta Environment, 2001. EPEA Approval 26-01-12 Mildred Lake Oil Sands Mine-Lease 17/22 Operation. EPEA 26-01-12, Alberta Environment, Edmonton.

Alley, W.M. 1984. On the treatment of evapotranspiration, soil moisture accounting, and aquifer recharge in monthly water balance models. *Water Resources Research*, 20:1137–1149.

Ambroise, B., Perrin, J.L., and Reutenauer, D. 1995. Multicriterion validation of a semidistributed conceptual model of the water cycle in Fecht catchment (Vosges massif, France), *Water Resources Research*, 31(6):1467–1481.

Anderson, E.A. 1968. Development and testing of snow pack energy balance equation. *Water Resources Research*, 4(1):19-37.

Anderson, E.A. 1976 . A point energy and mass balance of a snow cover. NOAA Tech. Rept. NWS 19, U.S. Dept. of Commerce, Washington, D.C.

Barton, P.M. and Tobias, A.M. 1998. Accurate estimation of performance measures for system dynamic models. *System Dynamics Review*, 14(1):85-94.

Bastiaanssen, W.G.M, Pelgrum.H, Droogers P, de Bruin, H.A.R. and Menenti, M. 1997. Area-average estimates of evaporation, wetness indicators and top soil moisture during two golden days in EFEDA. *Agricultural and Forest Meteorology,* 87:119-137.

Beven, K.J. 2000. Down to basics: runoff processes and the modeling process. Rainfall-Runoff Modeling: The Primer, John Wiley and Sons Limited, New York, pp.1-22.

Blaney, H.F. and Criddle. W.D. 1950. Determining water requirements in irrigated areas from climatological and irrigation data. Tech. Paper 96. USDA Soil Conservation Service. (In Doorenboss, J. and Pruitt, W.D. 1975. Crop Water Requirements. Irrigation and Drainage Paper No. 24, 179, pp. FAO. Rome)

Boegh, E., Thorsen, M., Butts, M.B., Hansen, S., Christiansen, J.S., Abrahamsen, P., Hasager, C.B., Jensen, N.O., van der Keur, P.,1, Refsgaard, J.C., Scheld K., Soegaard, A. and Thomsen, H. 2002. Incorporating remote sensing data in physically based distributed agro-hydrological modelling. *Journal of Hydrology*, 287:279–299.

Boese, K. 2003. The design and installation of a field instrumentation program for the evaluation of soil-atmosphere water fluxes in a vegetated cover over saline/sodic shale overburden. *M.Sc. Thesis, University of Saskatchewan*, Saskatoon, SK, Canada.

Brooks, R.H. and Corey, A.T. 1964. Hydraulic properties of porous media. Hydrol. Pap. 3, Colorado State University, Fort Collins.

Bruch, P. 1993. Evaporative fluxes in homogeneous and layered soils, M.Sc. thesis, Department of Civil and Geological Engineering, University of Saskatchewan, Canada.

Burnash, R.J.C. 1995. The NWS river forecasting system, In*:* Computer models of watershed hydrology. *Edited by* V.P. Singh. Water Resources Publications, LLC, Highlands Ranch, Colo., pp. 395–442.

Burt, C.M., Muziger, A.J., Allen, R.G. and Howell, T.A. 2005. Evaporation research: review and interpretation, *Journal of Irrigation and Drainage Engineering*, 131(1):37-58.

Campbell, G.S. 1974. A simple method for determining unsaturated conductivity from moisture retention data. *Soil Science,* 117:311-314.

Chang, C.H. 1968. Climate and Agriculture-An Ecological Survey. 304 pp. Aldine Publishing Co., Chicago, USA.

Christiansen, J.E. 1968. Pan evaporation and evapotranspiration from climatic data. *Journal of Irrigation and Drainage Division*, *ASCE*, 94:243-265.

Costanza, R. and Voinov, A. 2001. Modeling ecological and economic systems with Stella: Part III. *Ecological Modelling*, 143:1–7.

Costanza, R. and Gottlieb, S. 1998. Modeling ecological and economic systems with Stella: Part II. Special issue of *Ecological Modelling,* 112:81-247.

Costanza, R., Duplisea, D. and Kautsky, U. (Eds) 1998. Modelling ecological and economic systems with Stella. Part I. *Ecological Modelling,* 110:1-4.

Crawford, N.H., and Linsley, R.K. 1966. Digital simulation in hydrology: Stanford Watershed Model IV. *Tech. Rep. No. 39,* Stanford Univ., Palo Alto, California, USA.

CSIRO 1990. Soil water infiltration and movement. User`s manual. Division of Soils, Commonwealth Scientific and Industrial Research Organisation, Australia.

Cutris, W.R. 1974. Terraces reduce runoff and erosion on surface mine benches. *Journal of Soil and Water Conservation,* 26(5):198-199.

Deaton, M.L. and Winebrake, J.J. 2000. Dynamic modeling of environmental systems, Springer-Verlag Publication, New York, USA.

Dingman, S.L. 2002. Physical hydrology. Second edition, Prentice Hall, New Jersey, USA.

Diskin, M.H. and Simon, E. 1979. The relationship between the time bases of simulation models and their structure. *Water Resources Bulletin*. 15:1716-1732.

Donigian, A.S., Bicknell, B.R., and Imhoff, J.C. 1995. Hydrological simulation program — Fortran (HSPF). *In* Computer models of watershed hydrology. *Edited by* V.P. Singh. Water Resources Publications, LLC, Highlands Ranch, Colo., pp. 395–442.

Doorenboss, J. and Pruitt, W.D. 1975. Crop Water Requirements. Irrigation and Drainage Paper No. 24, 179 pp. FAO. Rome.

Elshorbagy, A. 2005. Learner-centered Approach to Teaching Watershed Hydrology Using System Dynamics. *International Journal of Engineering Education* (in press).

Elshorbagy, A. and Ormsbee, L. 2005. Object oriented modeling approach to surface water quality management, *Environmental Modeling and Software, (in press)*.

Elshorbagy, A. Simonovic, S.P. and Panu, U.S. 2000. Performance Evaluation of Artificial Neural Networks for Runoff Prediction. *Journal of Hydrologic Engineering, ASCE,* 5(4):424-427.

Elshorbagy, A., Jutla, A., Barbour, L., and Kells, J. 2005. System dynamics approach to assess the sustainability of reclamation of disturbed watersheds. *Canadian Journal of Civil Engineering,* (32):144–158.

Faria, D.A., Pomeroy, J.W. and Essery, R.L.H. 2000. Effect of covariance between ablation and snow water equivalent on depletion of snow covered area in a forest. *Hydrological Processes*, 14:2683-2695.

Fayer, M.J. and Jones, T.L. 1990 UNSAT-H Version 2.0: unsaturated soil water and heat floe model. Publication PNL-6779, Pacific Northwest Laboratory, Richland, WA, USA.

Fayer, M.J., Rockhold, M.L. and Campbell, M.D. 1992. Hydrologic modeling of protective barriers: comparison of field data and simulation results. *Soil Science Society of America Journal*, 56:690-700.

Fiering, M.B. and Kuczera, G. 1982. Robust estimators in hydrology. Scientific basis of water-resource management, Geophysics Study Committee, Geophysics Research Board, Assembly of Mathematical and Physical Sciences, National Research Council, Washington, D.C., USA.

Ford, A. 1999. Modeling the environment-An introduction to system dynamics modeling of environmental systems. Island Press, Washington, D.C., USA.

Forrester, J.W. 1964. Industrial dynamics. The MIT Pres, Cambridge, Massachusetts, USA.

Forrester, J.W. 1980a. Information sources for modeling the national economy. *Journal of the American Statistical Association,* 75:555-566.

Forrester, J.W. 1980b. System dynamics-future opportunities. *TIMS studies in the Management* Sciences, 14:7-21.

Gillespie, D.F, Robards, J.K., and Cho, S. 2004. Designing Safe Systems: Using System Dynamics to Understand Complexity. *Natural Hazards Review*, 5(2):82-88.

Gilley, J.E., Gee, G.W., Bauer, A., Willis, W.O. and Young, R.A. 1977. Runoff and erosion characteristics of surface mined sites in western North Dakota. *Transactions of American Society of Agricultural Engineers,* 20(4):697-704.

Granger, R.J. 1989. A complimentary relationship approach for evaporation from nonsaturated surfaces. *Journal of Hydrology*, 111:31-38.

Granger, R.J., Gray D.M., Dyck, G.E. 1984. Snowmelt infiltration to frozen prairie soils. *Canadian Journal of Earth Sciences,* 21:669-677.

Gray, D.M. and Tao, Y.X. 1994. Prediction of snowmelt infiltration into frozen soils. *Numerical Heat Transfer,* 26:643-665.

Gray, D.M., Landine, P.G. and Granger, R.J. 1985. Simulating infiltration into frozen prairie soils in streamflow models. *Canadian Journal of Earth Sciences,* 22:464-474.

Gray, D.M., Toth, B., Zhao, L, Pomeroy, J.W. and Granger, R.J. 2001. Estimating areal snowmelt infiltration into frozen soils. *Hydrological Processes,* 15:3095–3111.

Green, W.H. and Ampt, G. 1911. Studies of soil physics, Part 1-the flow of air and water through soils. *Journal of Agricultural Sciences*, 4:1-24.

Haigh, M. J. 2000. The aims of land reclamation. *Land Reconstruction and Management, A.A.Balkema Publishers, Rotterdam, The Netherlands*, 1: pp. 1-20.

Hakonson, T.E. 1986. Evaluation of geologic materials to limit biological intrusion into low-level radioactive waste disposal sites. LA–10286–MS, Los Alamos National Laboratory, Los Alamos, New Mexico.

Hann, C.T. 1972. A water yield model for small watersheds. *Water Resources Research,* 8:58-69.

Haan, C T, Johnson H P and Brakensiek, D L (ed) 1982. Hydrologic Modeling of Small Watersheds, Monogr. Ser., vol. 5, pp. 169-225, American Society of Agricultural Engineers, St. Joseph, Mich

Hanson, C.L. and Rauzi, F. 1977. Class A pan evaporation as affected by shelter and a daily prediction equation. *Agricultural Meteorology*, 18:27-35.

Haupt, F.H. 1967. Infiltration, overland flow, and soil movement on frozen and snow covered plots. *Water Resources Research*, 3(1):145-161.

High Performance Systems Inc. (HPS) 2001. Tutorial and technical documentation: STELLA® II. High Performance Systems Inc., Hanover, N.H. [now ISES Systems, Lebanon, N.H.].

Holtan, H.N. 1961. A concept for infiltration estimates in watershed engineering. Bulletin: 45-51, 25 pp. USDA, ARS, Washington, D.C..

Holtan, H.N., Stiltner, G.J., Hensen, W.H., and Lopez, N.C. 1975. USDAHL-74 revised model of watershed hydrology. Tech. Bull. 1518, 99 pp. USDA, Washington, D.C..

Horton, R.E. 1933. The role of infiltration in Hydrologic Cycle. *Transactions of American Geophysical Union* 14:446-460.

Horton, R.E. 1940. An approach toward a physical interpretation of infiltration capacity. *Soil Science Society American Proceedings*, 5:399-417.

Huggins, L.F. 1982. Surface runoff, storage and routing. In: Haan, C T, Johnson H P and Brakensiek, D L (ed) Hydrologic Modeling of Small Watersheds, Monogr. Ser., vol. 5, pp. 169-225, American Society of Agricultural Engineers, St. Joseph, Mich.

Huggins, L.F. and Monke, E.J. 1966. The mathematical simulation of the hydrology of small watersheds. TR1, 129 pp. Purdue Water Resources Research Centre, Lafayette, IN.

Hydrologic Engineering Center (HEC) 1981. HEC-1 flood hydrograph package: Users manual. U.S. Army Corps of Engineers, Davis, California, USA.

Illangasekare, T.H., Walter, R.J., Meier, M.F. and Pfeffer, W.T. 1990. Modeling of meltwater infiltration in subfreezing snow. *Water Resources Research.* 26(5):1001-1012.

Isrealson, O.W. and Hansen, V.E. 1967. Irrigation Principles and Practices, pp. 198-200. John Wiley, New Delhi.

Jakeman, A. and Hornberger, G. 1993 . How much complexity is warranted in a rainfall-runoff model? *Water Resources Research*, 29:2637–2649.

Johnston, P.R. and Pilgrim, D.H. 1976. Parameter optimisation for watershed models. *Water Resources Research*, 12:477–486.

Khire, M.V., Benson, C.H., and Bosscher, P.J. 1997. Water Balance Modeling of Earthen Final Covers. *Journal of Geotechnical and Geoenvironmental Engineering*, 744-754.

Kilmartin, M.P. 2000. Hydrological management of reclaimed opencast coal mine sites. *Land reconstruction and Management, A.A.Balkema Publishers, Rotterdam, The Netherlands,* 1: pp. 137-158.

Kim, W.H. and Daniel, D.E. 1992. Effects of freezing on the hydraulic conductivity of compacted clay. *Journal of Geotechnical Engineering,* 118:1083–1097.

Kite, G. 2000. Using a basin-scale hydrological model to estimate crop transpiration and soil evaporation. *Journal of Hydrology*, 229:59-69.

Kite, J.W. 1995 . The SLURP model. *In* Computer models of watershed hydrology. In: Singh, V.P. Water Resources Publications, LLC, Highlands Ranch, Colo., pp. 521–563.

Kostiakov, A.N. 1932. On the dynamics of the coefficient of water percolation in soils and on the necessity of studying it from a dynamic point of view for purpose of amelioration. Transactions of 6th Comm. Intern. Soil Science Society, Russian Part A.: 17-21.

Kristensen, K.J. and Jensen, S.E. 1975. A model for estimating actual evapotranspiration from potential evapotranspiration. *Nordic Hydrology*, 6:170-188

Kuczera, G., 1983. Improved Parameter Inference in Catchment Models. 1. Evaluating Parameter Uncertainty. *Water Resources Research*, 19(5):1151-1172.

Kuznik. I.A. and Bezmenov, A.I. 1964 Infiltration of meltwater into frozen soil. *Soviet Hydrology*, 665-670.

Lee, J. 1993. A formal approach to hydrological model conceptualization. *Hydrological Sciences Journal,* 38(5):391–401.

Li, L. and Simonovic, S.P. 2002 System dynamics model for predicting floods from snowmelt in North American prairie watersheds. *Hydrological Processes,* 16:2645–2666.

Licznar, P. and Nearing, M.A. 2003. Artificial Neural Networks of Soil Erosion and Runoff Prediction at the Plot Scale. *Catena,* 51(2):89-114.

Lusby, G.C. and Toy, T.J. 1976. An evaluation of surface mine spoils area restoration in Wyoming using rainfall simulation. *Earth Surface Processes,* 1:376-386.

Maidment, D.R. 1993. Handbook of Hydrology. McGraw Hill Publication, NY, USA.

Maxwell, T. and Costanza, R. 1997. An open geographic modelling environment. *Simulation Journal,* 68:265-267.

Mays, L.W. 2005. Water resources engineering. Hoboken, NJ : John Wiley & Sons, Inc., USA.

McKay, G.A. and Thompson, H.A. 1968. Snowcover in the prairie provinces of Canada,. *Transactions of ASAE*, 11(6):812-815.

Meiers, P. G. 2002. The use of Field Measurements of Hydraulic Conductivity to Characterize the Performance of Reclamation Soil Covers with Time. M.Eng. Thesis. Division of Environmental Engineering, University of Saskatchewan, Saskatoon, Saskatchewan, Canada.

Mein, R.G. and Larson, C.L. 1973. Modelling infiltration during a steady rain. *Water Resources Research* 9:384-394.

Mend 1993. SoilCover: user's manual for an evaporative flux model. University of Saskatchewan, Canada.

Miller, C. J., and Lee, J. Y. 1999. Response of landfill clay liners to extended periods of freezing. *Engineering Geology*, 51, 291-302.

Miller, C.J., and Lee, J.Y. 1999. Response of landfill clay liners to extended periods of freezing. *Engineering Geology*, 51, 291-302.

Moffatt, I. and Hanley, N. 2001 Modelling sustainable development: systems dynamic and input–ouput approaches, *Environmental Modelling & Software,* 16(6):545-557.

Mualem, Y. 1976. A new model for predicting the hydraulic conductivity of unsaturated porous media. *Water Resources Research,* 12:513-522.

Nash, J.E. and Sutcliffe, J.V. 1970. River flow forecasting through conceptual models. *Journal of Hydrology*, 10(3):282-290.

Ngah, S.A., Reed, S.M. and Singh, R.N. 1984. Groundwater problems associated with surface mining in United Kingdom. *International Journal of Mine Water,* 3(1):1-12.

O'Kane, M., Wilson, G.W. and Barbour, S.L. 1998. Instrumentation and monitoring of an engineered soil cover system for mine waste rock. *Canadian Geotechnical Journal,* 35:828-846.

Oke, T.R. 1992. Boundary Layer Climates, Routledge, New York, USA.

Osborn, H.B. and Lane, L.J. 1982. Chapter3-Precipitation. In Haan, C.T., Johnson, H.P. and Brakensiek, D.L.(ed) Hydrologic Modeling of Small Watersheds, American Society of Agricultural Engineers Monograph, 5:81-117.

Oudin, L., Hervieu, F., Michel, C., Perrin, C., Andre´assiana, V., Anctilb, F. and Loumagne, C. 2005. Which potential evapotranspiration input for a lumped rainfall–runoff model? Part 2—Towards a simple and efficient potential evapotranspiration model for rainfall–runoff modelling. *Journal of Hydrology*, 303:290–306.

Parmele. H.L. 1972. Error in output of hydrologic models due to errors in input potential evapotranspiration. *Water Resources Research*, 8:348-359.

Pelton, W.L., King, K.M. and Tanner, C.B 1960. An evaluation of Thornwaite and mean temperature method for determining potential ET. *Agronomy Journal*, 52:387-395.

Penman, H.L. 1956. Estimating evaporation. *American Geophysical Union*, 4:9-29.

Philip, J.R. 1957. The theory of infiltration. 1. The infiltration equation and its solution. *Soil Science,* 83: 345-347.

Potter, K.N., Carter, F.S. and Doll, E.C. 1988. Physical properties of constructed and undisturbed soils. *Soil Science Society of America Journal*, 52:1435-1438.

Prunty, L. and Kirkham, D. 1979. A drainage model for a reclaimed surface mine. *Soil Science Society of America Journal,* 43:28-34.

Rajurkar, M.P. Kothyari, U.C. and Chaube, U.C. 2004. Modeling of the Daily Rainfall-Runoff Relationship with Artificial Neural Network. *Journal of Hydrology,* 285(1-4):96-113.

Randers, J. 1996. Guidelines for model conceptualization. Modeling for Management 11: simulation in support of systems thinking (Ed: Richardson, G.P), Dartmouth Publishing Co. Ltd. Vermount, USA.

Richard, L.A. 1931. Capillary conduction through porous mediums. *Physics,* 1:318-333.

Rick, G., 1995. Closure considerations in environmental impact statements. *Mineral Industry International,* 1022:5-10.

Ringler, R.W. 1984. Spoil aquifer resaturation following coal strip mining. *Proceedings of American Society for Surface Mining and Reclamation, National Meeting (Kentucky):* 274-291.

Ritchie, J.T. 1972. Model for predicting evaporation from a row crop with incomplete cover. *Water Resources Research*, 8:1204-1213.

Rogowski, A.S. and Weinrich, B.E. 1981. Modeling water flux on strip mined land. *Transactions of American Society of Agricultural Engineers,* 24(4):935-940.

Sawatsky, L., McKenna, G., Keys, M. and Long, D. 2000. Towards minimizing the long tern liability of reclaimed mine sites, *Land reconstruction and Management, A.A.Balkema Publishers, Rotterdam, The Netherlands,* 1: 21-26.

Saxton, K.E. 1982. Evapotranspiration. In: Haan C T, Johnson, H P and Brakenseik, D L (ed) Hydrologic Modeling of Small Watersheds, ASAE Monograph No. 5., pp 229-273. American Society of Agricultural Engineers., Michigen.

Saxton, K.E., Johnson, H.P. and Shaw, R.H. 1974. Modeling evapotranspiration and soil moisture. *Transactions of ASAE*, 17:673-677.

Saysel, A.K. and Barlas, Y. 2001. A dynamic model of salinization on irrigated lands *Ecological Modelling*, 139:177–199.

Schaap, M.G. and Leij, F.J. 2000. Improved prediction of unsaturated hydraulic conductivity with the Mualem-van Genuchtan model. *Soil Science Society American Journal*, 64:843-851.

Schreoder, P.R, Morgan, J.M., Walski, T.M. and Gibson, A.C. 1994. Hydrologic evaluation of landfill performance (HELP) model. Volume 1, User`s guide, International Groundwater Modeling Centre, Colorado School of Mines, Colo., USA.

Schroeder, S.A. 1987. Runoff curve number estimations for reshaped fine textured spoils. *Reclamation and Revegetation Research*, 6:129-136.

Schwab, G.O., Fangmeier, D.D., Elliot, W.J. and Frevert, R.K. 2002. Soil and water conservation engineering, John Wiley and Sons, Toronto.

Shook, K. and Gray, D.M. 1997. Snowmelt resulting for advection. *Hydrological Processes*, 11:1725-1736.

Shurniak, R.E. 2003. Predictive Modeling of Moisture Movement within Soil Cover Systems for Saline/sodic overburden Piles, M.Sc. Thesis, University of Saskatchewan, Canada

Simonovic, S.P. 2002. World water dynamics: global modeling of water resources. *Journal of Environmental Management,* 66(3):249-267.

Simonovic, S.P. and Li, L. 2003. Methodology for Assessment of Climate Change Impacts on Large-Scale Flood Protection System *Journal of Water Resources Planning and Management*, 129(5):361-371.

Singh, V.P. 1988. Hydrological Systems-Volume 2, Prentice Hall, NJ, USA,

Singh, V.P. 1995. Watershed modeling. *Computer Models in Watershed Hydrology, Water Resources Publication, Highland Ranch, Colorado, USA*.

Skaggs, R.W. 1982. Infiltration. In: Haan, C.T., Johnson, H.P. and Brakenseik, D.L. (ed) Hydrologic Modeling of Small Watersheds. ASAE Monograph No. 5, pp. 121-165. ASAE, Michigan.

Smith, R.E. 1972. The infiltration envelop: Results from a theoretical infiltrometer. *Journal of Hydrology*, 17: 1-21.

Smith, R.E. 1976. Approximations for vertical infiltration rate patterns. *Transactions of ASAE*, 19:505-509.

Smith, R.E. 1981. Rational models for infiltration hydrodynamics, Proceedings of the International Symposium on Rainfall-Runoff Modeling, May 18-21, Mississippi State University, Mississippi State, Mississippi, USA.

Sorooshian, S. 1983. Surface water hydrology: online estimation. *Reviews of Geophysics and Space Physics,* 21(3):706-721.

Sorooshian. S. and Gupta, V.K. 1995. Model calibration. In: Singh V P (ed) Computer Models of Watershed Hydrology, Water Resources Publications. pp 20-68.

Stadler, D., Fluhler, H. and Jansson, P.E. 1997. Modelling vertical and lateral water flow in frozen and sloped forest soil plots. *Cold Regions Science and Technology*, 26:181-194.

Stahli, M., Jansson, P.E. and Lundin L.C. 1999. Soil moisture redistribution and infiltration in frozen sandy soils. *Water Resources Research*, 35(1):95-103.

Stave, K.A. 2003. A system dynamic model to facilitate public understanding of water management options in Las Vegas, Nevada. *Journal of Environmental Management,* 67:303-313.

Sugawara, M. 1995. The Tank Model. *In* Computer models of watershed hydrology. *Edited by* V.P. Singh. Water Resources Publications, LLC, Highlands Ranch, Colo. pp.165-215.

Suter, G. W., Luxmoore, R. J. and Smith, E. D. 1993. Compacted soil barriers at abandoned landfill sites are likely to fail in the long term. *Journal of Environmental Quality*, 22(2):217-226.

Swanson, D.A. Barbour, S.L. Wilson, G.W. and O'Kane, M. 2003. Soil-atmosphere modelling of an engineered soil cover for acid generating mine waste in a humid, alpine climate. *Canadian Geotechnical Journal,* 40(2):276-292.

Thornthwaite, C.W. 1948. An approach toward a rational classification of climate. *The Geophysical Review*, 38:55-94.

van Dam, J.C. and Feddes, R.A. 2000. Numerical simulation of infiltration, evaporation and shallow groundwater levels with the Richards equation. *Journal of Hydrology*, 233:72-85.

van Genuchten, M.T. 1980. A closed form equation for predicting the hydraulic conductivity of unsaturated soils. *Soil Science Society American Journal*, 44:892-898.

Vereecken, H. 1989. Estimating the soil moisture retention characteristic from text, bulk density and carbon content. *Soil Science*, 148:389-403.

Viessman, W. and Lewis, G.L. 2003. Hydrologic Simulation and streamflow analysis. Introduction to Hydrology. Prentice Hall, Pearson Education Inc., NJ, USA*,* pp. 453-536.

Voinov, A., Fitz, C., Boumans, R. and Costanza, R. 2004. Modular ecosystem modeling. *Environmental Modelling and Software,* 19:285-304.

Ward, A.D., Wells, L.G. and Phillips, R.E. 1983. Infiltration through reconstructed surface mined spoils and soils. *Transactions of American Society of Agricultural Engineers,* 26(3):821-830.

Waugh, W. J. and Smith, G. M. 1997. Effects of Root Intrusion at the Burrell, Pennsylvania, Uranium Mill Tailings Disposal Site. *GJO-97-5-TAR GJO-LTSM-4*, U.S. Department of Energy, Grand Junction.

Waugh, W.J. and Smith, G.M. 1997. Effects of Root Intrusion at the Burrell, Pennsylvania, Uranium Mill Tailings Disposal Site. *GJO-97-5-TAR GJO-LTSM-4*, U.S. Department of Energy, Grand Junction.

Williams, J.R. and Haan, R.W. 1972. HYMO-a problem oriented computer language for building hydrologic model. Water Research Laboratory. In: Singh, V.P. Water Resources Publications, LLC, Highlands Ranch, Colo., pp. 79-86.

Wilson, G.W., Fredlund, D.G. and Barbour, S.L. 1996. The effect of soil suction on evaporative fluxes from soil surfaces. *Canadian Geotechnical Journal*, 34:145-155.

Wooldridge, S.A., Kalma, J.D. and Walker J.P. 2003. Importance of soil moisture measurements for inferring parameters in hydrologic models of low-yielding ephemeral catchments. *Environmental Modelling & Software,* 18:35–48.

Woolhiser, D.A. and Brakensiek, D.L. 1982. Hydrologic modeling of small watersheds. In: Haan, C.T., Johnson, H.P. and Brakenseik, D.L. (ed) Hydrologic Modeling of Small Watersheds. ASAE Monograph No. 5. pp 3-15. ASAE, Michigan.

Woyshner, M.R. and Yanful, E.K. 1995. Modeling and field measurements of water percolation through an experimental soil cover on mine tailings. *Canadian Geotechnical Journal,* 32:601-609.

Wright, D.L., Perry, H.D. and Blaser, R.E. 1978. Persistent low maintenance vegetation for erosion control and aesthetics in highway corridors. *Reclamation of Drastically Disturbed Lands, American Society of Agronomy, Madison, USA,* pp. 553-583.

Wurbs, R.A. 1994. Computer models for water resources planning and management U.S. Army Corps of Engineers Institute for Water Resources Water Resources Support Center 7701 Telegraph Road Alexandria, Virginia 22315-3868, IWR Report 94-NDS-7.

Wurbs, R.A. 1998. Dissemination of generalized water resources models in the United States. *Water International,* 23:190–198.

Xu, Z.X., Takeuchi, K., Ishidaira, H. and Zhang, X.W. 2002. Sustainability analysis for yellow river water resources using the system dynamics approach. *Water Resources Management,* 16:239-261.

Yanful E.K., Mousavi, S.M. and Yang, M. 2003. Modeling and measurement of evaporation in moisture-retaining soil covers. *Advances in Environmental Research,* 7:783–801.

Ye, W., Bates, B.C., Viney, N.R., Sivapalan, M. and Jakeman, A.J. 1997. Performance of conceptual rainfall-runoff models in low-yielding ephemeral catchments. *Water Resources Research*, 33(1):153–166.

Zhao, L. and Gray, D.M. 1997. A parametric expressions for estimating infiltration into frozen soils. *Hydrological Processes,* 11:1761-1775.

Zhao, L., Gray, D.M. and Male, D.H. 1997. Numerical analysis of simultaneous heat and mass transfer during infiltration into frozen ground. *Journal of Hydrology,* 200:345-363.

Zhao, L.. and Gray, D.M. 1999. Estimating snowmelt infiltration into frozen soils. *Hydrological Processes*, 13:1827-1842.

Appendix A

Assembly of Model in STELLA®

STELLA® software consists of three layers for constructing an SD model. The two small arrows signs on the left hand side of Figure 3.4 are used to switch between the layers. Layer 1 is meant for those stakeholders who do not want to go into the details of the modeling. The user-friendly graphical user interface is developed in this layer of the software. The iconic based modeling is done in Layer 2, such as the one depicted in Figure 3.2. Layer 2 serves as the primary interface for constructing the model. Once the construction of a model is completed within Layer 2, a small globe, shown in Figure 3.4 on left hand side, is clicked to enable the equation sheet. Figure A.1 shows the small question marks (?) in each of the stocks, flows and converters that appear after clicking the small globe. The question marks indicate that the stocks, flows and converters need inputs, which can either be numerical or logical.The mathematical structure of the model is embedded in Layer 3. This layer facilitates the understanding of the mathematical and functional relationships among the stocks and flows.

Double clicking on a stock will open a dialogue box as shown in Figure A.2. This is a dialogue box for the stock called *Soil Water Storage* in Figure A.1. Moving down the dialog box, "Allowable Inputs" allows the modeller to input any of the inputs as an initial condition for the system or the modeller can enter a constant numeric value as the initial value. The calculator keypad, to right of the list, is useful for clicking in numerical values. Along the bottom of the dialog box are four buttons. The last two—"Cancel" and "OK"— require no explanation. The "Document*" button, when clicked, pops up a space into which the modeller can type text that describes assumptions, documents the source of numerical information, etc. Finally, the "Message…" button allows the modeller to "post" some sort of a message (e.g., play a movie or sound, navigate to a new screen, post a text message).

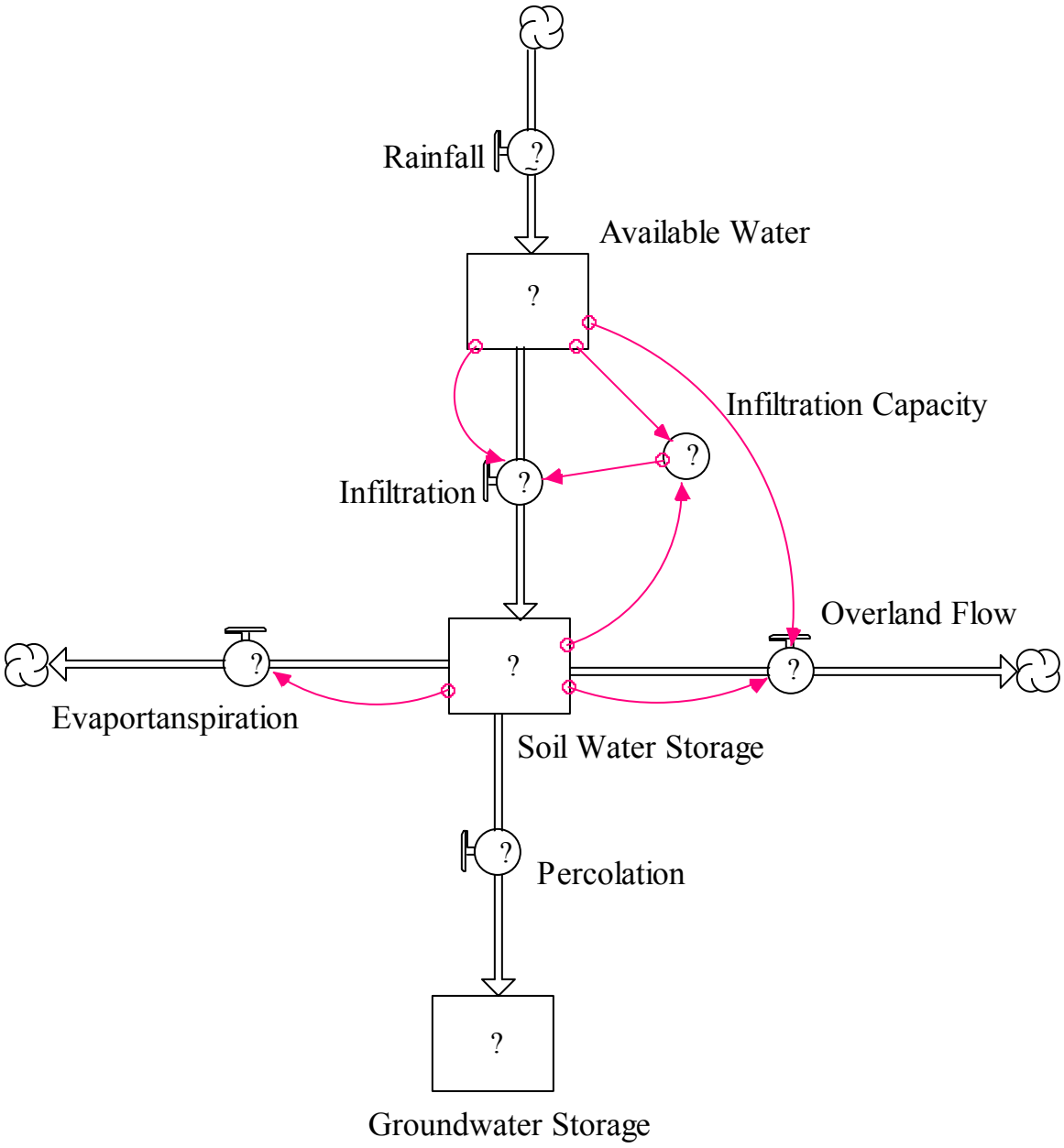

Figure A.1. Equation Sheet in STELLA Software.

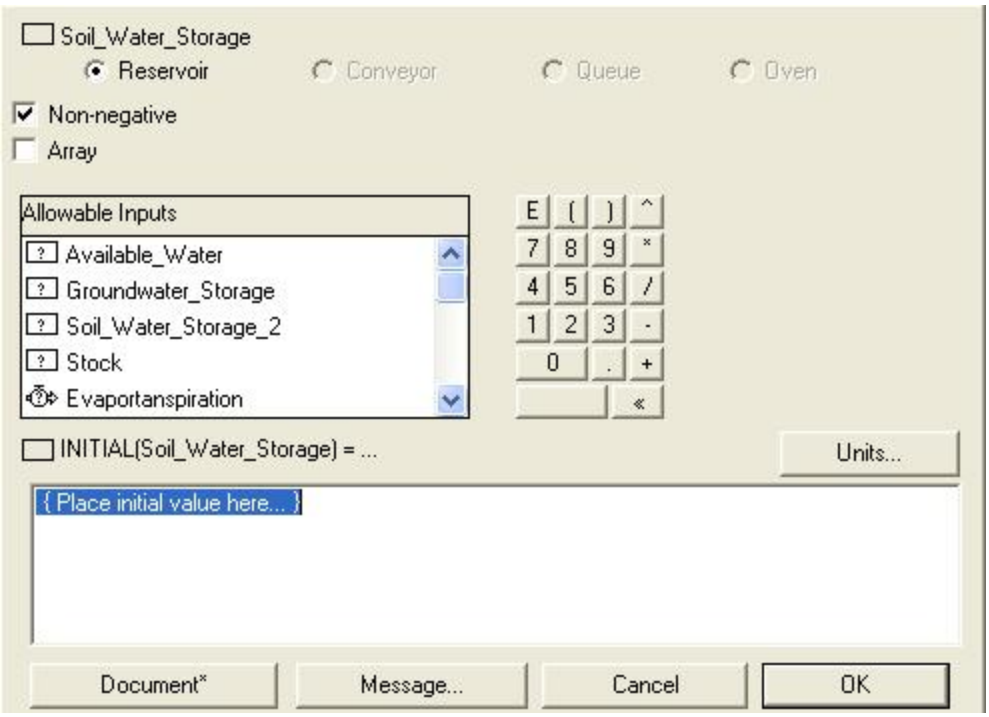

Figure A.2: Dialogue Box of a Stock.

The dialogue box shown in Figure A.3 will open when the modeller double clicks a flow (which is same for converters too). Here, a flow called *Infiltration* is shown. At the top of the dialog box, there is an option to make the flow a uniflow or a biflow. Uniflows allow flow only in the direction in which they point. Biflows allow flow to occur in either direction (either into or out of the stock). *Infiltration* is clearly the only flow into *Soil Water Storage*, so uniflow is the choice here (and the default). The "Required Inputs" list contains two variables, *Available Water* and *Infiltration Capacity*. These variables are in the list because the connectors are drawn from them to the *Infiltration* flow regulator. The sub-dialog box "Infiltration=" is prompting that a suitable mathematical relationship should be written in it using both variables in defining the *Infiltration* flow.

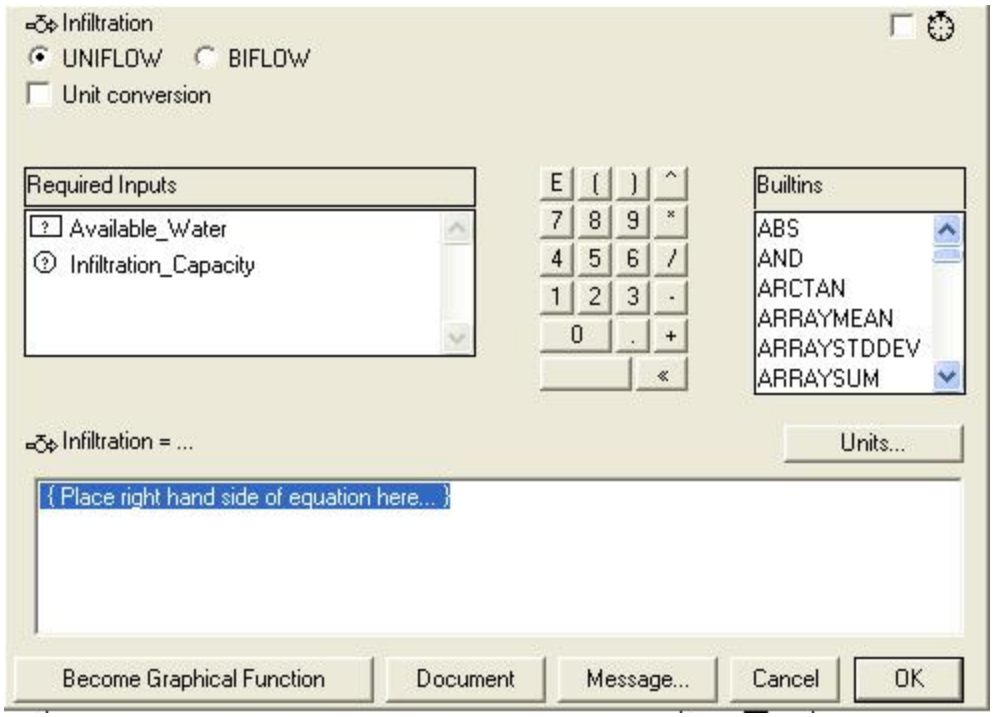

Figure A.3: Dialogue Box of a Flow.

At the bottom of the flow dialogue box, there is an additional button called "Become Graphical Function". This function facilitates in establishing the approximate graphical relationship between any two variables. This has been explained using a converter (Figure A.4) called *Infiltration Capacity,* where it is assumed that there is some relationship between the *Soil Water Storage* and *Infiltration Capacity.* The utility "Become Graphical Function" is especially helpful in hydrologic modeling in defining functional relationships such as between hydraulic conductivity and soil moisture content i.e., Soil water characteristic curve, SWCC, hence eliminating the need for using any regression equation.

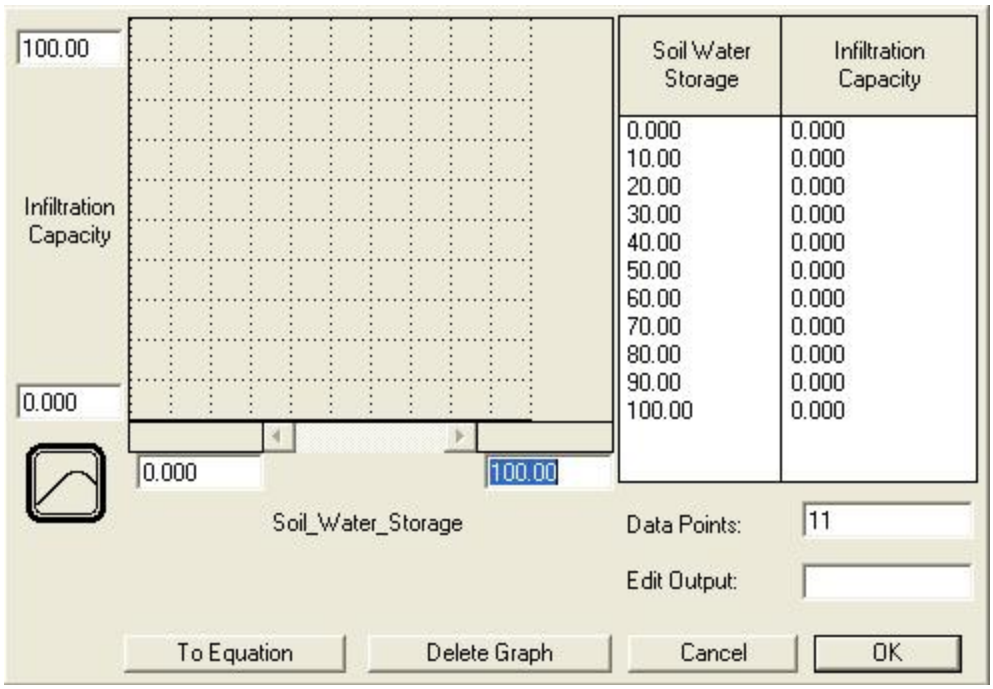

Figure A.4: Dialogue Box of "Become Graphical Function".

There should not be any more "?" left before the model is ready for simulation. The outputs of the model can be seen in graphical or tabular form. STELLA software provides flexibility for visualizing the results in Layer 1, the details of which are beyond the scope of this thesis. However, detailed information about the operation of the model is given in Ford (1999), Deaton and Winebrake (2000), and HPS (2001). Various online courses are available for detailed explanation for using STELLA software.

Appendix B

SDW Model Structure and Graphical User Interface

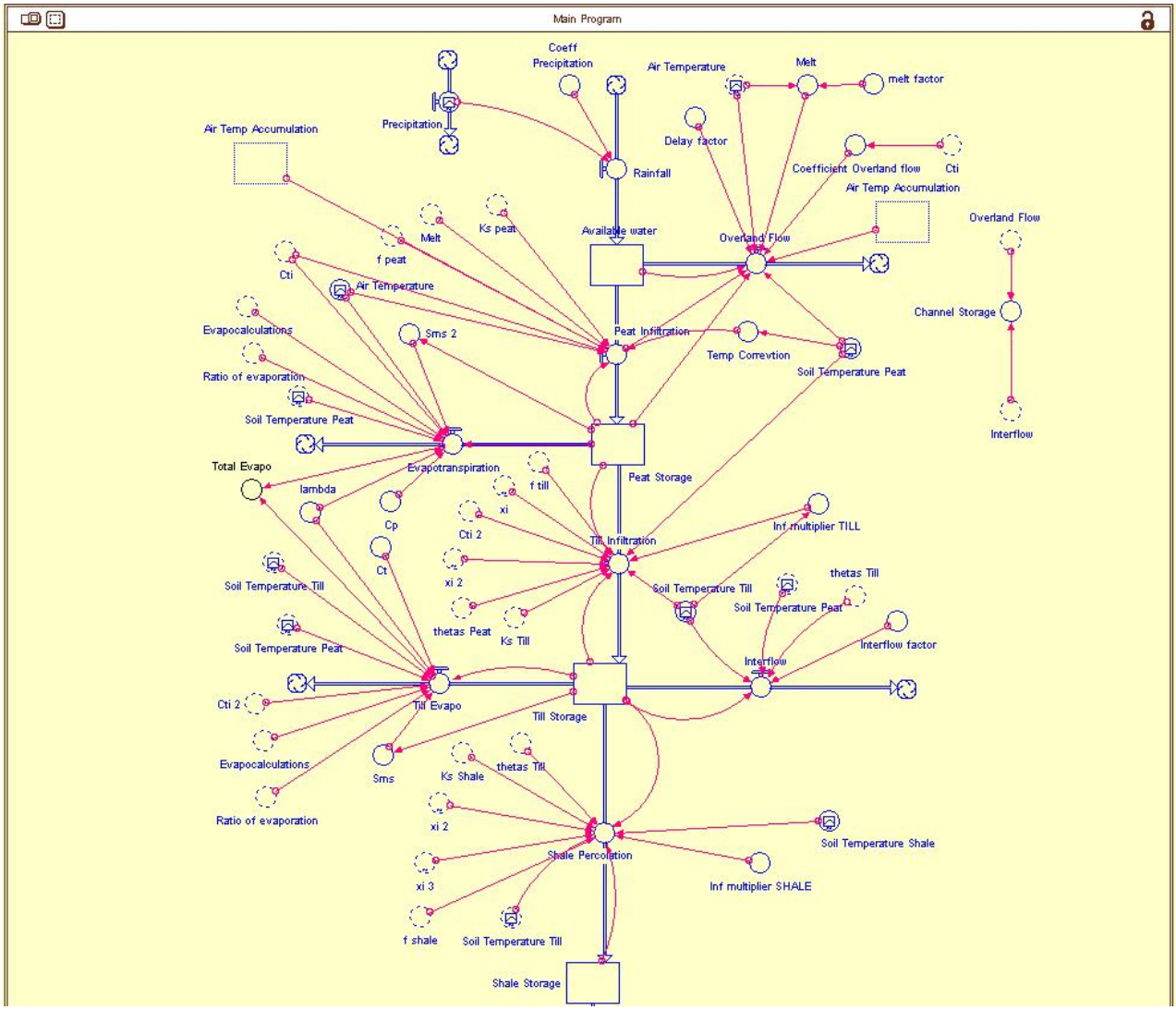

Figure B.1. Internal Model Structure (Only Partial Model is Shown for Illustration).

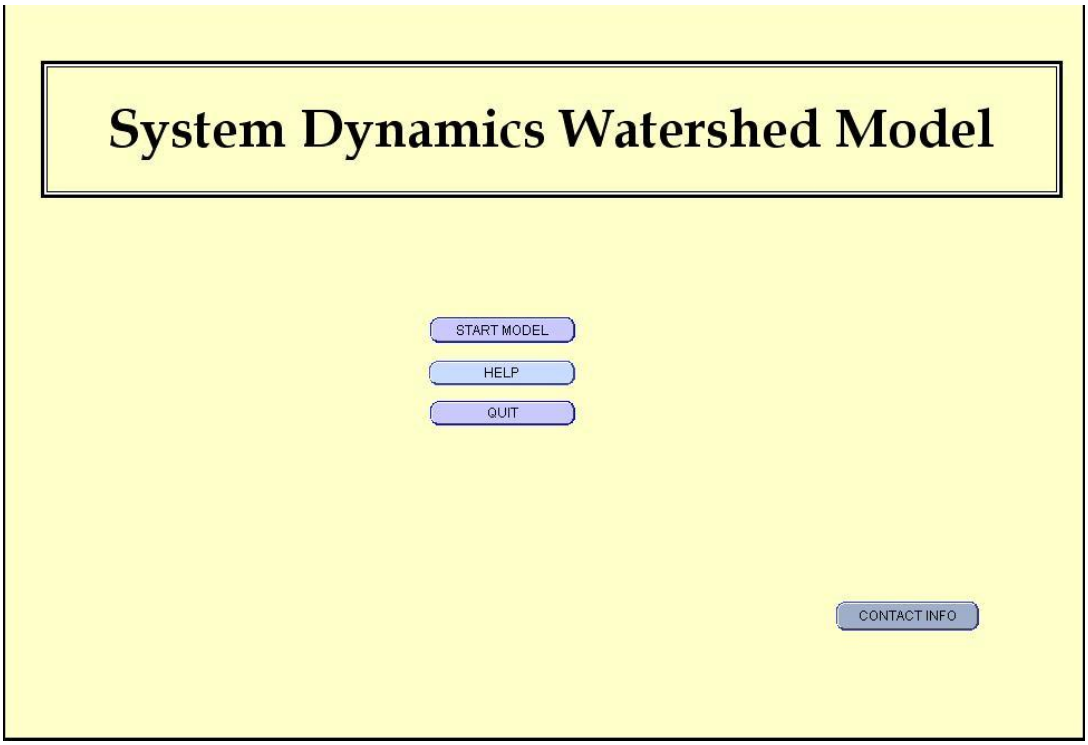

Figure B.2. First Screen during Model Run.

Figure B.3. Primary Screen having Master Controls for Running Model.

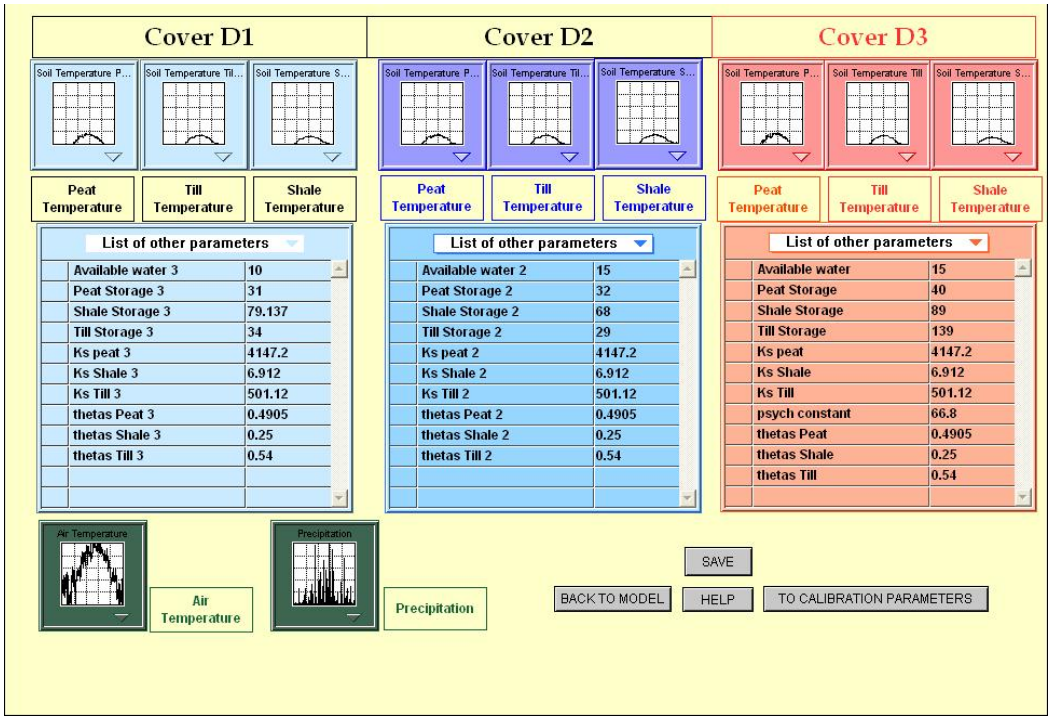

Figure B.4. Data Input Dialogue Boxes for all Sub-Watersheds.

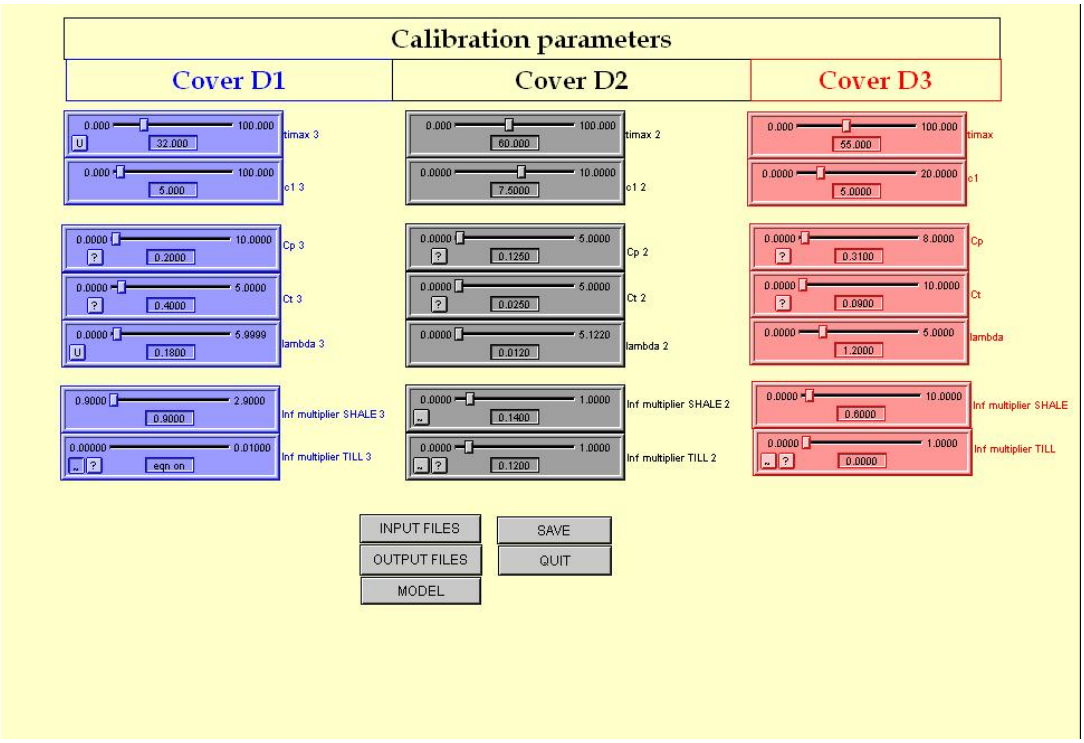

Figure B.5. Calibration Screen .

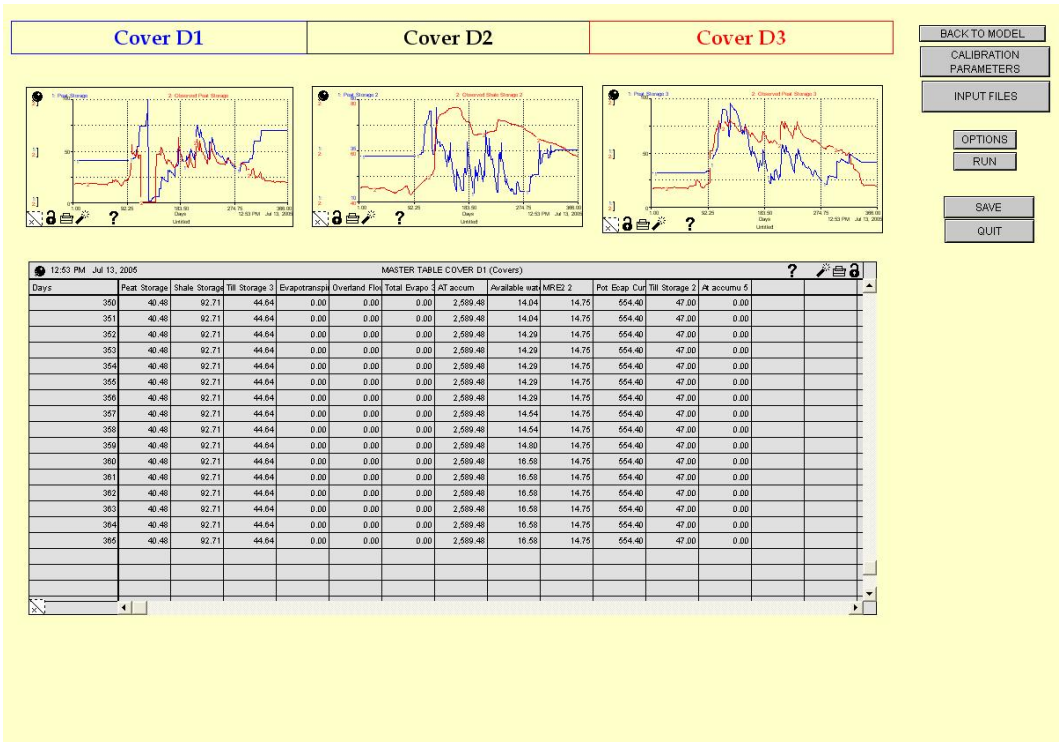

Figure B.6. Output Screen .

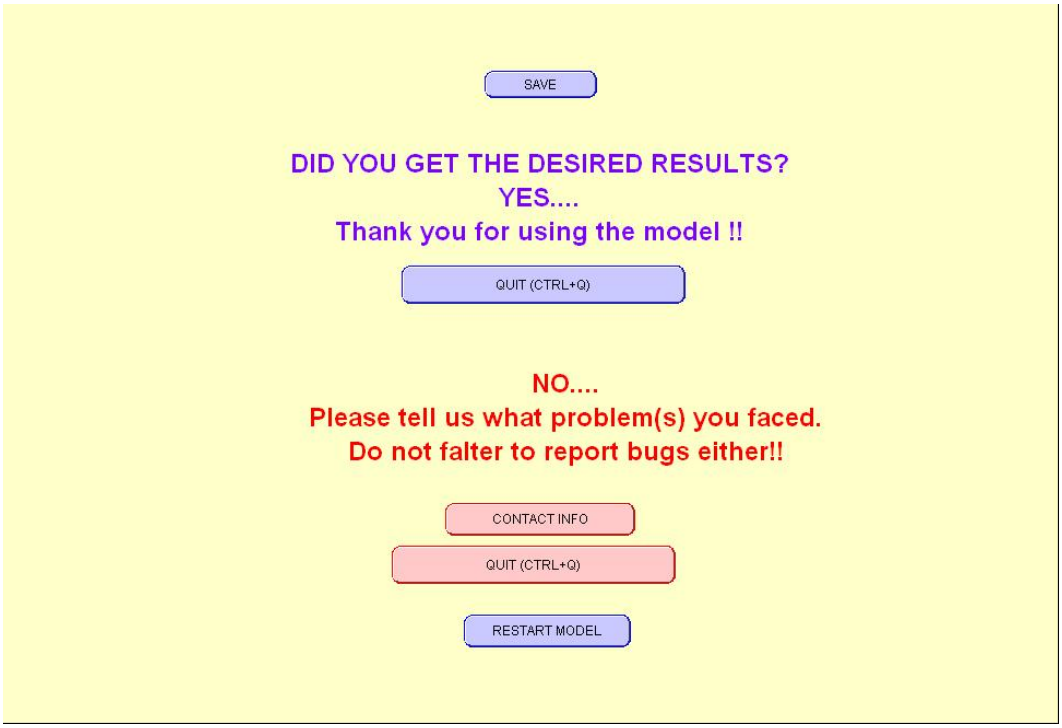

Figure B.7. Model Exiting.